

Technische Universität München

Wissenschaftszentrum Weihenstephan für Ernährung, Landnutzung und
Umwelt

Lehrstuhl für Chemie der Biopolymere

**Mapping disulfide bonds and free sulfides in the small hepatitis
B envelope protein S**

Nadine King

Vollständiger Abdruck der von der Fakultät Wissenschaftszentrum Weihenstephan für Ernährung, Landnutzung und Umwelt der Technischen Universität München zur Erlangung des akademischen Grades eines Doktors der Naturwissenschaften (Dr. rer. nat.) genehmigten Dissertation.

Vorsitzende/-r: Prof. Dr. Dietmar Zehn

Prüfende/-r der Dissertation:

1. Prof. Dr. Dieter Langosch
2. apl. Prof. Dr. Volker Bruß

Diese Dissertation wurde am 11.06.2019 bei der Technischen Universität München eingereicht und durch die Fakultät Wissenschaftszentrum Weihenstephan für Ernährung, Landnutzung und Umwelt am 23.09.2019 angenommen.

Contents

Acronyms	VI
1 Introduction	1
1.1 Historical background	1
1.2 Epidemiology and transmission	1
1.3 Classification	1
1.3.1 Genotypes and variants	2
1.4 Pathology and disease	4
1.5 Vaccination and treatment	4
1.5.1 The vaccine	4
1.5.2 Treatment methods	5
1.6 Genome Structure and proteins	5
1.6.1 Genome and open reading frames	5
1.6.2 Proteins	7
1.7 Particles secreted after infection	11
1.7.1 Dane particles	11
1.7.2 Subviral particles	11
1.8 Life cycle	12
1.9 The endoplasmic reticulum and disulfide bond formation	14
1.10 Aim of the project	16
2 Materials	17
2.1 Eukaryotic cell line	17
2.2 Cell culture media	17
2.3 Bacteria	17
2.4 Bacterial media and antibiotics	18
2.5 Plasmids	18
2.6 Primers	19
2.7 Enzymes	22
2.8 Antibodies	23
2.9 Kits	23

2.10	Chemicals	23
2.11	Solutions and buffers	25
2.12	Laboratory devices	27
2.13	Laboratory consumables	28
2.14	Software	29
3	Methods	30
3.1	Molecular and microbiological methods	30
3.1.1	Insertion of mutations using the QuickChange method	30
3.1.2	Agarosegel electrophoresis	32
3.1.3	Restriction enzyme digestion	32
3.1.4	Purification of DNA	33
3.1.5	Ligation	33
3.1.6	Preparation of chemical competent cells	33
3.1.7	Transformation of competent <i>Escherichia coli</i> (<i>E. coli</i>)	33
3.1.8	Plasmid preparation	34
3.1.9	Sequencing	34
3.2	Cell culture techniques	34
3.2.1	Cultivation of Huh7	34
3.2.2	Freezing of cells	35
3.2.3	Thawing of cells	35
3.2.4	Transfection of cells	35
3.2.5	Preparation of supernatant and lysate	36
3.3	Protein biochemical and immunological methods	36
3.3.1	Concentration of SVP	36
3.3.2	Sucrose density centrifugation	36
3.3.3	Protease protection assay	36
3.3.4	Labeling of thiols	37
3.3.5	SDS-PAGE	38
3.3.6	Western blot	38
3.3.7	Coomassie Blue staining	39
3.3.8	Immunofluorescence	39
3.3.9	FACS-FRET	40
4	Results	42
4.1	S protein oligomerization	42
4.1.1	Secretion of competent S constructs	42
4.1.2	Influence of the YFP/BFP fusion proteins on the topology	42

4.1.3	Functional characterization of the S-C65S-TM2polyA mutants	45
4.1.4	Oligomerization properties of C65S-TM2polyA-S	47
4.2	Secondary structure of the small hepatitis B virus surface protein	49
4.2.1	Secreted S protein forms a dimer	49
4.2.2	Exchange of cysteines in LL lead to impaired secretion	51
4.2.3	Restoration of secretion through particular cysteine residues	53
4.2.4	Cysteines in TM domains are free and do not influence secretion	58
4.2.5	Labeling with Mal-PEG is a way to detect and label cysteines in proteins	60
4.2.6	Mutation of glycosylation site is favorable in labeling experiments	63
4.2.7	Cysteines in CL influence secretion of wt and show free SH groups and intramolecular disulfides	64
4.2.8	Labeling of secreted SVP revealed intramolecular disulfide bond and seven oxidized cysteines in total	68
4.2.9	Native SVP carry an exposed free SH group on their surface	70
4.3	Influence of disulfide bonds on antigenicity	72
4.4	Comparison of human SVP and SVP from yeast for vaccination	74
5	Discussion	77
5.1	Mal-PEG labeling as a method for analysis of cysteine status in secreted viral particles	77
5.2	The main form of S in SVP was dimeric	79
5.3	A disulfide bond in the CL	81
5.4	Mapping of disulfide bonds and free sulfides in the S protein of HBV	85
5.5	SVP from yeast differ from human SVP	89
5.6	S protein oligomerization reveals influence of C65 and the TM2 domain	89
5.7	Outlook	90
6	Appendix	121
7	Acknowledgments	124

List of Figures

1.1	Global HBsAg endemicity	2
1.2	Geographic distribution of HBV genotypes	3
1.3	HBV genome organization	6
1.4	Linear map of HBV envelope proteins	9
1.5	S protein transmembrane topology	10
1.6	Life cycle of HBV	13
1.7	Disulfide bond formation in the lumen of the ER	15
2.1	Plasmid map of pSVBX24H-HA	19
3.1	QuickChange Site Directed Mutagenesis	31
3.2	Labeling of free sulfides with Mal-PEG	37
3.3	YFP and BFP absorption and emission spectra	40
4.1	Sucrose density centrifugation of secreted S constructs	43
4.2	Protease protection assay of YFP/BFP-S fusion proteins	44
4.3	Detection of the expression of the two constructs with different methods	46
4.4	FACS-FRET analysis of the oligomerization properties of different constructs	48
4.5	Dimers are the main form of S in different samples	50
4.6	Schematic Model of the localization of cysteines in the S protein	52
4.7	Exchange of all cysteines in TM and LL to serines impaire secretion	53
4.8	Three SingleCys constructs showed dimers and were secreted as SVP	54
4.9	Ratio of dimer intensities of different constructs to total intensity in lysate	55
4.10	One of the three cysteines C107, C147 and C149 are necessary for secretion	57
4.11	Cysteines in the TM domains do not influence dimerization	58
4.12	Accessability of cysteine residues in unfolded proteins	60
4.13	Identification of the shift size detectable after Mal-PEG labeling in WB	62
4.14	The exchange of the glycosylation motif did not impair secretion or dimerization	63
4.15	Co-transfection of S-HA with single CXXS echanges of cysteines in the CL	65
4.16	Labeling of free or oxidized cysteines in lysate	67
4.17	Labeling of S-HA and 4C+C107 in SN and lysate	69

4.18	Labeling of free cysteines in non-reduced secreted SVP	71
4.19	Analysis of the antigenicity of wt S	73
4.20	Analysis of the antigenicity of secretion competent constructs	74
4.21	Analysis of yeast HBs on sucrose gradient	75
4.22	Coomassie staining of yeast derived SVP +/- DTT and labeled for free and bound cysteines	76
5.1	Comparison of sequence similarities in HBsAg between fish and human	82
5.2	Variability at the cysteine position among sequences from NCBI	86
5.3	Proposed model of the S protein dimer	87
6.1	Labeling of disulfide bonds in lysate of different constructs regarding cysteines in TM domains	121
6.2	Graphic corresponding to the intensity analysis in Figure 4.9	122
6.3	Graphic corresponding to the intensity analysis in Figure 4.15	123

Acronyms

aa	amino acid
AGL	antigenic loop
BFP	blue fluorescent protein
BiP	binding proteins
CAD	cytosolic anchorage determinant
CL	cytoplasmic loop
cccDNA	covalently closed circular DNA
CHB	chronic hepatitis B
CMHBV	capuchin monkey hepatitis B virus
Da	Dalton
DHBV	duck hepatitis B virus
DNA	deoxyribonucleic acid
dpt	days post transfection
DTT	dithiothreitol
E.coli	Escherichia coli
ER	endoplasmic reticulum
ERGIC	ER-Golgi intermediate compartment
Ero1p	ER oxidase 1
ESCRT	endosomal-sorting-complex-required-for-transport
FACS	fluorescence-activated cell sorting

FDA	Food and Drug Administration
FRET	Förster resonance energy transfer
FSC	forward-Scater
fw	forward
GalT	galactosyltransferase
GFP	greenfluorescent protein
gp27	glycosylated S Protein
h	hour
HBsAg	HBV surface antigen
HBV	hepatitis B virus
HCC	hepatocellular carcinoma
Hsc-70	cognate heat-shock protein
HSPG	heparin sulphate proteoglycans
HT	high-throughput
IU	international unit
kDa	kilo Dalton
μ	micro
min	minute(s)
MVB	multivesicular-bodies
NA	nucleos(t)ide analogue
NEM	N-Ethylmaleimide
nt	nucleotide
NTCP	sodium taurocholate co-transporting polypeptides
o/n	over night

ORF	open reading frames
p24	non-glycosylated S Protein
PCR	polymerase chain reaction
PDI	protein disulfide isomerase
PEG	polyethylene glycol
Mal-PEG	methoxypolyethylene glycol maleimide
MW	molecular weight
pgRNA	pregenomic RNA
PMT	photomultipliertube
rcDNA	relaxed circular DNA
rev	reverse
RNA	ribonucleic acid
ROS	reactive oxygen species
S. cerevisiae	<i>Saccharomyces cerevisiae</i>
S	small envelope protein
SDS-PAGE	sodium dodecyl sulfate polyacrylamide gel electrophoresis
sec	second(s)
sgRNA	subgenomic RNA
SN	supernatant
SRP	signal recognition particle
SSC	sideward-Scater
SVP	subviral particles
TM	transmembrane domain
TMs	transmembrane domains

TP	terminal protein
v/v	volume per volume
w/v	weight per volume
w/w	weight per weight
WB	Western blot
WMHBV	woolly monkey hepatitis B virus
wt	wild type
YFP	yellow fluorescent protein
yHBsAg	yeast derived HBsAg

Abstract

The small envelope protein S (226 aa long) of the hepatitis B virus contains 14 cysteine residues and is synthesized as an integral membrane protein with 4 transmembrane regions (TM). Expression of S in eukaryotic cells causes the secretion of subviral particles (SVP) consisting of approximately 100 S chains and lipid. Nevertheless the structure and morphogenesis of particles is poorly understood, only two of the TM domains are experimentally proven. The influence of disulfide bonds on the structure and the epitope of S has been suggested early, but specific interacting cysteines have never been properly assigned.

We intend to map intra- and intermolecular cystin pairs and free cysteine residues in S by expression of a C-terminally HA-tagged S protein (S-HA) and derivatives carrying cysteine to serine exchanges in transient transfected Huh7 cells. The constructs were characterized with respect to SVP formation, cystin-linked oligomer formation, reactivity in an HBsAg-ELISA, and by determining the number of free and bound cysteines through labeling with Mal-PEG shifting the molecular mass of derivatized proteins. Besides, we compared, when applicable, these results with samples from infected donors and samples recombinantly expressed in yeast.

Approx. 90 % of S-HA in secreted SVP appeared as a cystin-linked dimer. Only a minor fraction formed monomers or higher oligomers. A S-HA mutant with an exchange of both cysteines present in TMs (C90S + C221S) was wt. A mutant (4C) with an additional exchange of all 8 cysteines in the luminal loop (LL) between TM2 and TM3 by serines was blocked in dimer and SVP formation. Only the restoration of single cysteines in this background at positions 107, 147, 149 restored dimer and SVP formation suggesting that these cysteines formed symmetric intermolecular disulfide bonds and that stabilization of S dimers by at least one cystin bond was essential for SVP formation. 4C carries only 4 cysteines (positions 48, 65, 69, 76) in the cytoplasmic loop (CL) between TM1 and TM2. Two of these cysteines were free and two were oxidized suggesting that two cysteins formed an intramolecular disulfide bridge. Besides, exchange of one of the four cysteines in wt background to serine had a dominant-negative effect on the secretion of co-transfected S-HA proteins.

In S-HA from SVP at least 6 free and at least 7 oxidized cysteines were found. One free SH group in LL could be labeled without prior denaturation of SVP suggesting that it was exposed on the particle surface. Due to calculations we propose one additional intramolecular bond to be present in LL, but we could not assign the position.

Zusammenfassung

Das kleine Hüllprotein S (226 aa lang) des Hepatitis-B-Virus enthält 14 Cysteinreste und wird als integrales Membranprotein mit 4 Transmembranregionen (TM) synthetisiert. Die Expression von S in eukaryotischen Zellen bewirkt die Sekretion von subviralen Partikeln (SVP), die aus etwa 100 S-Ketten und Lipiden bestehen. Dennoch ist die Struktur und Morphogenese der Partikel wenig verstanden, nur zwei der TM-Domänen sind experimentell belegt. Der Einfluss von Disulfidbindungen auf die Struktur und das Epitop von S wurde früh angenommen, aber bestimmte interagierende Cysteine wurden nie zugeordnet.

Wir beabsichtigen die inter- und intramolekularen Cystinpaare, sowie die freien Cysteinreste in S zu kartieren. Hierfür wird ein C-terminal HA-markierten S Proteins (S-HA), oder eine davon abgeleitete Mutante in Huh7 Zellen transfiziert und exprimiert. Die so entstandenen Proteine werden mit Bezug auf SVP Bildung, Cystin vermittelte Oligomerisierung, Reaktivität in einem HBsAg-ELISA und Anzahl der freien und oxidierten Cysteinreste, durch Mal-PEG-Markierung, untersucht. Außerdem haben wir diese Ergebnisse gegebenenfalls mit Proben von infizierten Spendern und Proben aus Hefe verglichen. Dieses in Hefe rekombinant hergestellte Material wird heute als Impfstoff verwendet.

Eine S-HA-Mutante mit einem Austausch beider Cysteine in den TMs (C90S + C221S) verhielt sich wie Wildtyp. Eine Mutante (4C) mit zusätzlichem Austausch aller 8 Cysteine zu Serinen in der luminalen Schleife (LL) zwischen TM2 und TM3 wurde in Dimer- und SVP-Bildung blockiert. Wiederherstellung einzelner Cysteine im 4C-Hintergrund an den Positionen 107, 147, 149 resultierte wieder in Dimer- und SVP-Bildung, was darauf hindeutet, dass diese Cysteine symmetrische intermolekulare Disulfidbrücken ausbildeten. Die Stabilisierung von S-Dimeren durch mindestens eine Cystinbindung war für die SVP-Bildung unerlässlich.

Circa 90 % von S-HA in sekretierten SVP lagen als Dimer vor, dieser würde über Disulfidbrücken vernetzt. Monomere oder höhere vernetzte Oligomere machten nur einen kleinen Teil des sekretierten Materials aus. 4C enthält nur 4 Cysteine (Positionen 48, 65, 69, 76) in der cytoplasmatischen Schleife (CL) zwischen TM1 und TM2. Zwei dieser Cysteine waren frei und zwei wurden oxidiert, was darauf hindeutet, dass zwei Cysteine eine intramolekulare Disulfidbrücke innerhalb von CL bildeten. Außerdem hatte der Austausch eines der vier Cysteine zu Serine im wt Hintergrund einen dominant-negativen Effekt auf die Sekretion von co-transfizierten S-HA-Proteinen.

In S-HA aus SVP wurden mindestens 6 freie und mindestens 7 oxidierte Cysteine gefunden. Eine freie SH-Gruppe in LL konnte ohne vorherige Denaturierung von SVP markiert werden, was darauf schließen lässt, dass sie auf der Partikeloberfläche exponiert wurde. Aufgrund der daraus resultierenden Berechnungen wird eine intramolekulare Disulfidbrücke vorgeschlagen, die in LL liegt. Die exakte Position konnte nicht bestimmt werden. Aber die Antigenität schien

in gewissem Maße von dieser Bindung abhängig zu sein, da sekretionskompetente Konstrukte, mit allen drei intermolekularen Disulfidbindungen, keine ELISA-Ergebnisse zeigten.

1 Introduction

1.1 Historical background

After a smallpox immunization campaign in Germany in 1883 an outbreak of hepatitis occurred. This was the first evidence that a form of hepatitis was transmitted by direct inoculation of blood or blood products¹. Although at this point in time it was not clear, that the causative agent was a virus.

In 1965 this changed when Blumberg and colleagues described an "isoprecipitin" which was found in the sera of Australian aborigines². This so called Australia antigen was subsequently shown to be related to hepatitis B virus (HBV) infections and finally was identified as the surface antigen of HBV³. What Blumberg described, however, was not the infectious particle, but, with diameters of 17-25 nm, subviral particles (SVP).

Dane and colleagues were the first to visualize and describe the infectious particles, which were then called "Dane particles", by electron microscopy⁴. They had a diameter of 42 nm and reacted with antisera to the Australia antigen.

1.2 Epidemiology and transmission

Hepatitis B virus has a worldwide distribution and it is estimated, that >2 billion people have been infected with HBV⁵. High endemic areas include China, Indonesia and Africa, around 60 % of the world's population lives in these regions⁶⁻⁹.

HBV can be spread via contact with blood or other body fluids from infected patients⁶. The main route in low endemic countries is horizontally, including sexual intercourse, needle sharing and working in the health care field^{6,10-14}. Whereas, in high endemic countries the main transmission route is from an infected mother to her newborn during birth^{15,16}.

1.3 Classification

HBV belongs to the family of *Hepadnaviridae* which contains two genera: *Avihepadnaviruses* and *Orthohepadnaviruses*. *Avihepadnaviruses* infect only birds, whereas *Orthohepadnaviruses* infect mammals and therefore include HBV^{17,18}. HBV was further subdivided into genotypes

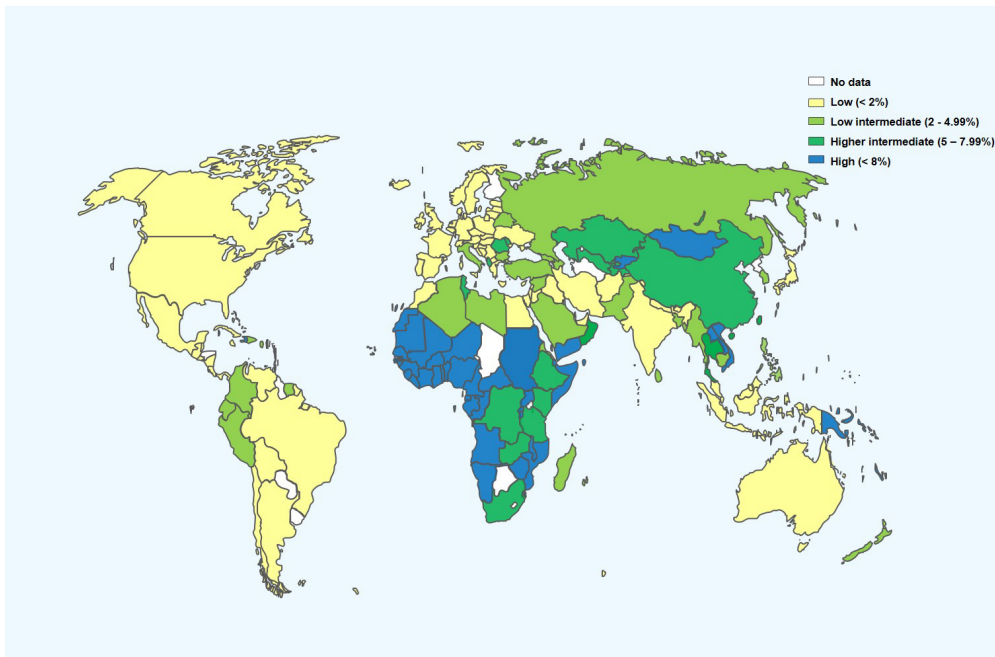


Figure 1.1: **Global HBsAg endemicity** Global HBsAg endemicity derived from published data generated from 1957-2013⁹. The higher the endemicity, the darker the color. No data available depicted in white. Template for the world map downloaded at <https://www.powerpointslides.net/powerpointgraphics/powerpointmaps.html>

and several subgenotypes based on sequence diversity of a minimum of 8 % and 4 %, respectively¹⁹⁻²⁵.

1.3.1 Genotypes and variants

The HBV genome has been estimated to evolve at an error rate of approximately 10^{-3} - 10^{-6} nucleotide substitutions per site per year²⁶⁻³². The genotypes differ in genome length, size of open reading frames (ORF), the translated proteins, as well as various mutations^{33,34}. Until now, based on an intergroup divergence of <7.5 % across the complete genome, HBV has been classified into 9 genotypes, A - I^{20,33,35}. Another genotype (J) has been proposed, but was only found in one individual so far³⁶. Intergroup diversities between 8 % and 4 % further subdivides genotypes A - D, F, H and I into a minimum of 35 subgenotypes^{20,21,33}. The genotypes are distributed throughout the world. The main genotypes in certain areas are displayed in Figure 1.2.

Another classification is dependent on the HBV surface antigen (HBsAg) heterogeneity. This defines 9 serological subtypes *ayw1*, *ayw2*, *ayw3*, *ayw4*, *ayr*, *adw2*, *adw4*, *adwq*, *adr* and *adrq*³³. The serological subtypes are significantly correlating with genotypes, i.e. *adw* is associated with genotypes A, B, F, G and H, and *adr* with C. However many exceptions do exist³⁴.

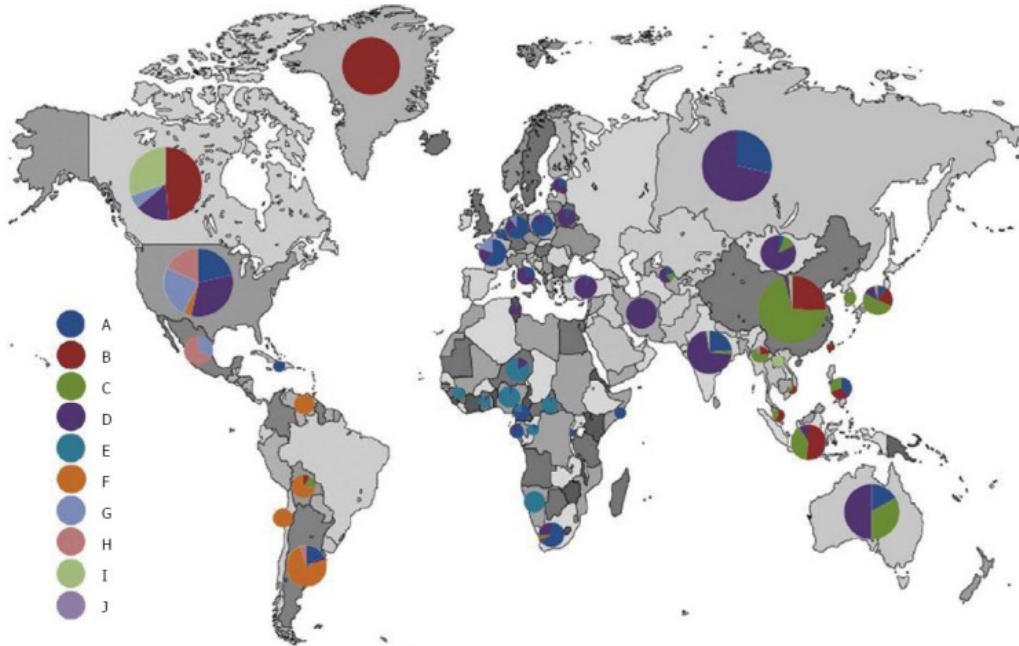


Figure 1.2: **Geographic distribution of HBV genotypes** The map was generated from published data. Only countries/regions with more than five full-length genome sequences available were included. This dataset included 46 countries/regions and 3179 full-length genome sequences. It should be noted that this geographic distribution of HBV genotypes may not represent actual seroprevalence in a country/region, as there are potential sampling errors due to the bias of including only whole genome analyses. In addition, the size of each circle does not represent the prevalence of HBV infection and burden of disease in the specified geographic region³⁷. (Reprinted with permission)

1.4 Pathology and disease

An infection with HBV can lead either to an acute self-limited or a chronic infection. In healthy adults an infection with HBV is cleared in 95 % of the cases. In 0.5 % of newly infected patients this can terminate in a fatal fulminant hepatitis³⁸⁻⁴¹. Clearance of the virus needs an effective CD4⁺ and CD8⁺ T cell response as well as a sufficient amount of neutralizing antibodies^{7,42-44}. Currently, up to 360 million individuals are chronically infected worldwide^{5,45,46}. They have a greatly increased risk of severe liver damage and, if progression continues, hepatocellular carcinoma^{5,38,39,46-50}. The pathogenesis is always caused by the immune system of the host, as the virus itself is not cytopathic⁵¹. The risk of developing a chronic infection decreases with age. When infected perinatal to 6 months of age the probability is around 90 %, between the age of 6 months and 5 years it decreases to 20-60 %⁹.

1.5 Vaccination and treatment

1.5.1 The vaccine

HBV is a preventable infection, due to the fact that a vaccine exists for more than 30 years⁵. In the case of HBV a single polypeptide is sufficient to elicit a protecting immune response against the infection. Nevertheless, these polypeptides need to be assembled into spherical particles^{52,53}. The first commercially available vaccine was derived from plasma of asymptomatic carriers^{52,54}. Due to safety issues a second generation of HBV vaccines without the use of human samples was developed. It became the first recombinant protein-based vaccine approved by the Food and Drug Administration (FDA) in 1986^{55,56}.

Nowadays, more than 150 countries use hepatitis B vaccines in their national immunization programs^{54,57}. The primary 3-dose vaccine schedule induces a protective antibody concentration in >95 % of healthy infants, children and young adults^{54,58-60}.

The second generation vaccine was based on a plasmid expressed in *Saccharomyces cerevisiae* (*S. cerevisiae*). a bacterial expression systems like *E.coli* did not work⁶¹⁻⁶⁴. However, yeast derived HBsAg (yHBsAg) has some shortcomings; in comparison to human HBsAg it is neither secreted from the yeast cells nor glycosylated^{52,63-71}. The usage of methylotrophic yeasts like *Hansenula polymorpha* or *Pichia pastoris* also did not lead to glycosylated yHBsAg^{65,66}. Until now, no clear evidence has been presented that the particle assembly occurs within the yeast cell⁷⁰. It is more likely, that the formation of 22 nm particles occurs during down-stream procession of the yeast cells and their proteins after lysis⁷⁰⁻⁷². A maturation of HBsAg can be achieved using chromatography and KSCN treatment⁷³, but also other chemicals are used. The purification can vary between microorganism and protocol between 3-13 steps (review of different protocols in⁷³).

1.5.2 Treatment methods

Up to date, there are two therapeutic approaches for the treatment of chronic hepatitis B (CHB) available. One is IFN- α 2b (interferon-alpha), which was the first agent to be approved in 1991^{74,75}. The main route of action is immune modulation. However, only a weak anti-viral effect is measurable⁷⁶. From 2005 on a new pegylated formulation of IFN- α was approved for CHB treatment, and is still in use⁷⁴.

The second mode of action is targeting the P protein with nucleos(t)ide analogue (NA). These can directly inhibit the polymerase or cause a DNA chain termination⁷⁷. Examples for this kind of substance class are Entecavir, Telbivudine and Tenofovir. There are, however, some major shortcomings of this therapeutic substances. Firstly, they need to be taken over a long period of time, secondly, they can lead to mutations in the HBV genome and therefore to resistances and thirdly they can cause severe side effects^{74,78,79}.

The discovery of the HBV entry receptor in 2012⁸⁰ opened the door to a new substance class, the entry inhibitors. The most promising candidate passed phase IIa of a clinical study in HBV and HDV co-infected patients⁸¹. It is a lipoprotein based on the pre-S1 domain of the envelope of HBV and known to block the entry of HBV⁸².

A functional cure of CHB is not available, as the covalently closed circular DNA (cccDNA) persists in the nucleus of infected cells and is the reservoir for HBV⁸³. Nevertheless, promising first results in the degradation of cccDNA in the nucleus could be achieved with a combination of IFN- α and activation of the lymphotoxin- β receptor⁸⁴ or with the use of CRISPR/Cas9⁸⁵.

1.6 Genome Structure and proteins

1.6.1 Genome and open reading frames

The hepatitis B virus has a complex genome with overlapping ORF and only 3.2 kb in size⁸⁶. The (-) strand, which is complementary to the pregenomic RNA (pgRNA) cf. section 1.8, harbors a short (9 nt) terminal redundancy⁸⁷⁻⁹⁰ whereas, the (+) strand is heterogeneous in length, terminating hundreds of nt before completion⁸⁶. Furthermore, there are two 11 nt long, direct-repeat elements (DR1 and DR2), which are located at the 5' end of the (-) stand and at the 3' end of the (+) strand⁹¹. The 5' ends of both strands are complementary, which leads to circularization⁹². The relaxed circular DNA (rcDNA) is covalently linked to the terminal protein (TP), which is part of the viral reverse transcriptase^{93,94}. Besides, the 5' end of (+) strand linked to a 18 nt long capped RNA oligomer^{90,95}.

HBV DNA carries four overlapping ORF which code for seven proteins: the preS/S-ORF codes for the envelope proteins, the X-ORF for the X protein, the P-ORF for the viral polymerase and the preC/C-ORF codes for the core and e protein.

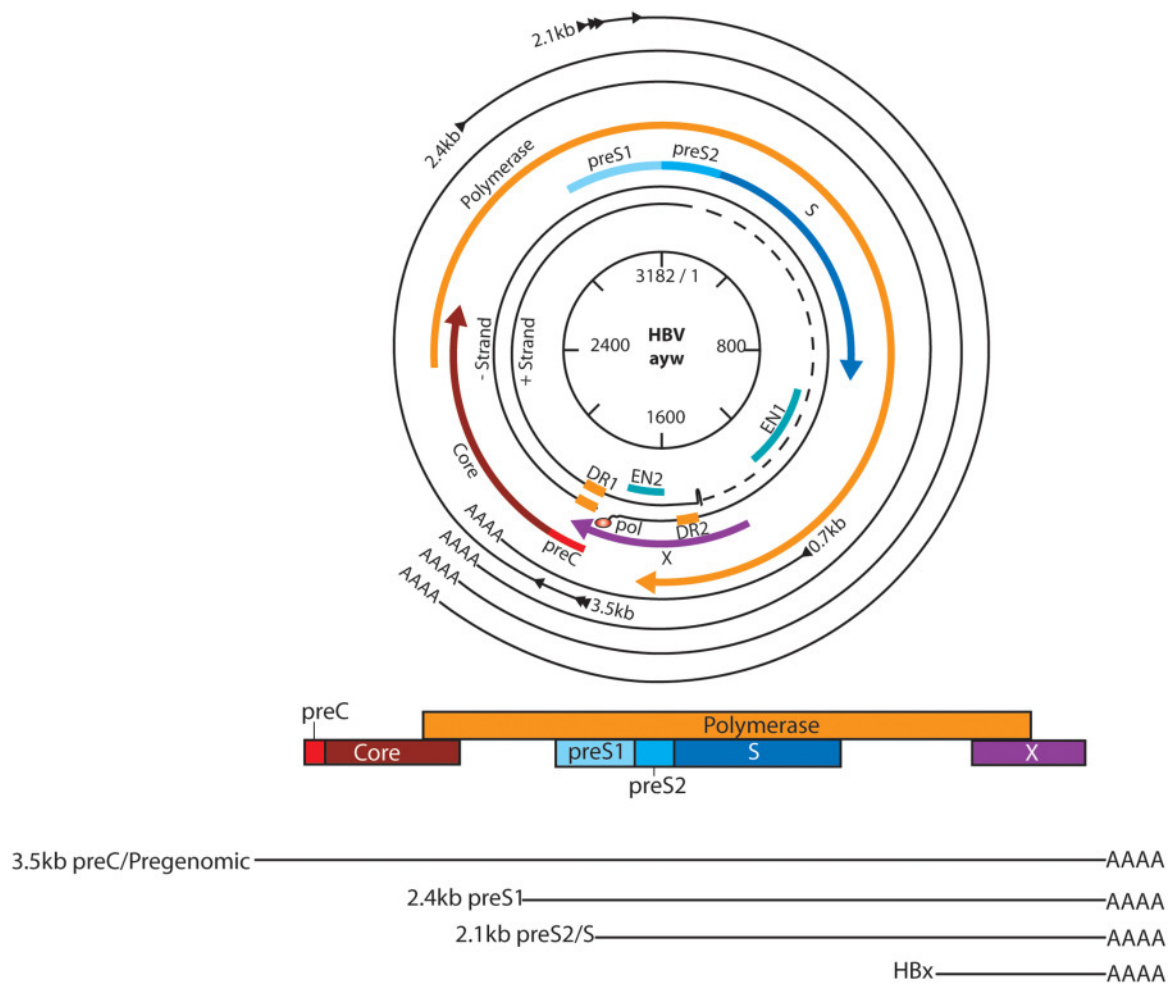


Figure 1.3: **HBV genome organization.**⁹⁶ The HBV genome is a partially double-stranded DNA. The central circle depicts the conventional numbering of the circular genome where positions 1 and 3182 usually represent a unique EcoR1 restriction site. Small differences in genome length among genotypes (and serotypes) exist; the ayw serotype is shown. The black circular lines represent the DNA genome with a completed negative-strand DNA ((-) strand) and a partially completed (dashed lines) positive-strand DNA ((+) strand). Also indicated are: direct repeats (DR1, DR2), enhancers (EN1, EN2), and polymerase (orange circle labeled “pol”). Colored arrows indicate the ORFs for preCore, core, polymerase, envelope (preS1, preS2, and S), and HBx proteins. Outer black arrows depict genomic and subgenomic polyadenylated transcripts transcribed from cccDNA, also depicted at the bottom of the figure, highlighting overlapping regions. Colored boxes below the circular genome indicate ORFs for HBV proteins, highlighting their overlapping regions. (Reprinted with permission)

1.6.2 Proteins

Core protein

The core protein is translated from the core-ORF of the pgRNA. Depending on the genotype it has a length of either 183 nt or 185 nt and weights of approximately 21 kDa. The protein can be divided into two domains with different functions. The 140 aa at the N terminus represent the assembly domain (NTD), which is sufficient to mediate capsid assembly^{97,98}. The C-terminal domain (CTD) is essential for packaging of pgRNA into nucleocapsids and the conversion of pgRNA to rcDNA⁹⁹⁻¹⁰¹.

Core protein dimers are the building blocks of capsids¹⁰². However, there are two distinct morphological capsid formed, with either 90 homodimers and a T=3 symmetry, or the main form with 120 homodimers and a T=4 symmetry^{103,104}. A functional influence of the two isoforms is not known so far.

e protein

The e protein, also called preC protein is translated from the preC mRNA. This mRNA is in-frame with the C-ORF but has its own start codon. Therefore, e equals C in 149 amino acid (aa), but carries a N-terminal signal peptide^{105,106}. It has a molecular weight of ~ 25 kDA intracellularly. When it enters the secretion pathway, first the signal sequence is cleaved off in the endoplasmic reticulum (ER). Then it undergoes further proteolytic processing steps before it is released from the cell as heterogeneous ~ 17 kDA e protein^{105,107,108}. Unlike C, preC is dispensable for viral infection, but is important to establish persistent infection by regulation of the host's immune response against C^{106,109-111}. Serologically, secreted e protein is referred to as Hepatitis B e Antigen (HBeAg)¹¹².

Reverse Transcriptase/ -Polymerase

The polymerase is the largest of the HBV proteins (~ 90 kDA) and is translated from the pregenomic RNA. It can be subdivided into four parts: TP, the spacer, the RT domain and the RNaseH domain¹¹³⁻¹¹⁹. TP is essential for priming the reverse transcription as it carries the essential tyrosine residue and interacts with the ε signal on the pgRNA to newly synthesize the (-) strand of rcDNA¹²⁰⁻¹²². The spacer is the most variable domain and is dispensable for the function of the polymerase. However, the ORF of P is overlapping with the ORF of the envelope proteins¹²³. Next, the RT domain carries the active polymerase site with a highly conserved tyr-met-asp-asp motif. This motif is also conserved among retroviruses and retrotransposons¹²⁴. While the pgRNA is transcribed into rcDNA, the RNaseH is degrading the already processed pgRNA^{113,125}. In conclusion, at the end only rcDNA is the only polypeptide in the mature capsids.

X protein

In contrast to the other HBV proteins, X does not have a single assigned function, so it is the least understood. Nevertheless, it is transcribed from the X mRNA and has a size of ~ 17 kDa. It is also known that it is not packed into infectious particles but is required for viral replication *in vivo*^{41,126,127}. Several functions of X have been described in literature, i.e. regulation of host and viral gene expression, Ca^{2+} signaling, DNA damage repair, cell cycle, apoptosis and autophagy¹²⁸⁻¹³³. There are also hints connecting HBx with the acceleration of hepatocellular carcinoma (HCC) progression¹³⁴⁻¹³⁶, but this is still under investigation.

Surface proteins

The three envelope proteins (S, M and L) are encoded by the E-ORF, which varies in length (389 or 400 codons) depending on the genotype. From this ORF two subgenomic RNA (sgRNA) are transcribed, one is initiated at a promoter upstream of the ORF, the other from a promoter upstream of the second translation initiation site^{137,138}. The longer (2.4 kb) sgRNA only codes for the large envelope protein, whereas from the shorter sgRNA (2.1 kb) the middle and the small envelope protein (S) are transcribed¹³⁷⁻¹³⁹. This is achieved through three different AUG codons for the initiation of translation which are in frame. But there is only one UAA stop codon where translation of all proteins terminate regardless of the start codon used. This means that the generated proteins only differ in length of their N-terminal domains (Figure 1.4) and all contain the S domain at the C terminus. The M protein contains in addition to S the preS2 domain and L the preS2 and a preS1 domains¹³⁷⁻¹³⁹.

So the largest of the envelope proteins is L with either 389 aa or 400 aa in size, depending on the genotype. This corresponds to a molecular mass of 39 kDa in the non-glycosylated form. The M protein is 281 aa long and weighs 30 kDa non-glycosylated and the small envelope protein is 55 aa shorter than M (226 aa) and weighs 24 kDa in non-glycosylated form¹³⁹. All three proteins can be N-glycosylated at asn146 of the S domain (open hexagon in Figure 1.4). There is also a second N-glycosylation site in the preS2 domain, which is only used in M proteins but not in L¹⁴⁰ (filled hexagon in Figure 1.4). A potential O-glycosylation site in the preS2 domain is only used in some genotypes¹⁴¹. PreS1 also contains additional N-glycosylation sites which are, however, not used.

The envelope proteins of HBV are typical membrane proteins, which means they are synthesized at the ER and gain a relatively complex topology (cf. Figure 1.5)¹⁴². The first topologic signal containing TM domain from residues 8- 22 (TM1) translocates the S protein into the ER membrane, but is not cleaved by the cellular signal peptidases¹⁴³. The second TM domain (TM2) from 80- 98 aa anchors the protein in the ER membrane, as it acts as a type II signal/anchor

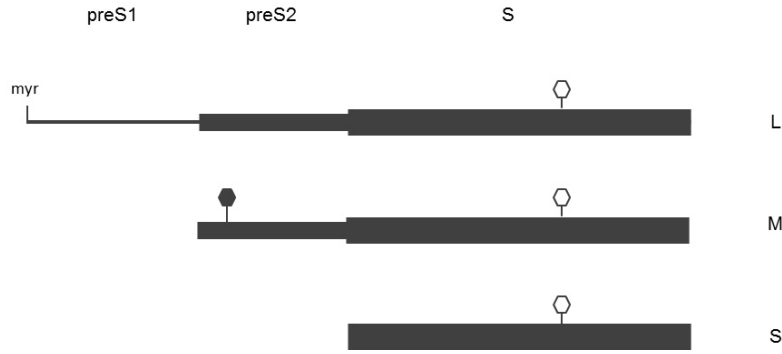


Figure 1.4: **Linear map of HBV envelope proteins.** The C terminus of all three proteins corresponds to the S protein. The M and L protein contain additionally the preS2 (M) or preS2 plus preS1 domain (L). The L protein is myristylated at glycine 2 (myr), the preS2 domain is N-glycosylated (filled hexagon) and the S domain is partially N-glycosylated (open hexagon).

domain¹⁴⁴. This results in a cytosolic loop (CL) between TM1 and TM2 and the C terminus locates to the ER lumen¹⁴⁵⁻¹⁴⁷. It is predicted that the hydrophobic C terminus crosses the ER membrane again twice with TM3 (173- 193 aa) and TM4 (202- 222 aa). Between TM2 and TM3 the luminal loop (LL) from 99- 169 aa is located^{144,146,148}. This loop contains the N-glycosylation site and the main epitope of S, also called antigenic loop (AGL)¹⁴⁹. Between TM3 and TM4 a short second cytosolic loop is formed^{146,147}.

S contains 14 cysteine residues. Cysteine residues are directly involved in disulfide bond formation^{150,151}. For maturation of S in the ER the cellular chaperon protein disulfide isomerase (PDI) is essential and catalyzes the formation of disulfide bonds¹⁵². Shortly after synthesis disulfide-linked homo- and heterodimers between S, M and L can be detected^{151,153}. An exchange of one out of three of the four cysteines in CL by serine blocks the secretion of SVP¹⁵¹. The reason for this remains unknown. A chemical modification of cysteine residues in CL could not be demonstrated^{153,154}. Also disulfide bridge formation by these aa has not been observed up to now.

The topology and biosynthesis of M is quite similar to S. Three different forms of M are detectable, a non-glycosylated version with a molecular weight of 30 kDa, a monoglycosylated form (33 kDa) and a double glycosylated form (36 kDa). The additional preS2 domain is cotranslationally translocated the ER lumen by the TM1 signal sequence^{140,155,156}. The role of M in the viral life cycle remains unclear, since its an absence (e.g. by mutation of its start codon)

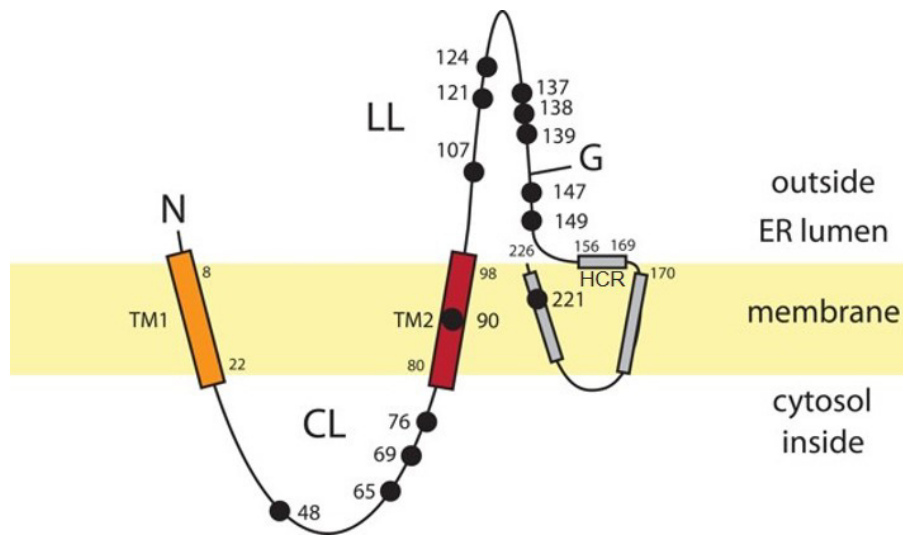


Figure 1.5: **S protein transmembrane topology.** Model for the transmembrane topology of the HBV S protein monomer in the ER membrane (light yellow area). TM1 and TM2, transmembrane domains 1 and 2; CL, cytosolic loop; LL, luminal loop; HCR, hydrophobic C-terminal region; (G), facilitative glycan N-linked to N146; cysteine positions are indicated with black dots and membranes correspond to the aa position. The shaded horizontal rectangle represents a putative amphipathic helix. Domains in the ER lumen become located on the surface of secreted SVP, and domains in the cytosol become located inside SVP.

does not disrupt particle morphogenesis or infectivity^{157,158}. In fact, avian hepadnaviruses do not code for an M protein¹⁴⁵. L is either present in its non-glycosylated form (39 kDa) or with a single glycosylation residue attached to asn146 (of S) leading to 42 kDa. Both forms are myristylated¹⁵⁴. However, in comparison to S and M, L has a more complex topology. Initially, the N terminus (preS1 and preS2) of L is in the cytosol of the ER, this topological form is called i-preS¹⁵⁹. Nonetheless, 50 % of L proteins in secreted virions show a different topology with the N terminus located outside on virions (e-preS)¹⁵⁹⁻¹⁶⁴. It is not fully understood how this "switch" is taking place. A topological element, mapped to residues 74-94 of preS1, called cytosolic anchorage determinant (CAD) interacts with the cognate heat-shock protein (Hsc-70), which in turn blocks the co-translational translocation of preS^{165,166}. Luminal chaperons, like binding proteins (BiP) could support the topological change^{167,168}. It is now widely accepted that the two distinct topologies serve two different functions, either recruitment of mature viral nucleocapsid for virion budding, or recognition of (co)receptors for viral entry^{142,159,169}.

1.7 Particles secreted after infection

1.7.1 Dane particles

In 1970 D. S. Dane identified the HBV virion via electron-microscopy. Therefore, the virion is called Dane particle in his honor⁴. It measures 42 nm in diameter and can therefore be distinguished from spherical and filamentous SVP, which have a diameter of only 22 nm⁴. Infectious virions consist of a nucleocapsid containing the rcDNA form of the viral genome and a surrounding envelope.

The capsid is generated by self-assembly of the capsid protein homo-dimers¹⁰². Two different symmetries are observable, either T=3 with 90 dimers, or T=4 with 120 dimers^{103,104}.

1.7.2 Subviral particles

Besides infectious Dane particles, infected or transfected cells secrete high amounts of non-infectious, spherical or tubular shaped SVP. In comparison to virions, SVPs are present in up to 10⁴ times higher numbers in plasma¹⁷⁰⁻¹⁷³. The function of this excessive amount of SVP is not completely understood, however, it seems to influence the immune system of the host. In order to favor a longterm persistent HBV infection¹⁷⁴⁻¹⁷⁸.

Spherical SVP have a diameter of 20 nm and consist mainly of S protein, low amounts of M, and very little L protein. Filamentous SVP also have a diameter of ~ 20 nm but differ in length. They also contain less L protein than virions^{137,172}. S alone or S and M combined are sufficient to form SVP, L alone cannot form SVP. L is even inhibitory to SVP secretion^{179,180}. Spherical SVP are made up by roughly 100 S proteins and around 25 % (w/w) lipids. SVP from patient serum contain mainly phosphatidylcholines, cholesteryl ester, and cholesterol (60 % / 15 % / 15 %) ¹⁷⁰. There is evidence that the lipids are not arranged in a lipid bilayer, but more probably a monolayer^{137,170}.

Dane particles are secreted via the endosomal-sorting-complex-required-for-transport (ESCRT) pathway. SVP, however, seem to be secreted through another pathway¹⁸¹⁻¹⁸³. Currently two theories how SVP are secreted are discussed. Both have in common that S proteins form dimers in the ER, with the help of PDI¹⁵². On the one hand side, Huovila et al. suggested that inside the ER-Golgi intermediate compartment (ERGIC) higher oligomers are formed. On the other hand side, others suggested that the dimers are already linked to filamentous structures in the perinuclear space of the ER and are transported to the ERGIC via vesicles. With the use of cellular chaperons spherical SVP are constricted from the long filaments in the ERGIC and transported to the Golgi^{67,145,184-186}.

1.8 Life cycle

The initial attachment of HBV to hepatocytes occurs through low-specificity interactions with heparin sulphate proteoglycans (HSPG) on the cell surface¹⁸⁷⁻¹⁸⁹. This process presumably leads to a conformational change of the surface proteins, which then can bind to the sodium taurocholate co-transporting polypeptides (NTCP) receptor^{80,190}. The domain responsible for the entry process is the myristoylated part of the preS1-domain, the N terminus from aa 1 to aa 75 of the preS1-domain and TM1 of the S-domain¹⁹¹⁻¹⁹⁷.

After entering the cell the envelope detaches from the capsid, by an until now unknown mechanism, and the capsid is transported to the nuclear pore complex^{41,198,199}. There, the rcDNA is released and enters the nucleus²⁰⁰. The rcDNA from intact capsids is repaired by cellular proteins to form the cccDNA^{41,83}.

The conversion step from rcDNA to cccDNA must change distinct features of the rcDNA, i.e. complete the (+) strand, recombine a longer than unit length (-) strand, and remove the linked protein and oligonucleotides^{93,114,201,202}. The establishment of the cccDNA minichromosome in the nucleus is not fully understood, however, participation of viral and cellular host proteins is described. For example the influence of the host DNA repair enzymes.^{83,203-205}. In one nucleus between 30- 50 cccDNA copies can be present^{203,206,207}, also an integration into the host genome has been observed. This is not essential for replication, but seems to influence the progression of HCC²⁰⁸⁻²¹⁰.

Four viral RNAs (0.7 kb, 2.1 kb, 2.4 kb and the pgRNA) are transcribed from the cccDNA via the host RNA polymerase II^{123,204}. The newly synthesized RNAs are not spliced, transported into the cytoplasm and translated into the seven viral proteins by the cellular ribosomes. The envelope proteins S, M, L and the viral protein e are synthesized at the ER membrane²¹¹.

The pgRNA is special as it does not only code for the core protein and the viral polymerase. It contains a 120 nucleotide (nt) redundancy and therefore the whole genome. This redundancy contains the encapsidation signal ε , a poly-A-tail and a second copy of DR1²¹³. After packaging into capsids it serves as template for the reverse transcription.

The conversion from pgRNA to rcDNA is a multistep mechanism. In brief; the viral polymerase binds to the 5' copy of ε on the pgRNA, this recruits core proteins to the RNA and causes autoassembly of the capsid^{89,94,214,215}. A conserved tyrosine residue in the TP domain of the polymerase serves as a primer for the initiation of reverse transcription. In the next step a short sequence in ε is reverse transcribed by the polymerase for the generation of a (-) DNA oligonucleotide^{89,216}. With this short DNA molecule the polymerase is recruited to DR1 at the 3' end of the pgRNA and starts there the complete synthesis of the (-) strand²¹⁷. At the same time the RNaseH domain of the polymerase degrades the pgRNA, leaving the DR domain at the 5' end not degraded¹¹³. This short RNA serves as a primer for the (+) strand after the

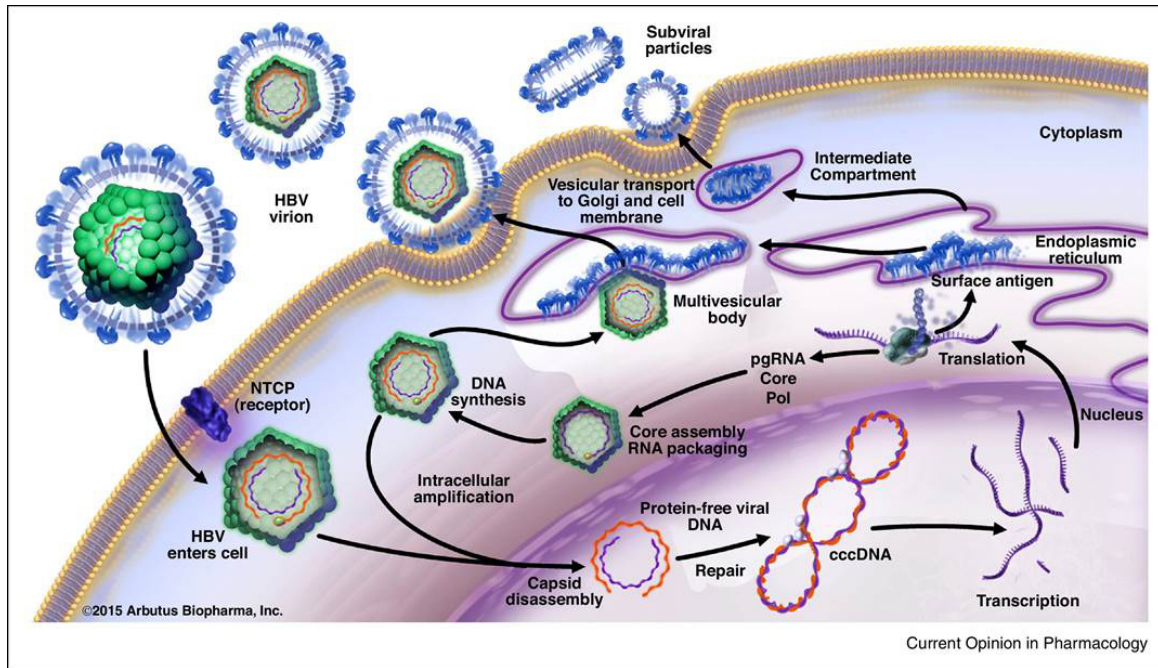


Figure 1.6: **Life cycle of HBV**²¹² Entry of the virus through NTCP receptor and disassembly of the capsid in the cytoplasm. Afterwards the rcDNA is repaired inside the nucleus to form the persistent cccDNA. From this minichromosome all RNAs are transcribed. Translation of the proteins occurs in the cytoplasm and surface antigens are inserted into the ER and secreted as subviral particles into the medium. Another pathway is the formation of infectious particles. There, the core protein is translated and pgRNA is packed inside the capsid. The capsid is then enveloped with surface antigens via budding into multivesicular bodies. In the end the virion is secreted. (Reprinted with permission)

translocation of the polymerase to DR2 on the DNA (-) strand^{95,218}.

It is suspected that during this process a conformational change in the capsid occurs, as only rcDNA containing nucleocapsids are incorporated into virions^{115,219}. Mature nucleocapsids can either be transported back into the nucleus to maintain persistence, or they can be enveloped and released from the cell^{25,220}.

Virions are secreted through the cellular ESCRT pathway, where they are enveloped, bud into multivesicular-bodies (MVB) and are then released from the cell^{67,184,221-225}. Besides also SVP are secreted from cells. These 22 nm particles are lacking internal capsids^{142,184}. They are exported through the ER and Golgi network^{67,152,224,226}.

1.9 The endoplasmic reticulum and disulfide bond formation

Disulfide bond formation is one of the post-translational modifications taking place during protein folding²²⁷. They are an essential step in folding and assembly of the extracellular domains of many membrane and secreted proteins²²⁸. They are not only necessary for correct folding, but also for stability and function^{227,229}. The only amino acid which can form disulfides is cysteine, as it carries an -SH group in its side chain²³⁰.

In eucaryotic cells disulfide bonds are formed in the lumen of the ER²²⁷. This is the largest organelle in the cell and participates in protein synthesis and transport, protein folding, lipid and steroid synthesis, carbohydrate metabolism and calcium storage²³¹⁻²³⁷. The initiation of translation takes place in the cytosol and the ribosome with mRNA is afterwards recruited to the membrane of the ER^{238,239}. The N terminus of the nascent polypeptide chain carries a signal sequence, which is recognized and bound by the signal recognition particle (SRP). The SRP binds to SRP receptors and the polypeptide is then co-translationally inserted into the ER through the translocon, a channel protein^{232,240-242}.

In the ER lumen there is an oxidation and a reduction pathway, so that native disulfide bonds can be formed, but also nonnative disulfides can be broken²⁴³. The most abundant oxidoreductases in the ER belong to the PDI family²⁴⁴. PDI has a broad substrate specificity and, depending on the conditions, can form, reduce or isomerize disulfides^{244,245}. The formation of disulfide in the disulfide exchange protein PDI is catalyzed by ER oxidase 1 (Ero1p)^{243,246,247}. In lower eucaryotes, like yeast Ero1p is sufficient, in mammalian cells two isoforms are present, Ero1 α and Ero1 β , which do not differ in function but in tissue distribution^{248,249}. Nonetheless, the electron flow in the Ero1p pathway is the same. PDI accepts electrons from the polypeptide chain, which oxidizes the active site cysteines. Ero1p contains two disulfides, one interacting with PDI and one with FAD. The one facing PDI is called shuttle disulfide and accepts the

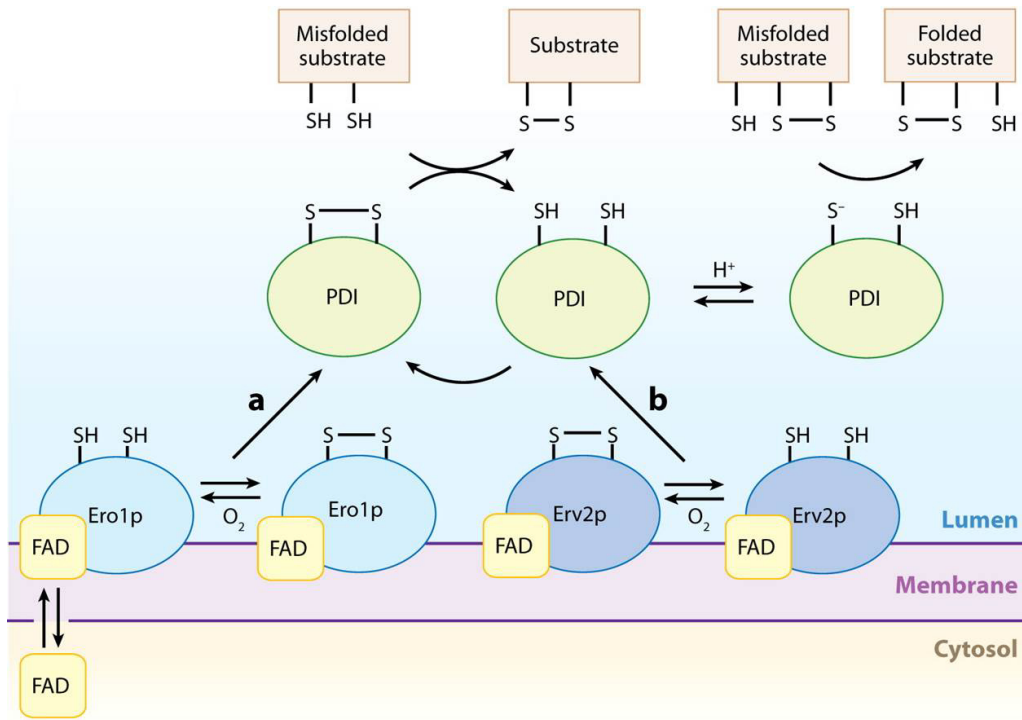


Figure 1.7: **Disulfide bond formation in the lumen of the ER**²²⁷ Formation of disulfide bonds in the ER occur through two different pathways. (a) the membrane associated Ero1p-FAD transfers oxidizing equivalents to PDI. PDI then transfers the oxidizing equivalents to the reduced substrate. In the second pathway (b) the difference is the membrane bound protein Erv2p, which carries the first oxidizing equivalents. Misfolded proteins can be isomerized through PDI. In this picture for simplicity only one active site of Ero1p, Erv2p and PDI is shown. (Reprinted with permission)

electrons from PDI. The second accepts the electrons from the shuttle disulfide and transfers them to FAD, generating FADH₂^{227,243,250}. This reacts with molecular oxygen, forming hydrogen peroxidase and thereby regenerating Ero1²⁴³. Without this pathway in the ER protein folding would be too slow and aggregation and degradation would be favored²³³.

In mammalian cells are at least 15 families of PDI present²⁴⁴. They all contain at least one active site with the CXXC motif. This motif can shuttle between the reduced and the oxidized form, which is dependent on the stability of the disulfide and the ability of an ER oxidase to catalyze its oxidation^{243,244}.

1.10 Aim of the project

The structure of S is relatively unknown, although it is used as the main compound of the HBV vaccine. Influences of disulfide bonds on the overall structure, the epitope and secretion are proposed (cf. chapter 1.6.2, 1.7.2). However, the proposed models are partially contradictory. So first we try to elucidate the form of S proteins generated through disulfide bonds. Here samples from different sources, like cell culture, patient material or material produced in yeast should be compared. A chemical which would only reduce S-S bonds was DTT, so the addition or removal from samples would show the influence on protein-protein linkage. Secreted particles could be analyzed to see if monomers, dimers or oligomers can be found. In a next step the single cysteines can be tested with regard to their influence on disulfides and/or secretion. It was assumed that secretion was the proof of a topology reassembling the wt phenotype close enough to pass the internal quality control system of the cell. As a minimal construct, S with only 4 cysteines in the LL was supposed. And then re-addition of single cysteines could be used to test the influence of single cysteine residues on secretion and disulfide bond formation.

A new method, Mal-PEG labeling, could be introduced to label free or oxidized cysteines in selected constructs. However, this method has neither been used on viral protein nor on secreted samples in cell culture supernatant. In conclusion this method needed to be tested and verified in this context first. When validated it could be used to determine the total number of free and oxidized cysteines in wt S and different constructs.

As a last step the influence of disulfide bonds and free sulfides on the antigenicity of S could be elucidated. Therefore a diagnostic ELISA should test different samples and constructs for their reactivity. With this the influence of different features and their influence on the epitope could be analyzed. Yeast samples should be included in this analysis to compare this material with cell culture samples.

2 Materials

2.1 Eukaryotic cell line

HuH-7

The work was conducted only using the HuH-7 cell line. It was derived from a liver carcinoma of a 57-year-old Japanese male²⁵¹. HuH-7 cells are growing adherent and are not infectable with HBV. Nevertheless, when transfected with the HBV genome, they produce viral proteins and release subviral particles.

2.2 Cell culture media

Component	Company	Stock concentration	Working concentration
DMEM high glucose (4,5 g/ml)	Sigma		
Fetal bovine serum (FBS)	Bio West	100 %	10 %
MEM Non essential amino acids	Lonza	100x	1x
Penicillin-Streptomycin	Lonza	100x	1x
Sodium pyruvate	Lonza	100x	1x
Trypsin/EDTA	Gibco		

2.3 Bacteria

The bacteria strain used was DH5 α with the genotype: supE44, Δ lacU169, (Φ 80dlacZ Δ M15), hsdR17, recA1, endA1, gyrA96, thi-1, relA1

2.4 Bacterial media and antibiotics

Component	Company	Stock concentration	Working concentration
LB-Media	Roth		
LB-Agar	Roth		
Ampicillin	Sigma	100 mg/ml	100 µg/ml
Kanamycin	Sigma	50 mg/ml	50 µg/ml

2.5 Plasmids

All plasmids used in this work are described in the following table. They were generated either directly in the corresponding backbone via QuickChange PCR, or generated and then cloned into the plasmid via the *XbaI*, *SpeI* or *EcoRV* restriction sites. The positions in the plasmid are indicated in Figure 2.1

Plasmid	Description
pSVBX24H ²⁵²	codes for the small envelope protein S
pSVBX24H-HA ²⁵³	codes for the small envelope protein S with a C-terminal HA-tag
pSVBX24H-HA derivatives	all constructs were cloned on the basis of pSVBX24H-HA. The corresponding mutations or deletions are described in the results part
pSVBX24H-YFP/BFP	codes for the small envelope protein S with N-terminal YFP or BFP
pSVBX24H-YFP/BFP derivatives	all constructs were cloned on the basis of pSVBX24H-YFP/BFP. The corresponding mutations or deletions are described in the results part
pCFP-GalT ²⁵⁴	codes for CFP-galactosyltransferase
pmTagBFP-eYFP ²⁵⁴	codes for the YFP+BFP fusion protein

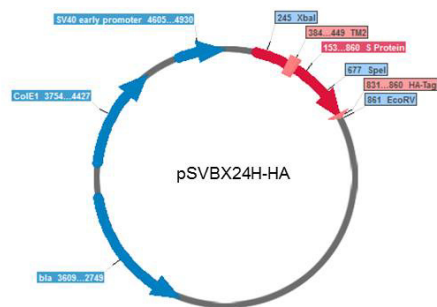


Figure 2.1: **Plasmid map of pSVBX24H-HA**. The main features are indicated on the 4930 nt long plasmid. The positions of the SV40 promoter, the ColE1 and the bla resistance are shown in darker blue. The S protein insert is indicated in red. Relative to S, the HA-tag and the TM2 are indicated in lighter red. The cutting sites used are shown in lighter blue. Picture designed with SerialCloner

2.6 Primers

All primers used for QuickChange are listed below. The mismatches introduced are marked in bold letters only in the forward (fw), not in the reverse (rev) primer.

Primer	Sequence 5'→3'	Description
C65S fw	ctcaccaacctct ct ctctccaatttgcc	Exchange of C65 to serine in S
C65S rev	ggacaaattggaggagaggaggttggtgag	Exchange of C65 to serine in S
C90S fw	catcctgctgctat cc ctcatcttcttattgg	Exchange of C90 to serine in S
C90S rev	ccaataagaagatgaggg g atagcagcaggatg	Exchange of C90 to serine in S
C221S fw	ag tctctgggtatacatttaaacc	Exchange of C221 to serine in S
C221S rev	aaagaaaattggtaacagcgg	Exchange of C221 to serine in S
S107C fw	ggtatggtgcccgttt g tctcttaattccagg	Re-exchange of S107 to Cys in S
S107C rev	cctggaattagaggacaaacgggcaacatacc	Re-exchange of S107 to Cys in S

Primer	Sequence 5'→3'	Description
S121C fw	ggaccat g caaaacctccacgactcc	Re-exchange of S121 to Cys in S
S121C rev	ggagtcgtggagggtttgcatggtcc	Re-exchange of S121 to Cys in S
S124C fw	ccaaaacct g cacgactcctgctcaagg	Re-exchange of S124 to Cys in S
S124C rev	ccttgagcaggagtcgtgcagggtttgg	Re-exchange of S124 to Cys in S
S137C fw	gttccctcatctt g ctctacaaaacctacggatgg	Re-exchange of S137 to Cys in S
S137C rev	ccatccgtaggtttgtagagcaagatgagggaaac	Re-exchange of S137 to Cys in S
S138C fw	gttccctcatctt g tacaaaacctacggatgg	Re-exchange of S138 to Cys in S
S138C rev	ccatccgtaggtttgtagagcaagatgagggaaac	Re-exchange of S138 to Cys in S
S139C fw	gttccctcatctt g tacaaaacctacggatgg	Re-exchange of S139 to Cys in S
S139C rev	ccatccgtaggtttgtacaggaagatgagggaaac	Re-exchange of S139 to Cys in S
S147C fw	gttccctcatctt g tacaaaacctacggatgg	Re-exchange of S147 to Cys in S
S147C rev	ccatccgtaggtttgtacaggaagatgagggaaac	Re-exchange of S147 to Cys in S
S147C fw	cggatggaaattccacct g tattccttcc	Re-exchange of S149 to Cys in S
S147C rev	ggatgggaatacaggtggaatttccatccg	Re-exchange of S149 to Cys in S
N146Q c fw	gctgtacaaaacctacggatggac ag tgcacctgtattccc atccc	Exchange of Asp to Glu
N146Q c rev	gggatgggaatacaggtgcactgtccatccgtaggtttgt acagc	Exchange of Asp to Glu in wt background
N146Q s fw	ccctacaaaacctacggatggac ag tccacctctattccc atccc	Exchange of Asp to Glu in Ser background
N146Q s rev	gggatgggaatagaggtggactgtccatccgtaggtttgt agagg	Exchange of Asp to Glu in Ser background

Primer	Sequence 5'→3'	Description
C69S fw	cctgtcctccaattttctcctggttate	Exchange of C69 to serine in S
C69S rev	cgataaccaggagaaaattggaggacagg	Exchange of C69 to serine in S
C65S (S69) fw	cctctcctccaattttctcctggttatecg	Exchange of C65 to serine in S if S69 mutation present
C65S (S69) rev	cgataaccaggagaaaattggaggagagg	Exchange of C65 to serine in S if S69 mutation present
C76S fwd	ggttatcgctggatgtctctgcg	Exchange of C76 to serine in S
C76S rev	cgcagagacatccagcgataacc	Exchange of C76 to serine in S
C48S fw	gggatctcccgtgtctcttgccaaaattcgcagtc	Exchange of C48 to serine in S
C48S rev	ggggactgcaatcttgccaaagagacacgggagatccc	Exchange of C48 to serine in S
S149C (C147) fw	cggatggaaattgcacctgtattcccatcc	Exchange of C149 to serine in S if C147 present
S149C (C147) rev	ggatgggaatacaggtgcaatttccatccg	Exchange of C149 to serine in S if C147 present
C107S fw	ggtatgttcccgtttctcctctaattccagg	Exchange of C107 to serine in S
C107S rev	cctggaattagaggagaaaacgggcaacatacc	Exchange of C107 to serine in S
C147S fw	cctacggatggaaattccacctctattccatc	Exchange of C147 to serine in S
C147S rev	gatgggaatagaggtggaatttccatccgtagg	Exchange of C147 to serine in S
C149S (S147) fw	cggatggaaattccacctctattcccatcc	Exchange of C149 to serine in S if S147 present
C149S (S147) rev	ggatgggaatagaggtggaatttccatccg	Exchange of C149 to serine in S if S147 present
C121S (S124) fwd	cgggaccatttextbfccaaaacctgcacgac	Exchange of C121 to serine in S if S121 present

Primer	Sequence 5'→3'	Description
C121S (S124) rev	gtcgtgcagggttttggatgggtcccg	Exchange of C121 to serine in S if S121 present
C137/ 138/ 139S fw	ctatgtttccctcatcttctctacaaaacctacggatg	Exchange of C147, C148 and C149 to serine
C137/ 138/ 139S rev	catccgtaggtttttagaggaagatgagggaaacatag	Exchange of C147, C148 and C149 to serine

2.7 Enzymes

Enzyme	Company	Buffer
T4 DNA Ligase	Thermo Scientific	T4 DNA Ligase Buffer
RNase I	Quiagen	-
Pfu Ultra HF	Agilent	Pfu ultra Buffer
T4 PNK	Thermo Scientific	T4 DNA Buffer
CIP	Thermo Scientific	-

Restriction Enzyme	Company	Buffer
EcoRV-HF	NEB	CutSmart
DpnI	NEB	-
SpeI-HF	NEB	CutSmart
XbaI	NEB	CutSmart
EcoRV	NEB	CutSmart

2.8 Antibodies

Primary Antibody	Company	Dilution
Anti-beta-Tubulin (rabbit)	NEB	WB 1:4000
Anti-GFP (rabbit)	NEB	WB 1:2000
Anti-HA (rabbit)	Sigma-Aldrich	WB 1:1000
Anti-S (HB1)(mouse)(IgG, S epitope AS 120-124)	Dieter Glebe (Gießen)	WB 1:2000
Anti-PDI (rabbit)	NEB	IF 1:100
Secondary Antibody	Company	Dilution
Goat-anti-mouse PO	Dianova	1:10000
Goat-anti-rabbit PO	Dianova	1:10000
Goat-anti-rabbit Alexa 633	Life Techn.	IF 1:2000

2.9 Kits

Kit	Company
NucleoSpin Gel and PCR Clean-Up	Macherey-Nagel
NucleoBond Xtra Midi I	Macherey-Nagel
NucleoSpin Plasmid	Macherey-Nagel
NucleoSpin Virus	Macherey-Nagel

2.10 Chemicals

Chemical	Company
Acrylamid Mix Rotiphorese Gel 30	Carl Roth
Agarose	Carl Roth
APS	Sigma-Aldrich
Bromphenol Blue	Sigma-Aldrich
BSA	Sigma-Aldrich
CaCl ₂	Carl Roth
Coomassie Brilliant Blue G-250	Bio-Rad
Dimethylsulfoxid (DMSO)	Sigma-Aldrich
Donkey sera	Sigma-Aldrich
DTT	Sigma-Aldrich
EDTA	Sigma-Aldrich

Chemical	Company
Ethanol	Carl Roth
Ethidium bromide	Carl Roth
Fugene HD	Promega
Glacial acetic acid	Merk
Glucose	Merk
Glycerin	Applichem
Glycine	Merk
Glycogen	Fermentas
H ₂ O ₂ (30 %)	Sigma-Aldrich
Isopropanol	Carl Roth
KCl	Carl Roth
KH ₂ PO ₄	Carl Roth
KOAc	Sigma-Aldrich
Luminol	Sigma-Aldrich
Mal-PEG2000	Sigma-Aldrich
Mal-PEG5000	Sigma-Aldrich
Methanol	Sigma-Aldrich
MnCl ₂	Carl Roth
MOPS	Carl Roth
Na ₂ HPO ₄	Carl Roth
NaCl	Carl Roth
NaOH	Merk
NEM	Sigma-Aldrich
Nonident P40	Fluka
p-Cumaric Acid	Sigma-Aldrich
PFA	Sigma-Aldrich
RbCl	Carl Roth
SDS	Sigma-Aldrich
skim milk powder	Carl Roth
Sucrose	Sigma-Aldrich
TEMED	Sigma-Aldrich
Tris base	Carl Roth
Tris-HCl	Carl Roth
Triton X-100	Applichem
Tween 20	Sigma-Aldrich

2.11 Solutions and buffers

Buffer	Composition
Antibody Dilution Buffer (IF)	1 x PBS 1 % BSA (w/v) 0.3 % Triton X-100
Blocking buffer (WB)	1 x PBS 10 % skim milk powder (w/v) 0.1 % Tween 20
Blocking buffer (IF)	1 x PBS 5 % goat serum (v/v) 0.3 % Triton X-100
Buffer I (Miniprep)	50 mM Glucose 25 mM Tris-HCl pH 8.0 10 mM EDTA
Buffer II (Miniprep)	0.2 M NaOH 1 % SDS (w/v)
Buffer III (Miniprep)	3 M K ⁺ 5 M Acetate-
Coomassie Staining solution	0.1 % Coomassie Brilliant Blue G-250 50 % Methanol 10 % Glacial acetic acid
Coomassie Destaining Solution	40 % Methanol 10 % Glacial acetic acid
Developing Solution A	1.41 mM Luminol 1 M Tris-HCl pH 8.6
Developing Solution B	7.61 mM p-Cumaric Acid in DMSO
FACS buffer	1 % FCS in PBS (w/v)
Lysis buffer	50 mM Tris-HCl pH 7.5 100 mM NaCl 20 mM EDTA

Buffer	Composition
	0.5 % (v/v) Nonident P40
PBS	1.4 mM NaCl 0.5 mM KCl 1 mM Na ₂ HPO ₄ 2.2 mM KH ₂ PO ₄ pH 7.4
PBS-T	1 x PBS pH 7.4 0.1 % Tween 20
5x SDS-PAGE loading buffer	250 mM Tris base 10 % SDS (w/v) 7.5 % Glycerol Bromphenol blue 25 % DTT (optional)
1x TBS	0.05 M Tris-HCl pH 7.5 0.15 M NaCl
TE	10 mM Tris-HCl pH 8.0 1 mM EDTA
TGS	25 mM Tris base 0.1 % SDS (w/v) 250 mM Glycine
TFB1	15 % Glycerine 10 mM CaCl ₂ 30mM KOAc 100 mM RbCl ₂ 50 mM MnCl ₂ Ad 500 ml sterile water, pH=5.8
TFB2	15 % Glycerine 75 mM CaCl ₂ 10mM MOPS 10 mM RbCl ₂ Ad 250 ml sterile water
TNE	50 mM Tris-HCl (pH 7.4) 100 mM NaCl

Buffer	Composition
	0.1 mM EDTA
Towbin	25 mM Tris base 0.1 % SDS (w/v) 192 mM Glycine 20 % Methanol (v/v)

2.12 Laboratory devices

Equipment	Company
Balance AC 100	Mettler
Centrifuge, ZK Biofuge Pico	Heraeus/ ThermoFisher Scientific
Centrifuge, ZK Labofuge 400 Function Line	Heraeus/ ThermoFisher Scientific
CO ₂ Incuator for cells, Hera Cell 150i	Heraeus/ ThermoFisher Scientific
Dounce tissue grinder set	Sigma-Aldrich
FACS Canto II	BD Bio Sciences
Freezer -20 °C	Liebherr
Freezer -80 °C, Hera Freeze	Heraeus/ ThermoFisher Scientific
Fridge 4 °C	Liebherr
Fusion FX7	Vilber Lourmat
Geldocumentation Apperature	BioRad
Hot water bath	Köttermann
Hybridization bottle	Biometra/ Analytic Jena
Hybridization oven, Compact Line OV4	Biometra/ Analytic Jena
Incubator for bacteria	Memmert
Magnetic Stirrer, Variomag Monotherm	Neolab
Micro scales, AC100	Mettler
Microscope, Ti Eclipse Spinning-Disc	Nikon
Microwave oven, Privileg 9029GD	Privileg
Mini-centrifuge, SproutR	Heathrow Scientific LLC
Nanodrop ND 2000c	Peqlab
PCR Machine, Mastercycler	Eppendorf
pH-meter, inoLab WTW series	WTW
Pipette	Eppendorf
Pipette	Gilson

Equipment	Company
Pipetting Aid, Accu JetR Pro	Brand
Refrigerated Centrifuge; Heraeus Fresco 17	Heraeus/ ThermoFisher Scientific
Scale, EG2200-2NM	Kern und Sohn
SDS-PAGE Minigel	Biometra/ Analytik Jena
SDS-PAGE Multigel	Biometra/ Analytik Jena
SDS-PAGE Multigel Long	Biometra/ Analytik Jena
Shaking Incubator	Infors AG
Sterile Bench, Lamina Air HLB2448 GS	Heraeus
Suction System, Vacusafe	Integra Biosciences AG
Thermomixer Comfort	Eppendorf
Thermomixer Compact	Eppendorf
Ultra Centrifuge, LC60	Beckmann
UV table 312 nm	Bachhofer
Voltage generator, Agarose Power Pack 300	Biorad
Voltage generator, SDS standard power pack P25	Biometra/ Analytic Jena
Vortex, MS3 Basic	IKA Schütt

2.13 Laboratory consumables

Consumable	Company
1.5 and 2.0 tubes	Sarstedt
15 ml and 50 ml tubes	Eppendorf or Sarstedt
Cell culture bottles	Sarstedt
Cell culture dishes and plates	Sarstedt
Cover slip	Menzel-Gläser
Cryo-vials	Sarstedt
Needle, Sterican	Braun
Nitrocellulose Membrane, Amersham Protran 0.45 NC	GE Lifesciences
Object plate	Carl Roth
PCR tubes	Kisker
Petridish	Sarstedt
Pipett tips	Sarstedt

Consumable	Company
Serological pipette (5 ml, 10 ml, 25 ml, 50 ml)	Sarstedt
Syringe	Becton Dickinson
Syringe filter unit, MillexGP 0.22 μm	Millipore/ Merck
Ultracentrifuge tubes	Beckmann
Whatman paper	Whatman GmbH
Zeba Spin Desalting Columns	ThermoFisher Scientific

2.14 Software

Software	Company	Usage
GraphPad Prism 5.01	GraphPad Software	Statistical analysis and diagrams
LATEX	LATEX Project, Opensource	Writing of the thesis
SerialCloner 2.5	Serial Basic	Cloning and maps of plasmids
Volocity 6.2.1	PerkinElmer	IF pictures
Office 2010	Microsoft	Diagrams and presentations

3 Methods

3.1 Molecular and microbiological methods

3.1.1 Insertion of mutations using the QuickChange method

Site directed mutagenesis with the QuickChangeTM method was used to substitute amino acids in plasmids. This method was developed by Stratagene (La Jolla, CA). It is able to introduce a mutation into the gene of interest in a single polymerase chain reaction (PCR). It would also be possible to delete or insert base pairs into the plasmid of choice.

The mechanism is based on amplifying the whole plasmid in a thermocycling reaction (cf. Table 3.1). Complementary primers carrying the mismatch are integrated in the newly synthesized DNA, generating a nicked plasmid. This nicked DNA cannot be used as a template for further amplification rounds, thus no exponential rate is reached, only a linear multiplication. The resulting DNA, a mix of original plasmid and newly synthesized nicked plasmid, is treated with 1 μ l of *DpnI*. This restriction enzyme cuts the parental methylated plasmid, leaving only the mutated plasmid intact. During transformation of *E. coli* the host machinery repairs the nick and the plasmid can be purified through mini- or midipreparation of the bacterial culture^{255,256}. Here we used 5 μ l of the digested PCR product with 50 μ l of bacteria for transformation.

Table 3.1: QuickChange scheme

Component	Amount
Primer [125 ng/ μ l]	1 μ l
DNA [25 ng/ μ l]	1 μ l
Pfu ultra	1 μ l
Buffer	5 μ l
dNTPs [10 mM]	2 μ l
Ad H ₂ O	50 μ l

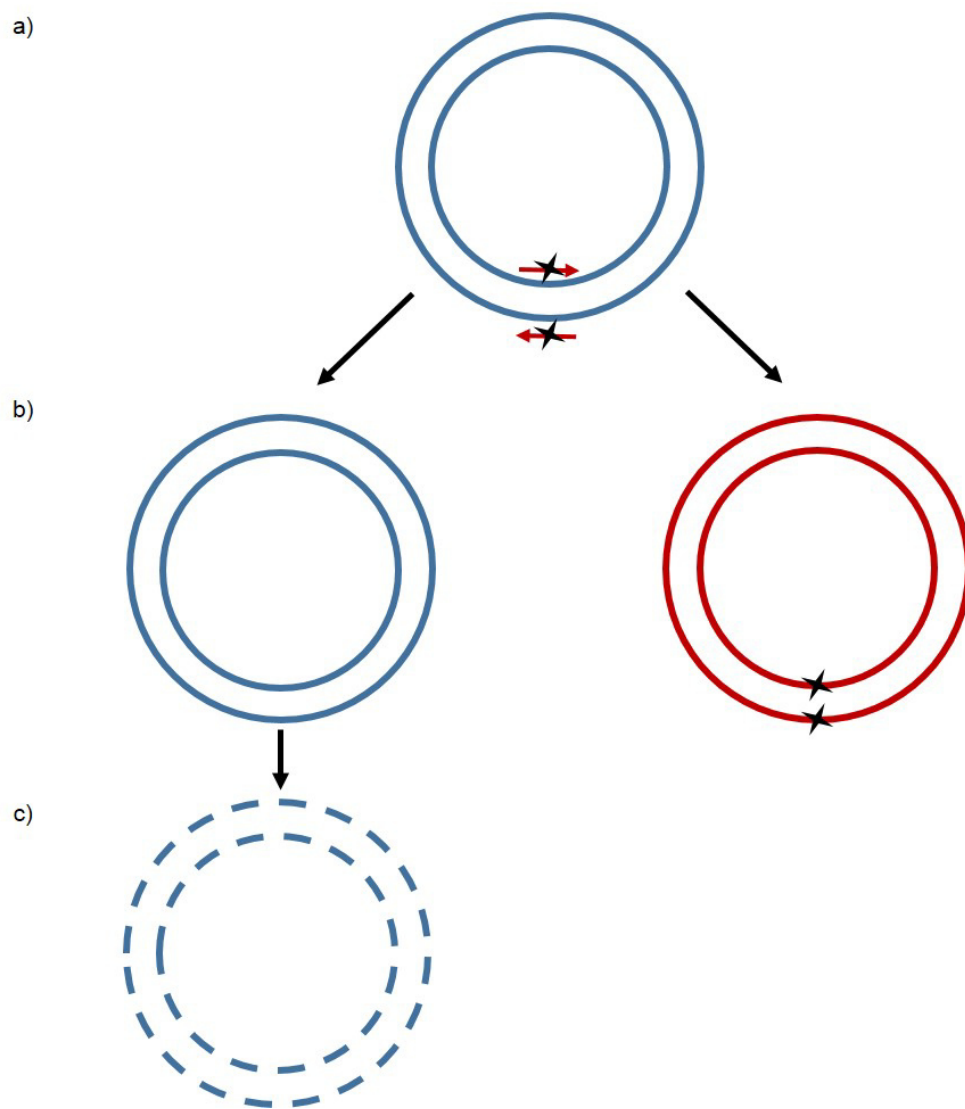


Figure 3.1: **QuickChange Site Directed Mutagenesis** a) Shows original plasmid (blue) and the two complementary primers, carrying the mutation (red arrows with black asterisk). b) New nicked DNA with the mutation is synthesized (dark red with black asterisk) and the original plasmid is still in the mix (blue plasmid). c) In a last step the methylated template DNA is digested with *DpnI* (dashed blue lines), leaving only the nicked plasmid from b) for transformation into *E.coli*.

Table 3.2: QuickChange Cyclor program

Step	Temperature	Time	Repetition
Initialization step	98 °C	2 min	
Denaturation step	95 °C	1 min	
Annealing step	50 °C	40 sec	x16
Extension/elongation step	68 °C	6 min	
Final elongation	68 °C	10 min	

3.1.2 Agarosegel electrophoresis

DNA is negatively charged and can therefore be separated according to its size in an electric field. 1 % Agarosegels with ethidiumbromide were used and the DNA was visualized with UV light. As a standard, the GeneRuler prestained Plus was used to determine the size of the DNA fragment. Small sized gels were run at 100 V for 1 hour (h), larger gels at 140 V up to 2 hours.

3.1.3 Restriction enzyme digestion

Restriction enzymes cut DNA at specific sites. To clone a fragment 1 µg of DNA was used, for a control digest 2 µl of a miniprep were used. The enzymes were used in the recommended buffers and according to manufacturer's instructions.

To avoid religation of the plasmids after cutting, the vector was dephosphorized with calf intestine phosphatase (CiP). The phosphatase removes phosphate residues at the 5' end of the vector. In Table 3.3 a restriction preparation can be seen.

Table 3.3: Restriction digestion

Component	Amount
Restrictionenzyme 1-10 U/µl	1 µl
Buffer	3 µl
DNA	1 µg
CiP	1 µl
Ad H ₂ O	30 µl

3.1.4 Purification of DNA

After restriction digest the fragments were resolved in an agarosegel. The fragments needed were cut and transferred into an Eppendorf tube. The extraction was performed using the PCR-Cleanup-Gel-Extraction-Kit from Macherey-Nagel. The vectors were eluated in 30 μ l, inserts in 20 μ l.

3.1.5 Ligation

For ligation of two fragments after restriction digest T4 Ligase was used. Therefore 5 μ l of the insert and 1 μ l of vector were used. An exemplified ligation pipetting scheme can be seen in Table 3.4. It was incubated either at 22 °C for 2 h or at 16 °C over night.

Table 3.4: Ligation scheme

Component	Amount
Plasmid	1 μ l
10x Ligation buffer	2 μ l
Insert	5 μ l
T4 DNA Ligase 5U/ μ l	1 μ l
Ad H ₂ O	20 μ l

3.1.6 Preparation of chemical competent cells

10 ml of LB-Media were inoculated with *DH5 α* over night. On the next day a 200 ml culture was inoculated (1:100) until the OD₆₀₀ reached 0.3- 0.5 (optimum 0.43). Then it was cooled for 15 min on ice. Afterwards the culture was centrifuged at 3000 rpm for 5 min at 4 °C. The pellet was resuspended in 15 ml TFB1 and again centrifuged for 5 min at 3000 rpm and 4 °C. As a last step the pellet was resuspended in 1 ml TFB2, split into aliquots, frozen in liquid nitrogen and stored at -80 °C until further use.

3.1.7 Transformation of competent *E. coli*

The cells were thawed on ice. Then 50 μ l of chemical competent cells were mixed with 0.5 μ g - 1.0 μ g of plasmid, incubated for 30 min on ice and shocked for 30 sec at 42 °C. Afterwards 1 ml of LB-Media was added the mixture incubated for 1 h at 37 °C on a shaking incubator. In a last step the bacteria could be plated on LB-Agar plates with either ampicillin or kanamycin.

3.1.8 Plasmid preparation

Miniprep

For the preparation of DNA on a small scale either 3 ml LB media (incubation for 7 h) or 5 ml (overnight) were inoculated with a single colony of *E. coli*. Then 1.5 ml of the bacteria were pelleted by centrifugation for 5 min at 13,300 rpm. The supernatant was removed and the pellet was resuspended in 100 μ l of buffer I. In the next step the cells were lysed adding 200 μ l buffer II. To neutralize buffer II, 150 μ l buffer III was added and it was incubated for 3 min on ice. After another centrifugation step, the supernatant was mixed with 900 μ l EtOH absolute. In this step the DNA precipitates and can be pelleted by centrifugation at 13,300 rpm for 10 min. After air drying it was resuspended in TE buffer and the concentration was measured.

Midiprep

The Macherey-Nagel NucleoBond Xtra Midi Kit was used. One day prior to the preparation 100 ml LB media with antibiotic was inoculated with a single colony. The next morning the DNA was purified according to the manufacturer's instructions. In the end the DNA was resuspended in 300 μ l of TE buffer.

3.1.9 Sequencing

For sequencing 30- 100 ng/ μ l of the plasmid and 10 pmol/ μ g of the primer were sent to GATC Biotech. The next morning the results were available online. Alignments were performed using Nucleotide BLAST of the National Center for Biotechnology Information (NCBI) (<http://blast.ncbi.nlm.nih.gov/BlastAlign.cgi>).

3.2 Cell culture techniques

3.2.1 Cultivation of Huh7

Under optimal conditions (37 °C , 5 % CO₂) Huh7 cells have a doubling time of 24 h. The cells were grown to a confluent monolayer and then split, to prevent overgrowing. First the cells were washed twice with PBS and 5 ml Trypsin/EDTA (T175 flask) was added. After incubation for 5 min at 37 °C and 5 % CO₂ the process was stopped by adding 25 mL DMEM++++. Then the cells were split with a ratio of either 1:5 or 1:10 and filled to a total volume of 25 ml. When cells were seeded for further experiments the ratio was 1:200 for 12 well (total 1 ml), 1:50 for 6 well (total 2 ml) and 1:25 for a 10 cm dish (total 10 ml).

3.2.2 Freezing of cells

To freeze cells the flasks were grown to confluence and trypsinized. Afterwards the trypsin was removed by centrifugation for 5 min at 3000 rpm and the cells were resuspended in 900 μ l FCS and 100 μ l DMSO. DMSO serves as a freeze protection. In the beginning the cells were stored at -80 °C in a freezer and subsequently transferred to liquid nitrogen.

3.2.3 Thawing of cells

To thaw the cells they were removed from the liquid nitrogen and shaken in a 37 °C water bath. When completely thawed the cells were transferred to 15 ml Falcon and 10 ml DMEM++++ was added drop wise. To sediment the cells they were spun down at 1000 rpm for 5 min at 4 °C. Subsequently the supernatant was removed, new media was added and the cells were divided into two T75 flasks.

3.2.4 Transfection of cells

To insert plasmid DNA into cells, they were transfected using Fugene HD transfection reagent from Promega. The reagent forms complexes with the plasmid and therefore shuttles the plasmid into the cells. The cells were seeded one day prior to transfection. Depending on the experiment a 12 well format, 6 well format or 10 cm dishes were used. For the transfection a mix of 100 μ l DMEM, DNA and Fugene was prepared, mixed and incubated at room temperature (RT) for 30 min. The amounts in the different scale can be seen in Table 3.5. Meanwhile the cells were washed twice with PBS and then fresh DMEM was added. The transfection mix was carefully pipetted to the cells and it was incubated for 6 h at 37 °C. Then the cells were again washed twice with PBS and medium was changed to DMEM++++. After three days cells and supernatant were harvested.

Table 3.5: Transfection scheme

Component	12 well	6 well	10 cm dish
Number of cells	1.5×10^5	3×10^5	3×10^6
DNA	0.5 μ g	1 μ g	5 μ g
Fugene HD	2.5 μ l	5 μ l	7.5 μ l
DMEM	100 μ l	200 μ l	400 μ l

3.2.5 Preparation of supernatant and lysate

The supernatant (SN) of the cells was harvested 3 days post transfection(dpt). To remove dead cells it was centrifuged for 10 min at 13,000 rpm. The SN was transferred into new tubes and either directly used or stored at -20 °C.

To collect the lysate the cells were washed once with PBS and 200 µl (1.5 ml) lysis buffer was added to the 6 well plates (10 cm dishes). After incubation on ice for 10 min the lysate was transferred to a reaction tube and the cell debris was spun down at 13,000 rpm for 10 min. The desired proteins were then in the clear supernatant. It was either directly used for further experiments or stored at -20 °C.

3.3 Protein biochemical and immunological methods

3.3.1 Concentration of SVP

To concentrate SVP the supernatant was harvested as described in subsection 3.2.5. For the following procedure 4 ml of supernatant was needed. 1 ml of 20 % sucrose (w/v) was transferred to an ultracentrifuge tube. The supernatant was loaded on top of the sucrose cushion. Centrifugation took place for 2 h at 50.000 rpm, 4 °C in a SW55Ti Rotor and a Beckman Ultracentrifuge. In the next step the liquid was discarded and 100 µl of PBS were used to resuspend the pellet.

3.3.2 Sucrose density centrifugation

The solutions used for the gradient were as followed: 0.5 ml of 60 % sucrose (w/w) and 1 ml of 45 %, 35 %, 25 % and 15 % sucrose (w/w) in TNE buffer. After the gradient was prepared in a centrifuge tube it was stored for 4 h at 4 °C. Then 500 µl of medium were added on top of the gradient and it was centrifuged for 16 h over night (o/n) at 10 °C and 38,000 rpm in an SW55Ti rotor. The next day the gradient was harvested in 15 fractions each containing 330 µl. These fractions were analyzed using SDS-PAGE and Western blot.

3.3.3 Protease protection assay

The protection assay was performed as described earlier¹⁵⁹. In brief, cells were transfected and 3 dpt washed once with TBS. Then they were incubated in 1.2 ml in 0.1x TBS for 10 min on ice. The swollen cells were then scraped of the dish and homogenized by douncing (20 strokes) on ice. After that 130 µl of 10x TBS were added to generate 1x TBS. In a next step the cell debris was removed by centrifugation at 2,500 rpm at 4 °C for 15 min. To pellet the microsomes, the clear solution was layered on top of a 3.7 ml 10 % sucrose (w/w) cushion and centrifuged in a

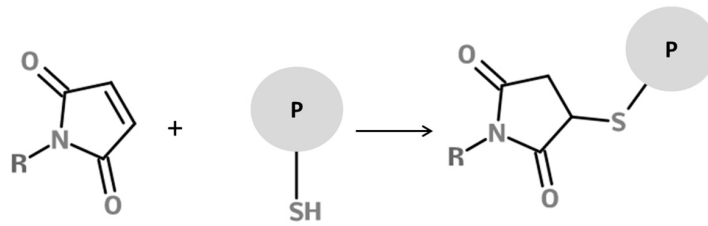


Figure 3.2: **Labeling of free sulfides with Mal-PEG** The maleimide is chemically bound to the SH group of a protein (P) in a Michael reaction. The PEG tail (R) causes a mass-tag detectable in WB or mass spectrometry.

SW55Ti rotor for 45 min at 38,000 rpm and 4 °C. The pellet was washed once in 1 ml TBS and resuspended in 100 µl TBS by passing it through a 24G needle. Subsequently, the microsome preparation was divided into three 33 µl samples. Nothing was added to sample A, to B 6.6 µl of trypsin (5 mg/ml) were added and to sample C 1.8 µl of 10 % NP-40 (v/v) and 6.6 µl of trypsin (5 mg/ml) were added. The three samples were first incubated for 30 min at 37 °C and then cooled for 30 min on ice. To inhibit the enzyme 2 µl of TBS and 3 µl of 5x Lämmli buffer were pre-heated to 95 °C and 10 µl of the samples were added and boiled for another 5 min. The samples were then used for Western blot analysis.

3.3.4 Labeling of thiols

Mal-PEG is a derivate of the maleimide carrying a polyethylene glycol (PEG) mass tag. The maleimide is an acceptor in Michael reaction, meaning it adds nucleophiles. This creates thioethers with thiols at pH ranges of 6.5-7.5.

Free thiols

The labeling of the thiols is performed with freshly collected lysate or supernatant. To 45 µl of the lysate 5.5 µl of 5 M Mal-PEG was added to achieve an end concentration of 0.5 mM. This mixture was incubated for 30 min on ice. Afterwards the reaction was stopped by adding 40 mM DTT and incubation for 10 min on ice. This samples could then be used for Western blotting.

Optionally, SDS at an end concentration of 1 % was added in the beginning and incubated for 10 min at room temperature. This denatured the protein and therefore made the cysteines more accessible.

Oxidized thiols

Besides the free thiols it was also possible to detect cystines in disulfide bonds. To achieve this, the lysate was first treated with 1 % SDS and incubated for 10 min at RT. Afterwards 50 mM NEM was added and incubated for 30 min also at RT. NEM binds, like Mal-PEG to -SH groups, but does not cause a detectable shift. So it was used to shield the free -SH groups from binding Mal-PEG later in the process.

In order to make the S groups in the bonds accessible, 100 mM DTT was added for 30 min at RT. However, DTT can bind to Mal-PEG and therefore hinders binding to the now existing -SH groups. So it was removed via Zeba Micro Spin Desalting Columns. They were used according to manufacturer's instructions. In brief: the storage buffer was removed by spinning it down at 1000 g for 1 min. Then the column was washed three times with the PBS buffer always spinning at 1000 g and applying 50 μ l of buffer. In the last step 12 μ l of sample and 3 μ l of blank buffer were loaded and centrifuged for 2 min at 1000 g.

These 15 μ l of sample were then labeled adding 0.5 mM of Mal-PEG for 30 min on ice. The reaction was stopped by adding 40 mM DTT. For detection these samples were used for Western blotting.

3.3.5 SDS-PAGE

With SDS-gels it is possible to separate proteins according to their molecular mass. Essential for this process is the fact that the proteins carry a charge, so they can be separated in an electric field. This is achieved by adding SDS to the proteins, causing a negative charge.

The samples were mixed with 5x SDS loading dye (if not stated otherwise with 0.125 g DTT in 500 μ l of buffer) to achieve a 1x end concentration. This mixture was heated for 5 min at 98 °C and centrifuged for 1 min at 13,000 rpm and 4 °C. The prepared gel was loaded with 2-20 μ l of the samples. As a standard, 2 μ l of *PageRuler Prestained Plus* was used. The samples were separated 2-4 h using 130- 170 V. The composition of the gel can be seen in table Table 3.6.

3.3.6 Western blot

For detection the proteins were transferred from the SDS-PAGE gel to a nitrocellulose membrane. Therefore, Whatman paper and a nitrocellulose membrane in the size of the gel were required. First all components were soaked in Towbin buffer, and arranged as follows: a fibrepad, two Whatman papers, the gel, the membrane, two Whatman papers and the second fibrepad. The cassette was closed and put into the Wet blotting Chamber from Bio-Rad. Either it was transferred for 90 min at 400 mA or overnight at 200 mA.

After the blotting, the membrane was blocked for 30 min in blocking buffer and was afterwards decorated with the primary antibody over night. Next, the membrane was washed 3 times in

Table 3.6: SDS-gel components for one gel

Component	Stacking Gel (3.9 %)	Running gel (12 %)
H ₂ O	4950 µl	3400 µl
30 % Bis-Acrylamide	6000 µl	850 µl
1.5 M Tris (pH 8.8)	3750 µl	-
1 M Tris(pH 6.8)	-	650 µl
10 % SDS	150 µl	50 µl
10 % APS	150 µl	50 µl
TEMED	6 µl	5 µl

PBS-T and incubated with the secondary antibody coupled with horseradish peroxidase for 1 h. In the last step the membrane was washed again in PBS-T, covered with detection reagent and developed using the Fusion FX7 camera.

3.3.7 Coomassie Blue staining

A second method to detect proteins in a SDS-gel was to stain them with Coomassie. The gel was rinsed for 20 min in the Coomassie solution until it appeared completely stained. Then the gel was destained several hours during which the buffer was replenished several times. In the end the gel was stored in Mili-Q water and documented.

3.3.8 Immunfluorescence

Immunocytochemistry or Immunfluorescence (IF) is used to detect cellular or viral proteins using an fluorescence microscope. The proteins can either be tagged with a fluorochrome and be expressed in the cells or be detected via fluorochrome-coupled antibodies.

One day after transfection the cells were washed twice with PBS and fixed with 4 % PFA in PBS (RT, 15 min). After washing 3 times with PBS, the cells needed to be permeabilized adding 100 % Methanol and freezing the cells for 10 min at -20°C. This step is necessary to open the cell walls and allow binding of the antibody intracellularly. Afterwards the methanol was washed away once with PBS and the specimen were blocked in blocking buffer for 1 h. Then the blocking solution was aspirated and the diluted primary antibody was applied over night at 4 °C.

On the next morning the cover slips were washed three times in PBS and the fluorochrome-conjugated secondary antibody was added for 1 h at RT in the dark. As a last step the samples were fixed with MOWIOL on slides and either analyzed directly or stored at 4 °C.

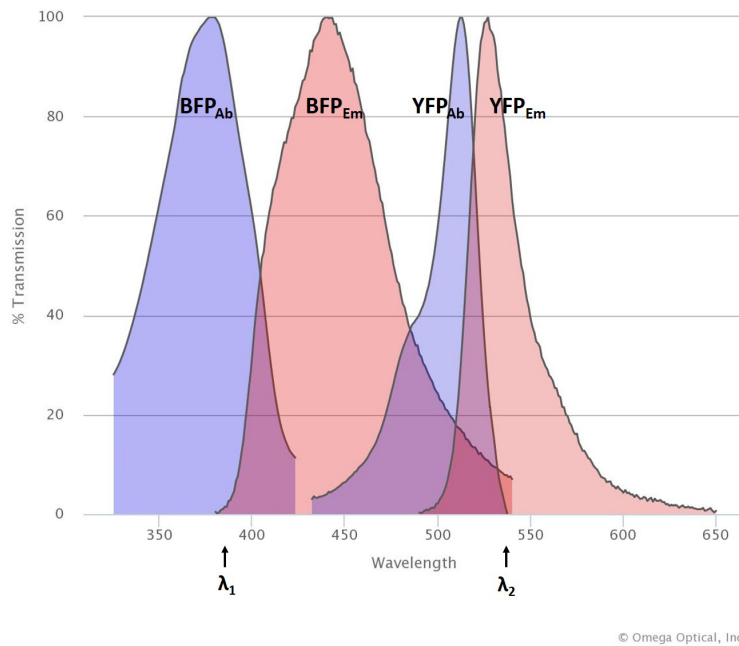


Figure 3.3: YFP and BFP absorption and emission spectra Figure generated at <https://www.omegafilters.com/curvomatic/index.php?fluorophores=BFP%7CYFP>

3.3.9 FACS-FRET

The underlying principle is the Förster resonance energy transfer (FRET), which describes the transfer of energy from a donor to an acceptor chromophore. The donor molecule is excited with a wavelength λ_1 and transfers its energy through dipole-dipole coupling to the acceptor chromophore. This protein then excites at a higher wavelength λ_2 . The two prerequisites are that the emission spectrum of the donor needs to overlap with the absorption spectra of the acceptor and that the proteins are in close proximity (up to 10 nm). In this work yellow fluorescent protein (YFP) was used as acceptor and blue fluorescent protein (BFP) as donor chromophore both attached to the N terminus of the constructs. The spectra can be seen in Figure 3.3.

FRET was now combined with the fluorescence-activated cell sorting (FACS), which allows high-throughput screens. This method was developed by Banning et. al.²⁵⁴.

To measure FRET with a flow-cytometer, the controls and gating-strategy were essential. The Huh7 cells were seeded two days prior to the measurement in 12 well plates. On the next day the cells were transfected with either YFP or BFP alone for the gating, YFP alone + BFP alone as a negative control, a fusion protein YFP-BFP as a positive control and the proteins of interest.

After 24 h the cells were harvested. The supernatant was removed, the cells were washed twice with PBS and 200 μ l trypsin was added. After the cells were pelleted at 4500 rpm for 5 min at 4 °C, they were resuspended in 500 μ l FACS-buffer.

As a first measurement mock cells were analyzed to set the parameter for the granularity and size of living cells. To achieve this, a gate was set using the forward-Scater (FSC) and the sideward-Scater (SSC). In a next step, the photomultipliertube (PMT) was adjusted using the YFP alone and BFP alone controls, so that the double-positive cells could be measured. As YFP is not only excited with the 455 nm laser but also to a small extent with the 405 nm laser, this false positive values needed to be eliminated. For that reason the FRET signal was plotted on the YFP signal and the cells were gated out. In a next gating step, the BFP signal was plotted on the FRET signal. Here the negative control is gated out, to remove "random" close proximity. As a last step, the fusion protein were analyzed after the gates were set and now showed high FRET signal.

4 Results

4.1 S protein oligomerization

4.1.1 Secretion of competent S constructs

The S protein of HBV is secreted in subviral particles^{137,172}, which consist only of lipid and approximately 100 copies of S²⁵⁷. In previous experiments only two domains of S were found not to be essential for secretion of SVP²⁵³. Firstly, the TM1 domain, which could be exchanged to a poly-alanine sequence, and secondly, the C terminus from aa 178 on, which can be depleted. Transfection of these two constructs resulted in detectable amounts of secreted particles after three days post transfection (dpt) (cf. Suffner²⁵³). To further analyze if the proteins detected in the supernatant (SN) were incorporated in SVP, sucrose density gradient centrifugation was performed (cf.4.1).

S-HA had its main peak fraction in fraction number 9, but was spreading from fractions 7 to 13 (cf.4.1). Whereas the S- Δ 178 construct sediments more slowly and has its peak fraction in fraction 8, but beginning in 7 and reaching till 12. So it was shifted one fraction upwards in comparison to wt-S. Besides, the S-TM1polyA-HA constructs had the main abundance in fraction 9 with expansion to fractions 8 and 10. So the sedimentation was comparable to S-HA. Single proteins would stay on top of the gradient and would not sediment.

4.1.2 Influence of the YFP/BFP fusion proteins on the topology

The oligomerization of different constructs was further investigated by FRET in combination with FACS²⁵⁴. This method allows detection of interacting proteins in an high-throughput (HT) screen. Besides, the constructs can also be secretion deficient as the method was applied on living cells and not SN.

For this analysis, S protein fusion constructs were generated, which carried either YFP or BFP at the N terminus. To investigate if this tag influenced the insertion into the ER membrane and therefore the folding of S, a protease protection assay was performed. The YFP/BFP-S constructs carried a signal sequence at the N terminus of YFP/BFP to initiate the insertion of the fluorochrome into the ER lumen. For this experiment, control constructs were generated in which the signal-sequence was removed. This generated the constructs YFP*-S and BFP*-S.

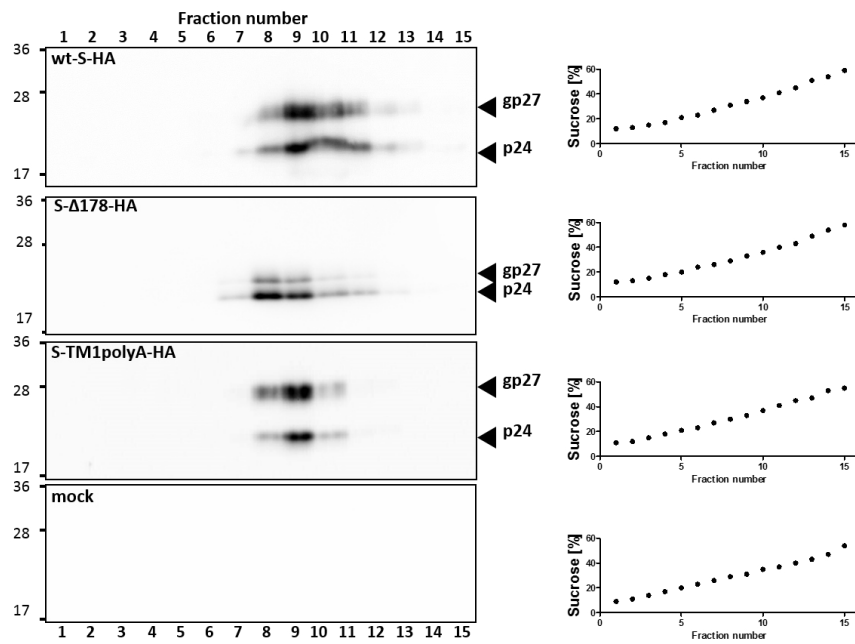


Figure 4.1: **Sucrose density centrifugation of secreted S constructs** Supernatant of transfected Huh7 cells were collected three dpt and loaded onto sucrose gradients. After an o/n centrifugation, the gradient was harvested into 15 fractions. The fractions were analyzed via Western-blot analysis and an HA-antibody. The right panel shows the corresponding sucrose densities in the fractions determined via refraction indices.

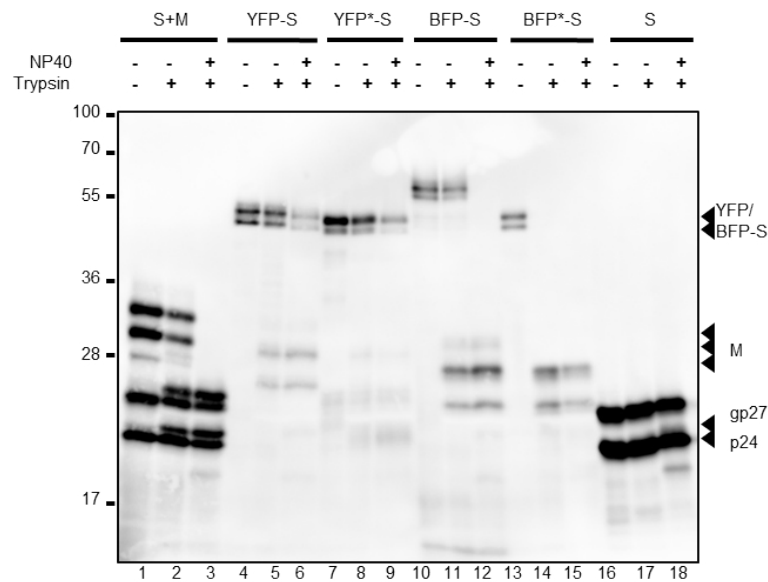


Figure 4.2: **Protease protection assay of YFP/BFP-S fusion proteins** Lysate was harvested three dpt and microsomes were prepared. These microsomes were then treated with either trypsin alone, trypsin and NP40 or nothing. The samples were analyzed using Western blot and HB1-antibody. * indicated lack of signal sequence before the tag.

Additionally to the controls, the S and M protein or the S protein alone were used. As it is known that M, in contrast to S, can be cleaved by trypsin, the correct orientation with the added tags was determined¹⁵⁹.

The cells were dounced, thereby creating microsomes in which the membrane proteins were accessible for the protease. In Figure 4.2 the results of the experiments analyzed via Western blot can be seen. The constructs were either untreated (lanes 1, 4, 7, 10, 13, 16), treated only with trypsin (lanes 2, 5, 8, 11, 14, 17) or treated with a detergent (NP40) and trypsin (lanes 3, 6, 9, 12, 15, 18). The detergent opened the membranes of the microsomes so that proteins were completely accessible for trypsin.

Firstly, the M protein was cleaved by trypsin as described earlier. When the membranes were opened with detergent first, trypsin degraded the M protein. The bands between 28 kDa and 36 kDa marker band in the lanes 1 and 2 were no longer visible in lane 3. The small loss in intensity from an untreated construct to a construct treated with trypsin (i.e. lanes 1 and 2 of Figure 4.2) was due to the fact that during the microsome preparation not all membranes reformed with the correct topology. So some proteins were inserted the wrong way and could thereby be degraded. Nevertheless, the S protein at 24 kDa and 27 kDa did not loose intensity in the blot. Also, when S was used alone (lanes 16, 17, 18) the addition of detergent and trypsin did not lead to a cleavage of the S protein. Secondly, the YFP-S and YFP*-S constructs did

not differ in their behavior upon trypsin and detergent treatment. Both constructs were not fully degraded with NP40 (lanes 6 and 9), indicating that YFP is partially resistant to protease cleavage by trypsin. However, BFP was susceptible to cleavage with trypsin. Nevertheless, BFP-S was only degraded after disintegration of the membranes (lanes 11 and 12). But when the signal-sequence was deleted, BFP*-S could be degraded with trypsin without additional treatment (lane 14).

Besides, it was visible that BFP-S in comparison to BFP*-S was bigger, with a difference of about 10 kDa. This was due to post-translational modification occurring when BFP is inserted into the lumen of the ER²⁵⁸.

4.1.3 Functional characterization of the S-C65S-TM2polyA mutants

In a previous work, Sascha Suffner²⁵³ could show that intermolecular disulfide bonds are not the only linkers which support oligomerization of S. The exchange of the eight cysteines in the cytoplasmic loop (CL) to serines (construct CS) did not show a significant reduction in the FRET-signal. It was shown that the transmembrane domain (TM)2 and one cysteine in the luminal loop (C65) are necessary for oligomerization of S.

As a next step, these two exchanges were combined in the wild type (wt) and CS background, generating the constructs S-C65S-TM2polyA and S-C65S-TM2polyA-CS in which the aa in TM2 were exchanged by alanine.

To begin with, the new constructs were tested for their expression in WB (cf. Figure 4.3 b)). All three constructs were detected with a greenfluorescent protein (GFP) antibody, as YFP and GFP are highly similar in their structure. The size of S alone is 24 kilo Dalton (kDa) (non-glycosylated S Protein (p24)) and 27 kDa (glycosylated S Protein (gp27)) in a glycosylated state. YFP alone is 26 kDa in size. So the YFP-S fusion protein has calculated sizes of 50 kDa (p24+YFP) and 53 kDa (gp27+YFP). In the WB analysis the two bands were clearly visible for all three constructs at sizes around 50 kDa, which matches the calculated size. In the mock control (lane 4), in which no YFP was present, no bands were visible. Besides, it could also be seen that the glycosylated form of the protein was expressed stronger than the non-glycosylated form, as the upper band was stronger than the lower band. As a loading control, the same samples were stained for tubulin, a house-keeping gene. In this blot the bands had the same intensity, so equal amounts of protein were loaded on the gel.

Alongside the WB analysis, the expression was also measured using FACS (cf. Figure 4.3 c)). Here both fluorophores were measured. In almost all constructs analyzed, the BFP constructs were expressed weaker than the YFP constructs. An exception was the S-C65S-TM2polyA-CS protein, in which BFP and YFP were both expressed in around 9 %. Nevertheless, all constructs could also be detected in FACS analysis.

In addition, the localization inside the cell was analyzed. To achieve this, cells were transfected

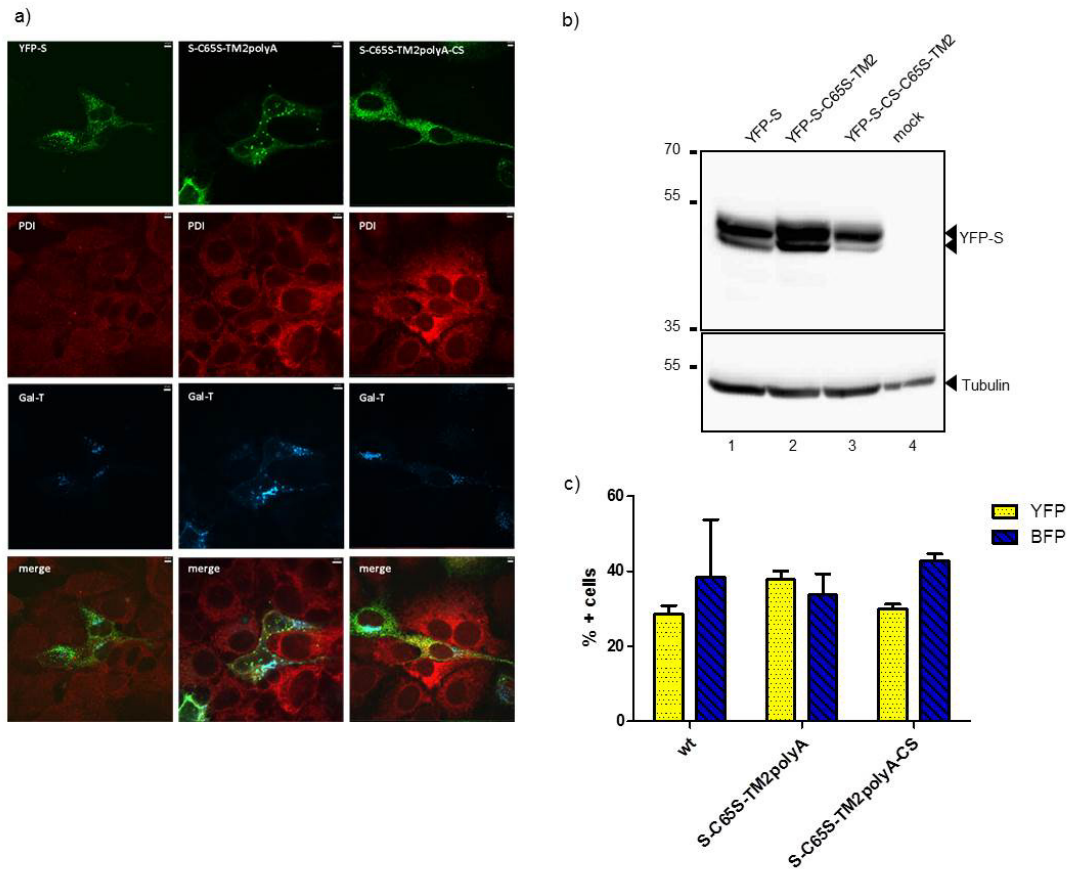


Figure 4.3: Detection of the expression of the two constructs with different methods

The two constructs S-C65S-TM2polyA-CS and S-C65S-TM2polyA were analyzed with respect to their expression and localization after transfection. a) Representative pictures of the localization throughout the cell. YFP fusion constructs were co-transfected with GalT, a marker for the Golgi, and stained with an antibody against PDI, an ER marker. As secondary antibody, Alexa Fluor 633 was used. b) Shows a Western blot in comparison to wt S in which the proteins were detected with a GFP antibody, and as loading control the lysates were stained for tubulin. Lysates were used three dpt. c) The expression pattern of the two constructs in comparison to wt S and S-CS in FACS-analysis. The fusion constructs, which were tagged with either YFP or BFP, were transfected and the cells analyzed one dpt.

with YFP constructs and galactosyltransferase (GalT)-CFP and stained for PDI. GalT served as a marker for the Golgi-network, whereas PDI was only present in the ER. The cells were analyzed using a fluorescence microscope. Representative picture can be seen in Figure 4.3 a). In the lowest panel the localization of the YFP-S protein is shown. S was distributed throughout the Golgi-ER network, but the signals were stronger in the ER regions. The S-C65S-TM2polyA construct was also localized throughout the ER and the Golgi apparatus. However, this construct showed dots with higher fluorescence intensity. These were mainly localized surrounding the nucleus. Nevertheless, they were low in number, with less than 20 dots per cell. In contrast, the S-C65S-TM2polyA-CS construct did not show dots or areas with higher intensity. It was equally distributed throughout the Golgi and ER network. As expected, in none of the pictures the S protein was detectable inside the nucleus of the transfected cells.

We could therefore show that the addition of a fusion protein did not alter the protein in its folding process. As the expression and localization status was comparable to YFP-S, the construct could be used for further experiments.

4.1.4 Oligomerization properties of C65S-TM2polyA-S

The FACS-FRET analysis, described by Banning et al.²⁵⁴, was used to investigate the oligomerization properties of the constructs. Sascha Suffner showed in his PhD thesis, that the FACS-FRET technique can be used for the S protein and he also demonstrated that the expression rate and the FRET value are not dependent on each other.

In Figure 4.4 a) the newly generated constructs were measured in comparison to some already existing controls. The first control were YFP and BFP, as YFP and BFP are not interacting inside cells. This gave the background noise of the method. A YFP-BFP fusion construct served as a positive control, as the proteins were fused and therefore should generate the maximum value. As specific controls, which were already measured before, YFP/BFP-S, YFP/BFP-S-CS, YFP/BFP-S-TM2polyA-CS and YFP/BFP-S-TM1/TM2polyA-CS were used. To validate the gate setting, the values were then compared to already measured data. The findings were consistent with the values generated before, with one exception: S-TM1polyA-TM2polyA-CS. Here, it was measured with lower values than in the measurements conducted before.

In a next step the constructs S-C65S-TM2polyA-CS and S-C65S-TM2polyA were analyzed in the same gates. S-C65S-TM2polyA oligomerized strongly and showed a FRET signal comparable to S. The values were above 90 %, whereas the construct S-C65S-TM2polyA-CS showed almost no FRET signal with an arithmetic mean of 1.83. This was around the range of the negative control with a mean of 2.54. So S-C65S-TM2polyA-CS was no longer interacting with itself to form dimers and/or higher oligomers.

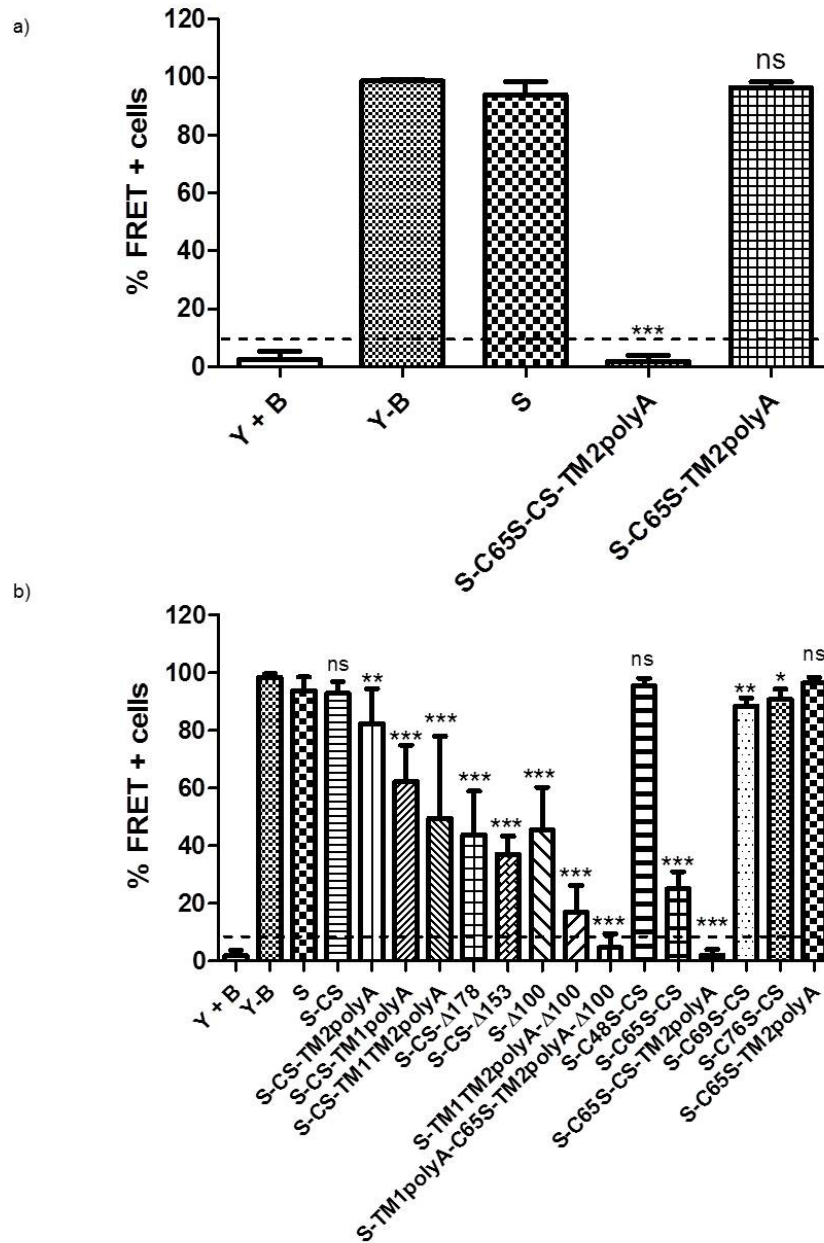


Figure 4.4: **FACS-FRET analysis of the oligomerization properties of different constructs** a) Constructs of S-C65S-TM2polyA and S-C65S-TM2polyA-CS in comparison to the controls. b) Summary of all the results obtained, including results from S. Suffner. (Co)-transfected Huh7 cells were analyzed via FACS-FRET one dpt. Indicated are mean and standard deviation of a minimum of three independent measurements with a minimum of two replicates. For each experiment a minimum of 50,000 cells were analyzed. FRET values $\leq 10\%$ were assumed as interaction. Statistical analysis was performed using the Mann-Whitney-test by GraphPad Prism. *** = $p < 0.001$, ** = $p < 0.01$, * = $p < 0.05$, ns = not significant.

4.2 Secondary structure of the small hepatitis B virus surface protein

SVP only consists of lipid and S protein, the number of proteins and the diameter of SVP are described^{137,172}. However, the arrangement of S in the particles and their secondary structure are only proposed with *in silico* methods. Gilbert et al. described, after his microscopic studies, that S seems to be arranged in a dimeric structure²⁵⁹. But this was not further investigated on molecular biological level. So we analyzed the structure of S in SVP and the influence of disulfide bonds on the tertiary structure.

4.2.1 Secreted S protein forms a dimer

To find out if disulfide bonds influence the dimerization/ oligomerization of S in secreted particles, we added or removed DTT in loading dye. DTT selectively opens disulfide bonds. We used plasma samples from an infected donor which were taken at the TUM Klinikum Rechts der Isar (thanks to Dr. Marc Ringelhan) and compared them to SVP collected in cell culture. The samples were either wt S or S-HA, which carries an HA-tag at the C terminus. Lysate and supernatant were collected three days after transfection of the cells.

In Figure 4.5 the influence of disulfide bonds on the structure of S proteins in SVP was analyzed. Normally proteins are completely unfolded before they are loaded onto an SDS-gel. Addition of SDS and DTT as well as heating the samples disrupt hydrogen bonds, disulfide bonds and lipid membranes. We optionally removed DTT from this pre-treatment and therefore left the possible disulfide bonds intact.

In Figure 4.5 a) plasma samples of an infected donor were used. The plasma samples contained infectious virions, but in excess SVP. These were mainly detectable in the gel. When the samples were treated with DTT (+DTT, lane 4), S proteins were fully reduced and were detected in the non-glycosylated (p24) and the glycosylated (gp27) form. Between around 30 kDa to approximately 50 kDa the three different versions of M were detectable. However, when DTT was removed from the samples, M was no longer visible, but at 50 kDa two stronger and one weaker band appeared. This corresponded in size to the dimers of S. So the main form of S in patient samples was dimeric. Monomers were still visible, but they ran lower than the completely reduced ones. An explanation could be that intramolecular disulfide bonds were present inside the monomer, which caused a more compact structure running differently on the gel.

In comparison to this result, it was analyzed if this dimeric phenotype could be reproduced in cell culture through transfection of plasmids. First we used a very well established plasmid (pSVBX24H, cf. Materials), which after transient transfection lead to intracellular and secreted

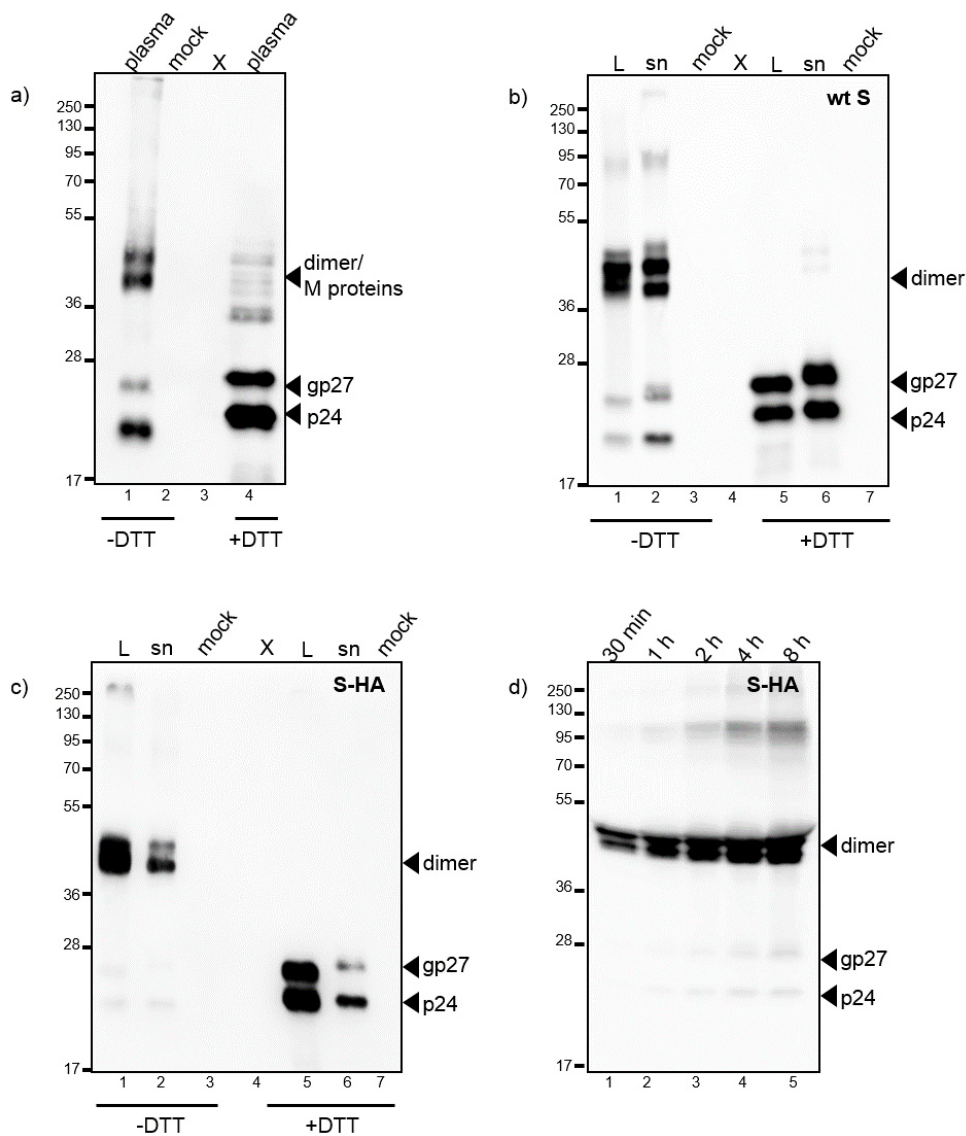


Figure 4.5: **The main form of S in SVP is a disulfide-linked dimer** Samples were either treated without (-DTT) or with DTT in the buffer (+DTT) a) Shows plasma from an HBV infected donor. In b) wt S was used from cell culture, either lysate (L) or cell culture supernatant (SN). c) was comparable to b), only the construct used was tagged with an HA-tag at the C terminus. d) Cells were transfected, after three dpt the medium was changed to fresh DMEM+++. This was collected after the indicated time points and loaded -DTT. L was lysate, sn supernatant, X means loading buffer without DTT. HB1-ab. 1:1000, harvested three dpt.

S and/or SVP. The SN and lysate were harvested three dpt and the samples were either treated with (+DTT) or without (-DTT) DTT. In Figure 4.5 b) the results can be seen. The proteins were expressed and secreted as expected (lane 5 and 6). Without DTT the dimeric pattern, already known from the patient sample, was visible. Notably, in lysate and SN dimers were present to around the same extent.

Due to the fact, that the antibody used for this experiments (HB1) carries cysteines in its epitope and mutation of this positions seemed necessary in further experiments, we wanted to use S with an HA-tag. This construct was generated and described before²⁵³. In c) we performed the same experiment as in b) but with S-HA. The tagged protein resembled wt S. Without DTT the main form of S is dimeric at approximately 50 kDa (lane 1 and 2). When DTT was added (lane 5 and 6) the two versions of S became the dominant form.

So the use of transiently transfected S proteins showed the same phenotype as human samples. Also the addition of the HA-Tag did not notably influence the formation of dimers through disulfide bonds.

As a last step, the S-HA construct was tested in a time-course experiment (d)). Cells were transfected with S-HA and three dpt the medium was removed from the cells and they were washed twice with PBS. Fresh medium was added and harvested after 30 min, 1 h, 2 h, 4 h and 8 h. With the removal of the old medium all secreted particles were diminished and also the effect of "aging" particles in cell culture was ruled out. As the cells already produced SVP before the medium exchange it was not surprising, that after 30 min dimers were found in the supernatant. Over time the dimer signal was increasing, and also weaker higher migrating bands became visible. However the effect seen here was, that the cells secreted dimers, which were relatively stable in SN. So the effect of further oxidizing effect in SN on the particles could be ruled out.

4.2.2 Exchange of cysteines in LL lead to impaired secretion

The 14 cysteines present in the S protein were assigned into three categories, according to where they are located in the S protein. In Figure 4.6 a) localization of the cysteines in the LL, the CL and the TM domains can be seen. In Figure 4.6 b) the construct 4C is depicted, it only carries the four cysteines in the CL. This minimal construct was expressed in Huh7 cells and analyzed like the samples before: with and without the addition of DTT in lysate and supernatant. The construct carried an HA-tag, so that the samples can be detected in WB, as the HB1 antibody can not bind to constructs lacking C121 and/or C124.

4C was not secreted into cell culture media (cf. Figure 4.7), despite its strong signal in the lysate. Also the removal of DTT did not influence 4C, as there were only minor dimeric bands upcoming. So the main form of 4C was monomeric and secretion-deficient. The intermolecular disulfide bonds stabilizing the dimer needed to be in either the TM domains or the LL.

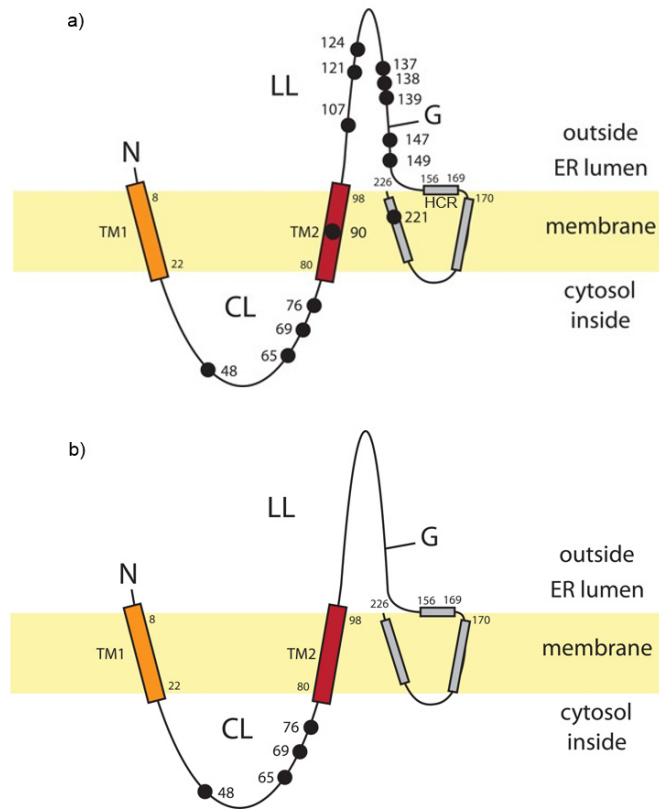


Figure 4.6: **Schematic Model of the localization of cysteines in the S protein** a) wt S with all 14 cysteines. b) Construct 4C with only four cysteines in LL. The black dots represent the cysteine residues.

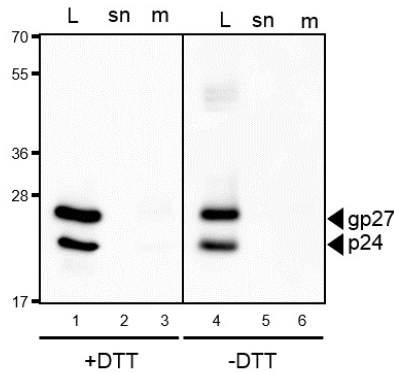


Figure 4.7: **Exchange of all cysteines in TM and LL to serines impair secretion and dimerization** Lysate and supernatant from transfected Huh7 cells was collected three dpt and analyzed via Western blot. Supernatants were concentrated by centrifugation through a 20 % sucrose cushion. The samples were either treated with or without DTT prior to loading. Samples were detected using HA-antibody.

4.2.3 Restoration of secretion through particular cysteine residues

Subsequently the restoration of the secretion competence through re-addition of particular cysteines in the TM domains or in LL was under investigation. So ten constructs were generated carrying 4C plus one additional cysteine at the indicated position (4C+CXXX) through site-directed-mutagenesis. These ten constructs were transfected and expressed in liver cells and three dpt the lysate and supernatant were analyzed, again either with or without DTT added prior to loading on the SDS-gel.

All constructs were expressed in the lysate. When only 20 % of S-HA were loaded, the expression patterns had equal intensities and were easier to analyze. So the 4C+CXXX constructs were made 20 % as efficient in lysate as S-HA. When DTT was removed from the lysate samples, the dimers became visible, but also some higher bands at 100 kDa and above were detectable. As observed before, the main form of S-HA was dimeric.

However, in the other constructs also dimers appeared. So the ratio of intensity of the dimer band to the total intensity of the monomer+dimer bands ($\frac{dimer}{monomer+dimer}$) was quantified using ImageStudio Lite. Thus the bands were marked (cf. Appendix), the background was set using the mock control and the signals were quantified. The total intensity was calculated adding up the intensity of the monomer bands and the dimer bands. The results can be seen in Figure 4.9. So the ratio of dimer to total intensity in S-HA was almost 1, indicating that the main form

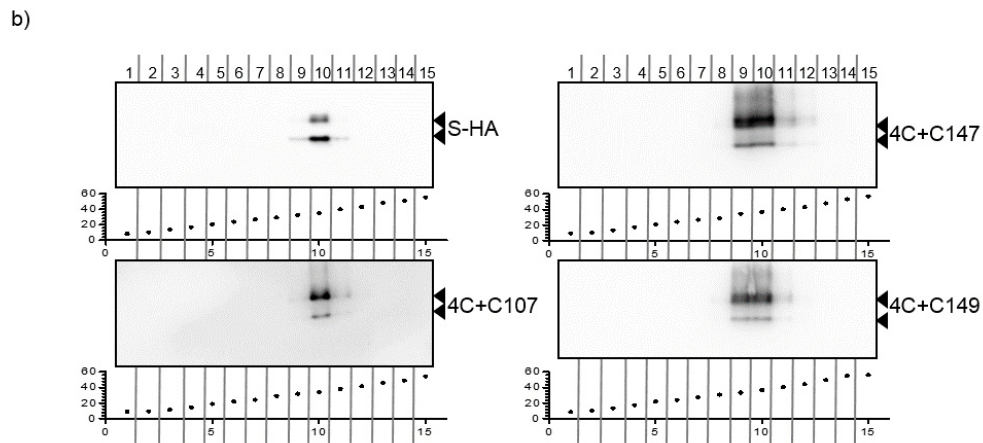
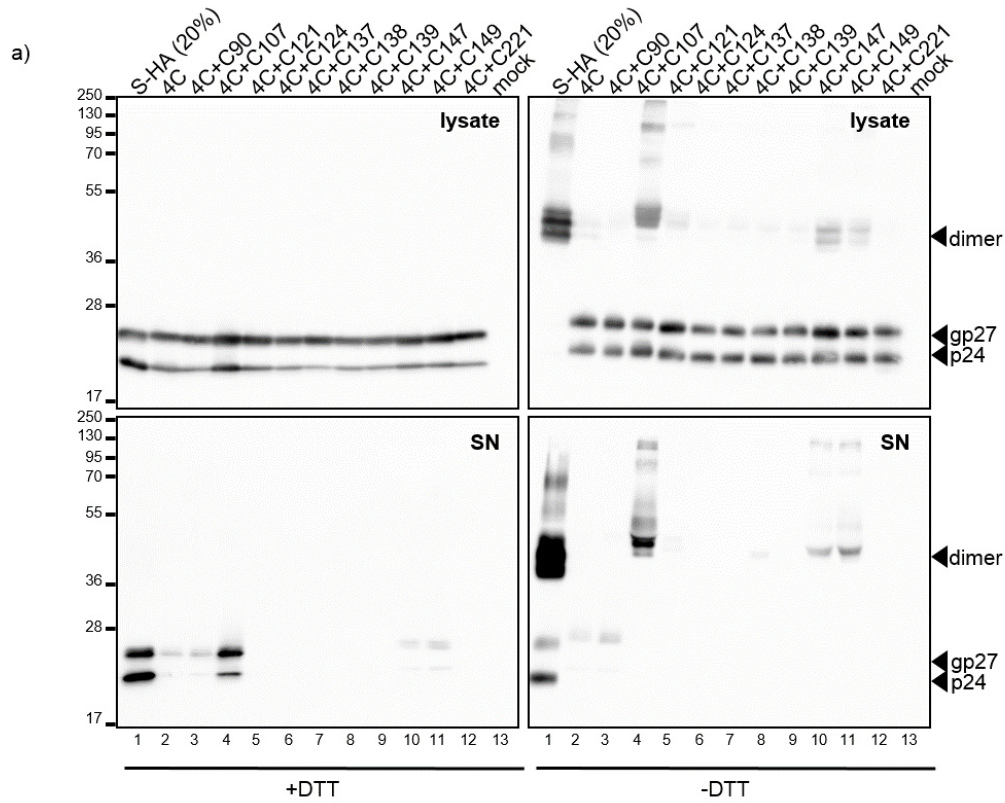


Figure 4.8: **Three SingleCys constructs show dimers and are secreted as SVPLysate** and supernatant from transfected Huh7 cells was collected three dpt and analyzed via Western blot. a) Only 20 % of S-HA were loaded in comparison to the other constructs. SN was concentrated by centrifugation through a 20 % sucrose cushion. The samples were either treated with or without DTT prior to loading. b) Supernatant was loaded on top of a sucrose density gradient and centrifuged o/n. Gradient was fractionated into 15 samples, which were then analyzed via Western blot. Samples were detected using HA-antibody.

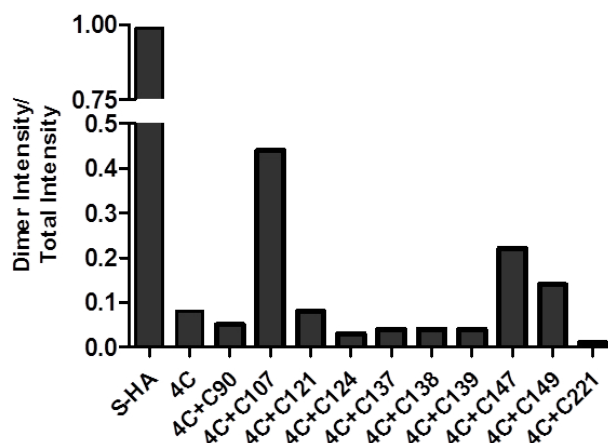


Figure 4.9: **Ratio of dimer intensities of different constructs to total intensity in lysate** Analysis of band intensities with ImageStudio Lite. Total intensity per construct was calculated adding dimer and monomer intensities.

was a dimer. Only three more constructs had values above 0.1. 4C+C107 with 0.44, 4C+C147 with 0.22 and 4C+C149 had 0.14. The other mutants were within the range of 0.01 and 0.08. In SN only a few samples could be detected, namely S-HA, 4C, 4C+C90, 4C+C107, 4C+C147 and 4C+C149. When loaded without DTT, S-HA and 4C+C107 resembled a strong dimer signal at around 50 kDa. But also higher bands at approximately 100 kDa and higher appeared. These bands were comparable to the ones visible in lysate, although they were stronger in SN. 4C+C147 and 4C+C149 also formed dimers and partially higher shifts. However, 4C and 4C+C90 were only weakly expressed and only visible in a monomeric form. The only other monomer detectable was a minor proportion at S-HA.

Additionally, the three constructs with the strongest dimer signal in SN were analyzed through sucrose density centrifugation. On the one hand, it was possible to see, if the secreted proteins were incorporated in SVP, and on the other hand, possible differences in the size and/or density could be analyzed. To begin with, S-HA accumulated in fraction 10 of 15, with 1 being on top of the gradient and 15 being the bottom. The other three constructs were also sedimenting into the gradient, indicating SVP formation. All of them showed proteins in fraction 10, but 4C+C147 and 4C+C149 showed the same intensity also in fraction 9. So their peak was wider and it sedimented also slower.

The corresponding sucrose densities of the fractions can be seen below the WB pictures. Anyhow, there was no significant difference in the values.

Consequently we generated two new constructs. One which carried all three cysteines C107, C147 and C149 together in the 4C background (4C+CCC) and a construct in S-HA background

where these three cysteines were exchanged into serines (S-SSS). All mutants were expressed in lysate S-SSS, however was as weakly expressed as 4C (Figure 4.10). When we left out the DTT in the buffer, we found strong dimers in S-HA as well as in 4C+CCC, besides some higher migrating bands at around 100 kDa. In S-SSS we saw a very weak dimer band in lysate, which was as weak as the dimers in Figure 4.8 4C+C137 for example. When we looked at the secreted particles in the SN blots, we only found S-HA and 4C+CCC in the cell culture supernatant, which in conclusion leads to the fact that none of the other cysteines were capable of forming a stable dimer which entered the secretion pathway.

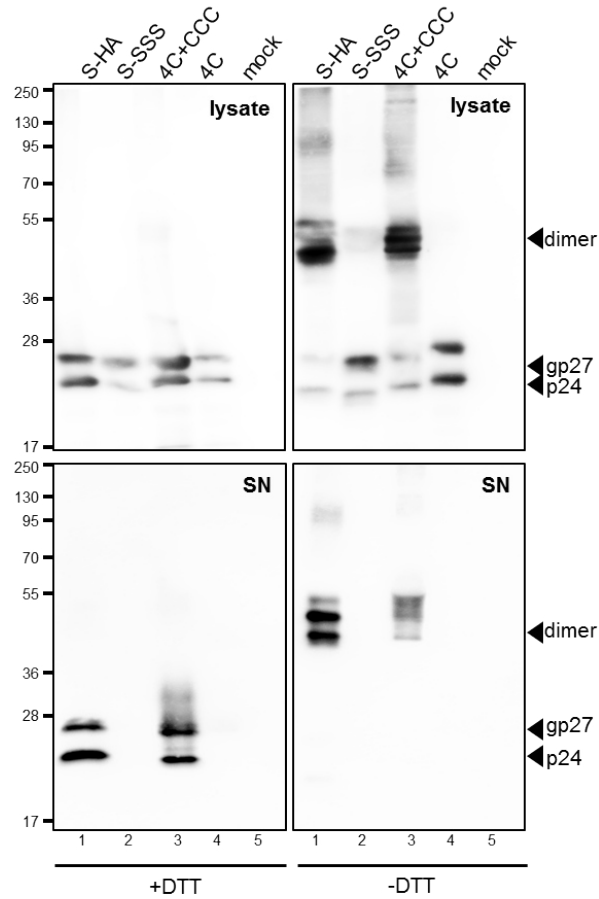


Figure 4.10: **One of the three cysteines C107, C147 and C149 are necessary for secretion** Lysate and supernatant from transfected Huh7 cells was collected three dpt and analyzed via Western blot. Supernatants were concentrated by centrifugation through a 20 % sucrose cushion. The samples were either treated with or without DTT prior to loading. Samples were detected using HA-antibody. S-SSS corresponds to S-HA with cysteine to serine exchanges at position 107, 147 and 149. 4C+CCC corresponds to 4C with cysteines positions 107, 147 and 149.

4.2.4 Cysteines in TM domains are free and do not influence secretion

Similarly, the cysteines in the TM domain were investigated further. The S-HA and the 4C construct served as a control. Another construct, already described by Suffner et al., was used²⁵³. It carries six cysteines (6C construct), namely 4C with addition of C90 and C221. Another construct was generated using S-HA and exchanging C90 and C221 to serines (construct S90+S221). All four constructs were expressed in lysate (cf. Figure 4.11), the S-HA samples were diluted 1:1 before loading onto the SDS-gel.

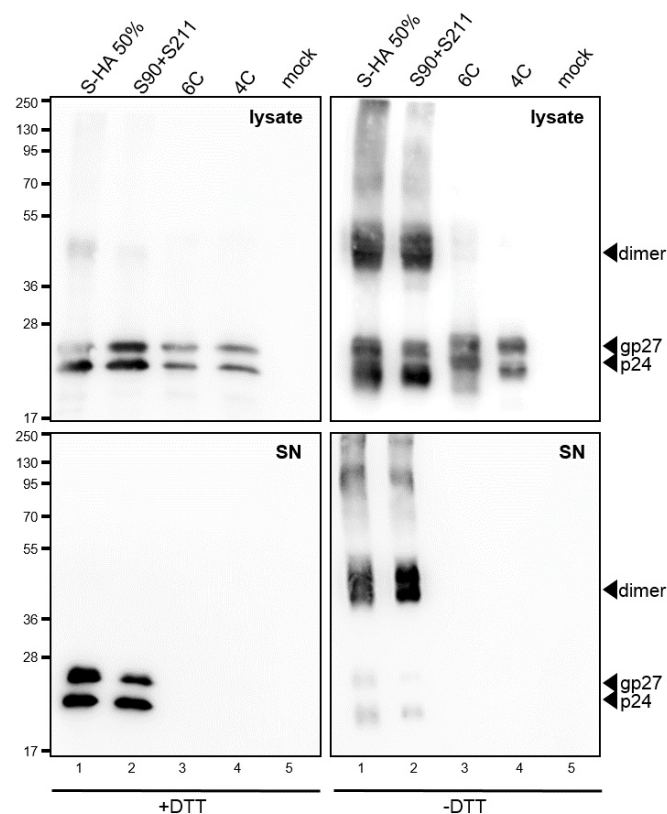


Figure 4.11: **Cysteines in the TM domains do not influence dimerization** Lysate and supernatant from transfected Huh7 cells was collected three dpt and analyzed via Western blot. Supernatants were concentrated by centrifugation through a 20 % sucrose cushion. The samples were either treated with or without DTT prior to loading. Samples were detected using HA-antibody.

4C and 6C were not secreted, as well as no strong dimers were visible in lysate. The -DTT lysate blot in this figure appeared blurry, yet the -DTT supernatant blot seemed sharper. So

the S90+S221 protein was secreted and formed dimers in lysate and supernatant (lane 2 in - DTT). The intensity was as strong, or even stronger than 50 % S-HA, which indicates that they were secreted at more or less the same level. Higher bands appeared also when DTT was left out of the buffer, though in lysate it was not possible to distinguish single bands, which made size quantification invalid. In SN this was more feasible, with one stronger signal at a size of around 120 kDa. So the cysteines in the TM domains did not alter secretion and dimerization, when they were exchanged and were not sufficient to restore secretion in 4C background.

4.2.5 Labeling with Mal-PEG is a way to detect and label cysteines in proteins

It was described earlier in various different fields that Mal-PEG can bind to free and/or oxidized cysteines²⁶⁰⁻²⁶². So we used this method to label either free -SH groups directly or to target bound cysteines. The second method was more complex, with respect to three more steps in the protocol. Firstly, the potential free cysteines were blocked with NEM, which does not cause a detectable increase in mass. Afterwards cystin bonds were reduced with DTT. To avoid interference of DTT on the labeling step, the samples were desalted through a column to remove DTT. In the last step, the now reduced disulfide bonds were labeled.

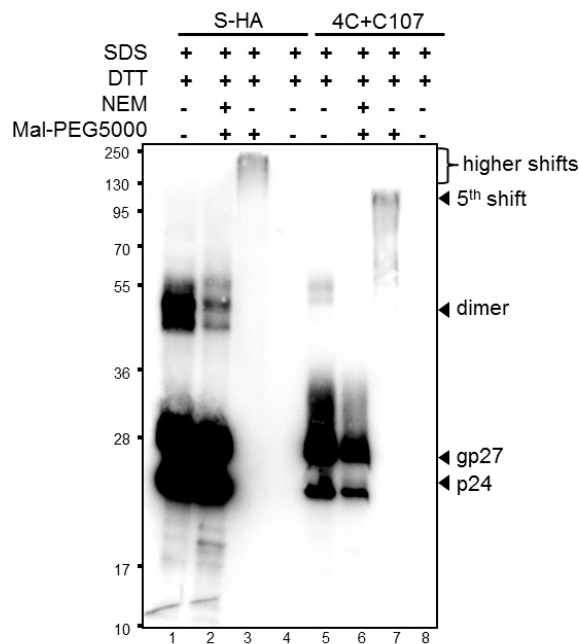


Figure 4.12: **Accessibility of cysteine residues in unfolded proteins** Either supernatant after three dpt of S-HA or 4C+C107 were left untreated or labeled with Mal-PEG5000. Before labeling the proteins were treated with SDS and DTT to unfold them and then the cysteines were either blocked with NEM and, in the last step, labeled with Mal-PEG (lane 2 and 6) or the unfolded protein was directly labeled (lane 3 and 7).

Accessibility

As this protocol has never been used before on a HBV protein, we tested the accessibility of cysteines to the chemicals first (Figure 4.12). All samples were completely denatured with SDS and DTT. After this step, all cysteines should be accessible. Then in one sample all cysteines

were blocked with NEM and then Mal-PEG was added (lane 2 and 6). Here no shifts were visible, as expected, only p24 and gp27 were strongly detectable. When, after denaturing, Mal-PEG was added, all 14 or five cysteines (depending on the construct) should be tagged, when they were sterically accessible. This could be seen in lane 3 and 7. The monomeric form was gone and higher migrating bands appeared. In S-HA the size of the complex could not clearly be determined, as it ran above the highest marker band (250 kDa). The calculated size of the band in 4C+C107 (lane 7) corresponded to approximately 125 kDa. This indicated five labeled cysteines. The intensity of the labeled band was weaker than the bands from the monomeric form of the proteins. In the very strongly expressed proteins (lane 1 and 2) there were dimers visible at a height of around 50 kDa, although DTT was added to the buffer. In comparison to the intensities of p24 and gp27 the dimer intensities were negligible. So all cysteines could be accessed at the same time and there seemed to be no sterical hindrance in the 4C+C107 construct. However, the accessibility of the cysteines in the LL could not be determined, as the sizes in S-HA were no longer distinguishable. So the closest distance in the primary structure of cysteines in 4C+C107 were two cysteines within five aa, which were taggable. It needs to be stressed that in LL there are three consecutive cysteines from 137-139 aa.

Shift size

The maleimide head of the Mal-PEG is the reactive part of the compound, whereas the PEG-tail causes the mass-shift in WB and is not restricted to a certain length. The suppliers sell the Mal-PEG compounds with molecular weight (MW) between 750 g/mol and 20,000 g/mol. The most common ones for use in WB seemed to be PEG2000 and PEG5000. However, due to the extensive hydrate shell which surrounds the PEG-tail in solutions, the shift detectable in WB is significantly bigger than 2 kDa or 5 kDa per Mal-PEG added.

To determine the shift size, two WB were analyzed. First the distance from the top of the membrane to the different marker bands was measured (Figure 4.13 a) and b)) indicated by the gray arrows in the pictures. The $\log(\text{MW})$ is directly proportional to the distance the marker band migrated in a gel. As a next step we plotted the graph and calculated the line of best fit (c) and d)).

In a last step we measured the distance of the signal bands to the top of the corresponding gel and calculated the MW of the proteins (d)). When the bands of non-glycosylated and glycosylated proteins could no longer be distinguished, the upper part of the band was measured. The results of this calculations can be seen in Figure 4.13 e).

With these results we then calculated a mass increase per Mal-PEG5000 added of 13.1 ± 2.8 kDa. When two bands were clearly distinguishable, the increase was calculated accordingly. When only one band was visible, for example in b) at a size of two shifts, the upper part

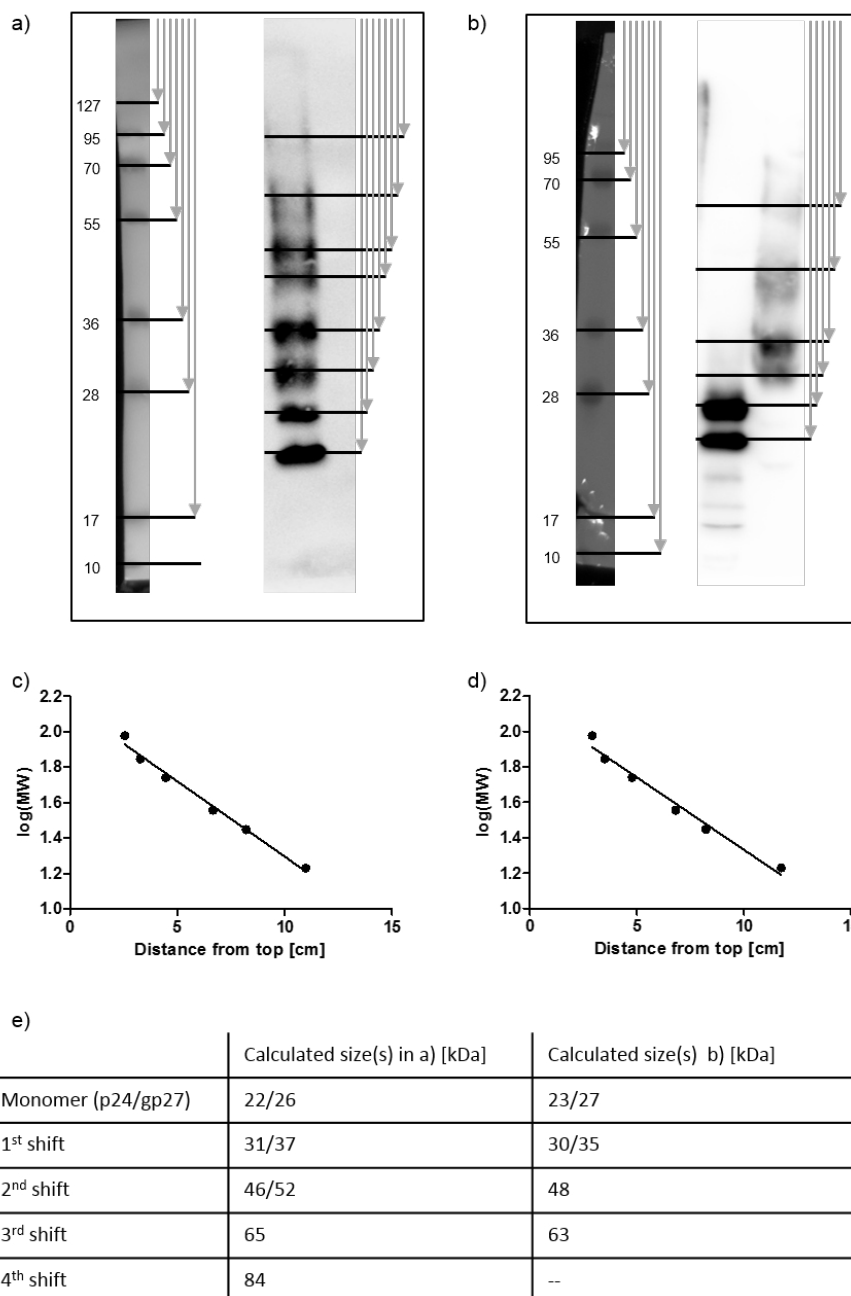


Figure 4.13: **Identification of the shift size detectable after Mal-PEG labeling in WB**

Two exemplary labeling experiments were analyzed with respect to the shift size. The supernatants were harvested three dpt and labeled with Mal-PEG5000. In a) free sulfides were labeled in S-HA. b) Labeling of disulfide bonds in 4C+C107 (cf. Figure 4.17b)). In a) and b) the original pictures of the marker are visible and the length from the top of the picture to the bands was marked (arrows) and measured. In the signal picture, the bands were marked and measured (arrows). c) and d) Graph of $\log(\text{MW})$ and the distance from the top of the marker bands and the corresponding line of best fit. e) Table of the calculated sizes of the signal bands.

was measured and the difference was calculated to the glycosylated band below. This was conducted, assuming the upper border was corresponding to a glycosylated band.

4.2.6 Mutation of glycosylation site is favorable in labeling experiments

The size of the mass-tag used for labeling experiments causes either a shift of ≥ 10 kDa (Mal-PEG5000) or ≥ 5 kDa (Mal-PEG2000). The smaller tag would therefore migrate at the same height as the glycosylation band in WB. So the N at position 146 in S was exchanged to Q to block the glycosylation of the protein. This was already shown not to dramatically influence the secretion of S²⁶³. So we tested this in our S-HA and 4* constructs. In Figure 4.14 the results can be seen.

In lanes 1-4 the controls can be seen. S-HA was present in lysate and secreted into the SN, unlike 4C, which was not secreted and only visible in lysate. The knock-out of the glycosylation site led to the loss of the gp27 band, but also to a decrease in signal intensity. The proteins were produced in lysate in a sufficient amount, though, and S*-HA was secreted. So the constructs were expressed lower, but the intensities in WB were strong enough to use them in further experiments.

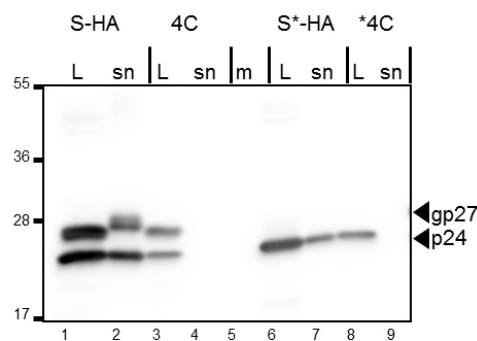


Figure 4.14: **The exchange of the glycosylation motif did not impair secretion or dimerization** Lysate and supernatant from transfected Huh7 cells were collected three dpt and analyzed via Western blot. Supernatants were concentrated by centrifugation through a 20 % sucrose cushion. The samples were treated with DTT prior to loading. Samples were detected using HA-antibody.

4.2.7 Cysteines in CL influence secretion of wt and show free SH groups and intramolecular disulfides

It was shown before by Mangold and Streek¹⁵⁰ that C48, C65 and C69 are essential for secretion of S. In addition Suffner showed in his PhD thesis that all four cysteines in the CL are necessary for secretion²⁶⁴. We investigated this effect further and co-transfected the constructs with S-HA. In Figure 4.15 a) the published results were reproduced. None of the single cysteine to serine exchange was secreted, also a 1:1 transfection with S-HA did not favor SVP in the cell culture supernatant. In b) the amount of DNA per transfection was still 1 µg in total but the ratio of the corresponding mutant to S-HA differed from 1:1 to 1:32.

All co-transfections caused a detectable amount of S proteins in lysate. Nevertheless the strongest signal was caused by S-HA alone. The lower the amount of CXXS constructs in comparison to S-HA, the stronger the signal was in lysate. So co-transfection caused a reduction in expression of S inside the cells. The effects in SN was stronger, as no signals were detectable with ratios from 1:1 up to 1:8 independently from the CXXS construct used. So it could be demonstrated that S-HA needed to be 16 times increased in the transfection solution to be secreted from the cells with a detectable amount.

Nevertheless, in three out of four constructs a ratio of 1:32 was not sufficient to restore the signal intensity to S-HA alone levels. The only one was C69 which resembled S-HA alone in a ratio of 1:32. Quantifications of the band intensities of 1:16 were performed and can be seen in Table 4.1. This experiment demonstrated a dominant-negative effect of the four C48S, C65S, C69S and C78S construct on S-HA secretion.

As a next step, we labeled free and bound cysteines in lysate to determine the status in the CL. It was well known that in the reducing environment of the cytosol disulfide bonds are rather unlikely. Nevertheless, there are viruses known which form disulfide bonds in the cytoplasm through unique mechanisms²⁶⁵. Hence, we did not rule out this possibility and analyzed the cysteines in the CL. For this labeling experiments the * variants were used.

In lane 1 and 2 of Figure 4.16 *4C and S*-HA were labeled either with respect to oxidized thiols or free thiols. The number of shifts in S*-HA labeled for oxidized thiols is hard to calculate, as it was a very strong smear rather than distinguishable bands. It was calculated that a minimum of five cysteines were labeled when the end of the smear was set to around 50 kDa. In *4C two main shifts were visible independent of the labeling technique used. As we did not find a high proportion of dimers (dimer/monomer ratio 0.08:1) an intermolecular bond was unlikely. So the two shifts, which were detectable after labeling for oxidized thiols, indicated an intracellular disulfide bond. To narrow down the exact position, double cysteine constructs which only contained two cys at the positions indicated in * background were cloned. It was expected that the double shift will be gone when the pair of cysteines which harbor the bridge

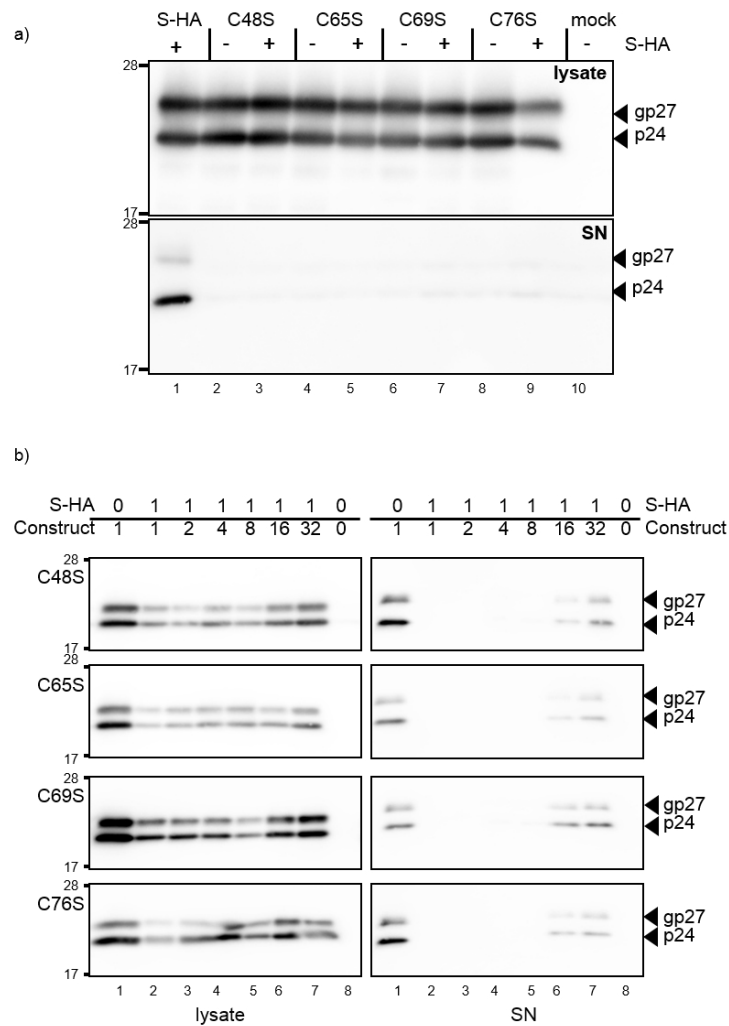


Figure 4.15: **Co-transfection of S-HA with single CXXS exchanges of cysteines in the CL** Lysate and supernatant from transfected Huh7 cells were collected three dpt and analyzed via Western blot. Transfection was conducted with different ratios of S-HA/CXXS with constant total volume. a) Only the construct alone or in a 1:1 ratio with S-HA was transfected. b) Different ratios of S-HA and the constructs were used during transfection.

Table 4.1: Measured intensities of secreted SVP at a ratio of 1:16. Values are indicated relative to wt in the corresponding Western blot

Construct	Intensity at 1:16 in SN in relation to S-HA [%]
C48	8.7
C65	15.1
C69	11.1
C76	48.4

were exchanged to serines. Contrary to the expectations, none of the combinations completely lost both labels. In *C48+C69 the labeling was very weak and only one band was detectable and in *C65+C69 and *C69+C76 the intensity of the shifts was rather weak, but still two shifts were detected. When the double cysteine constructs were labeled for free thiols in all constructs (lane 3-8) two shifts were nicely detectable. Unlike the oxidized thiols, the intensity of the bands in the free thiols were equal.

So the data suggested that cysteine pairs could be free and oxidized in different S chains at the same time. This could be possible because, in both experiments, we found unlabeled monomers at 24 kD. This proportion could represent the other moiety. Thus, unlabeled material in the oxidized blot, could represent the bands labeled in the free blot and vice versa.

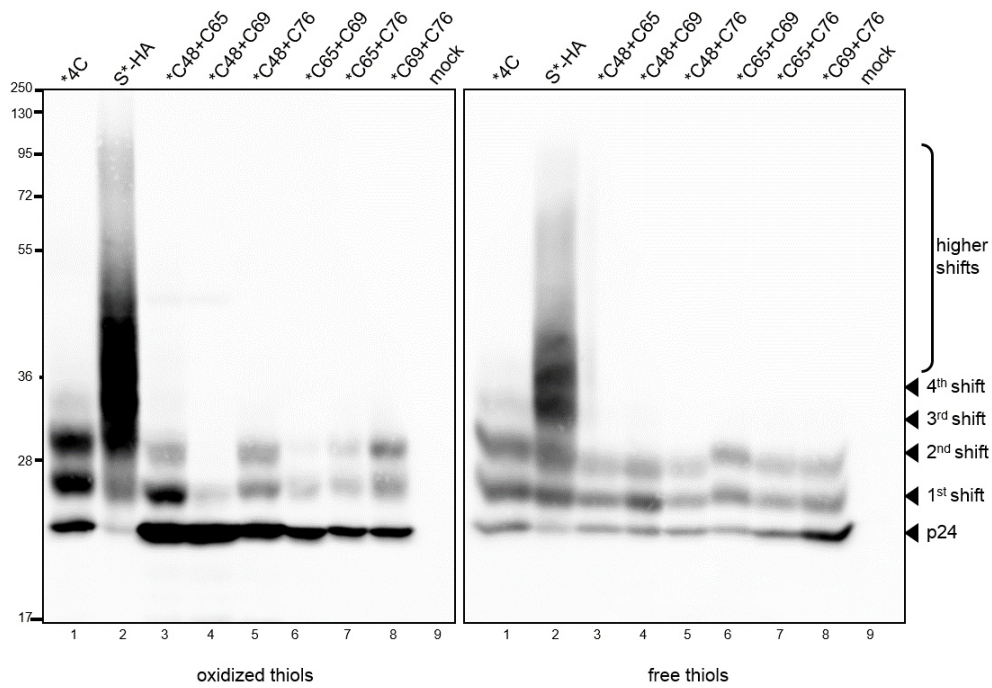


Figure 4.16: **Labeling of free or oxidized cysteines in lysate** Lysates of *constructs were harvested three dpt and either labeled for oxidized thiols or for free thiols. As controls *4C and S*-HA were used. The samples were detected using an anti-HA antibody, labeling was performed with Mal-PEG2000.

4.2.8 Labeling of secreted SVP revealed intramolecular disulfide bond and seven oxidized cysteines in total

S-HA and 4C+C107 were labeled in lysate (Figure 4.17 a)) and SN (Figure 4.17 b)) for oxidized thiols. In lanes 1 and 3 the untreated samples could be seen. These samples were diluted according to the labeling procedure steps to depict the same overall intensity. In total, the signals in the labeled samples were weak and blurry. However, in 4C+C107 single shifts were easily distinguishable. 4C+C107 showed in SN (Figure 4.17 b) lane 4) three shifts. This was predicted, as C107 forms a symmetrical intermolecular disulfide bond and an intra-molecular disulfide bond was expected from the results obtained in Figure 4.16. In the lysate sample this restriction to three bands was not as strict as in SN. There might be higher migrating bands in lysate samples. This could be due to the fact that in lysate the samples were not all in the same maturation step, as lysate is a mixture of freshly synthesized proteins and almost secreted proteins after the ER and Golgi.

The quantification of the number of shifts in S-HA was more difficult. In lysate (Figure 4.17 a) lane 2) it was only possible to state that there were more than four shifts detectable, with the majority being in this region. In SN the bands were not so strong and it seemed that the signal intensity was significantly below the intensity in the loading control. After all, the shift number could be calculated to be 6-7, as they had a clear boundary at the top.

This could also be seen in Figure 4.17 c). Here S-HA was labeled in SN for free sulfides (lane 1) and disulfide bonds (lane 2). So the labeling lane 2 in b) and lane 2 in c) show the same result. Nevertheless, in c) the signal was stronger, as it was developed longer. The result was the same with a calculated shift number of 7 at the highest band.

Labeling for free sulfides led to six shifts (lane 1 in c)). Interestingly, when labeling for free sulfides, a stronger "ladder-like" structure was visible with smaller shift sizes. The number of the shifts, corresponding to the bands was indicated in the picture. However, the band corresponding to the 4th shift was not clearly visible and was only marked at the calculated height with a gray arrow head.

Labeling of free and disulfide bonded cysteines in S-HA should cover both states the sulfide in the side chain could be in. This means, that the addition of the shifts visible in both states should sum up to the total number of cysteines present in the protein. Here we found 6 free sulfides and seven oxidized sulfides, only adding up to 13 not to 14 as expected. So one cysteine was not labeled at all by Mal-PEG5000.

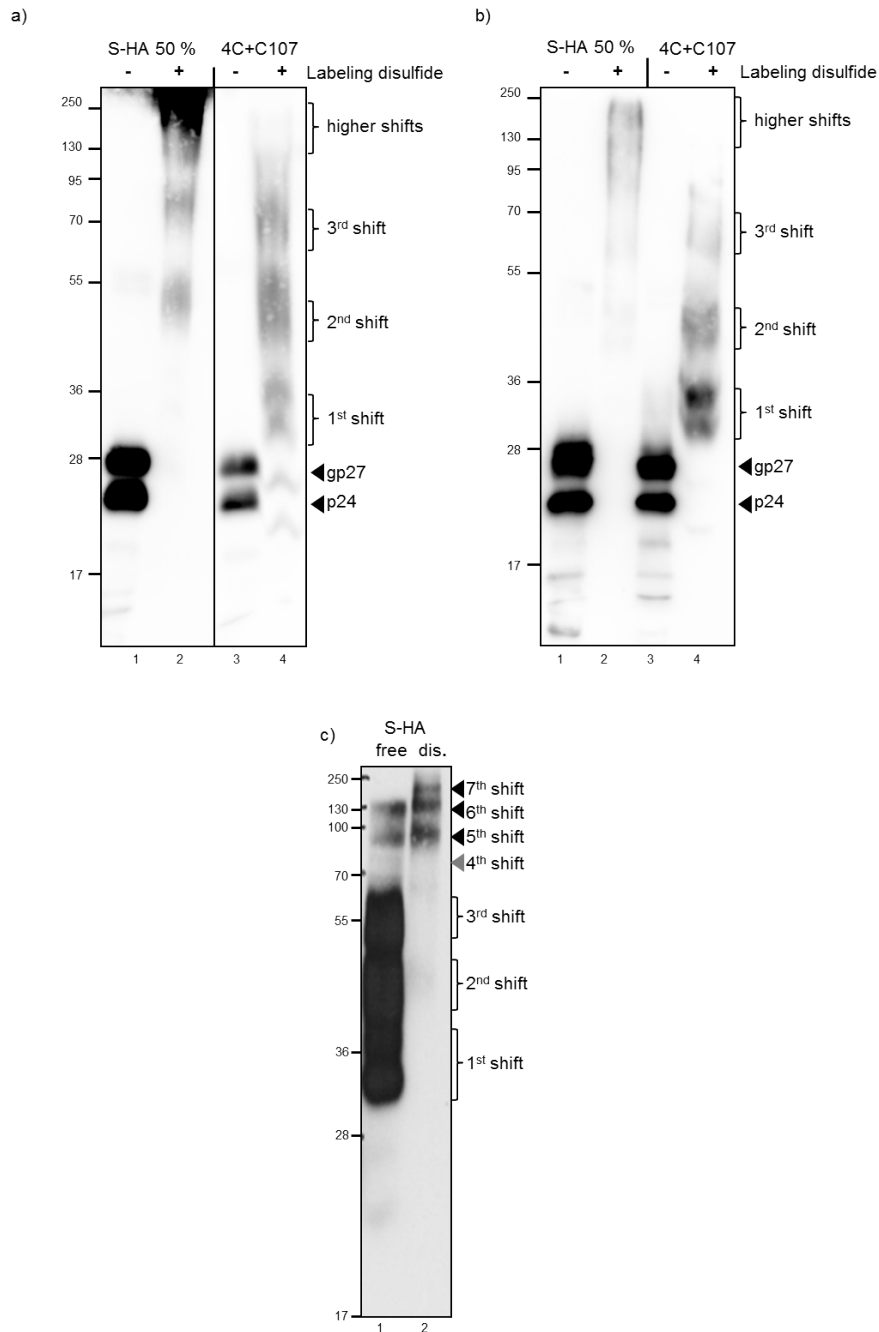


Figure 4.17: **Labeling of S-HA and 4C+C107 in SN and lysate** a) Represented lysate fractions of S-HA and 4C+C107 either untreated (-) oder labeled for disulfides. b) Represented SN fractions of S-HA and 4C+C107 either untreated (-) oder labeled for disulfides. c) Shows a direct comparison of labeled SN S-HA samples, either labeled for free or oxidized thiols (dis.). Lysate and SN were collected three dpt and SN samples were concentrated through ultracentrifugation. Then the samples were labeled using Mal-PEG5000. As controls untreated samples were loaded on the gel and to achieve equal intensities only 50 % of S-HA were loaded in comparison to 4C+C107. Samples were detected using an anti-HA antibody.

4.2.9 Native SVP carry an exposed free SH group on their surface

Mal-PEG of any size cannot cross membranes, if they are not denatured. So incubation of secreted SVP should only tag SH groups which are easily accessible on the surface of the particles. When we treated S-HA with Mal-PEG5000 directly after concentration in the ultracentrifuge, one shift was visible. Compared to the band intensity of p24 and gp27 the shift was weaker with around 50 % of the intensity. In another experiment (data not shown) it was suggested that one of the cysteines in the epitope of HB1 might influence the binding of the antibody when the sample was labeled for free cysteines. So we focused on the two cysteines C121 and C124 as a next step. Three constructs were cloned all in S* background. Either one cysteine was exchanged to serine (S*-S121, S*-S124) or both of them (S*-S121/124). All three constructs were expressed and secreted in Huh7 cells. When analyzing the concentrated SN we saw that S*-S121 and S*-S124 were strongly secreted (Figure 4.18 b) lane 2 and 3), but the double mutant was drastically reduced in SN (lane 4).

Labeling of the SVP without addition of SDS or DTT prior to labeling revealed one shift in S*-HA. But also the S*-S121 and S*-S124 showed one tag added. As seen in the S-HA, the labeling band was only a minor proportion of the overall intensity. Nevertheless, both mutants resembled the S-HA phenotype, indicating that none of the two positions carried the exposed cysteine. In the double exchange construct no shift was detectable. However, the signal was very weak in comparison to the other samples. So it could be easily attributed to the signal of the shift being too weak to be detectable with this antibody.

Further experiments were conducted using a construct in which the three remaining cysteines C137, C138 and C139 were all exchanged to serines. Similarly to S*-S121/124 the construct S*-S137/138/139 was very weakly secreted (data not shown), which made it impossible to detect any shifts in non-reduced SVP.

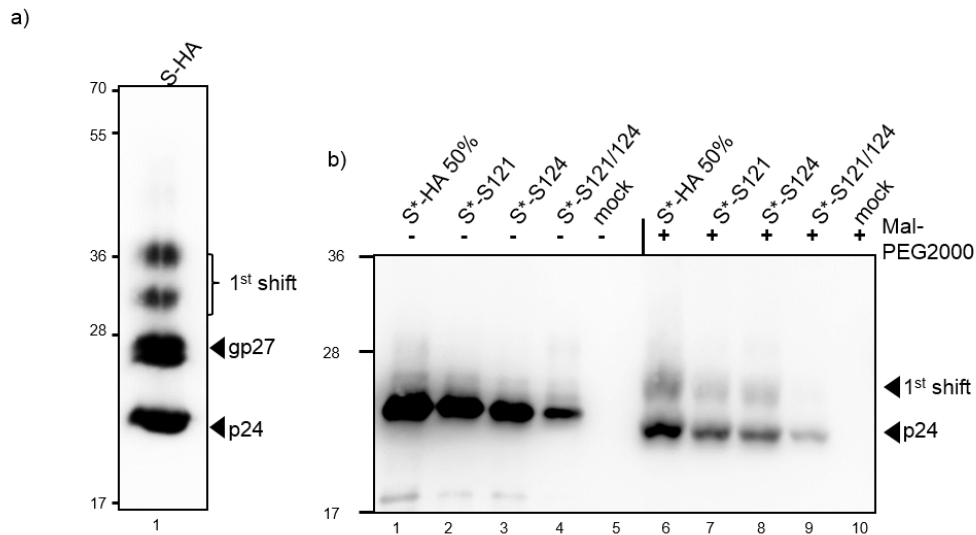


Figure 4.18: **Labeling of free cysteines in non-reduce secreted SVP SN** was collected three dpt and SN samples were concentrated through ultracentrifugation. Labeling was performed without prior denaturing of the samples. Reduction only took place prior to loading on the SDS-gel. In a) S-HA was used in combination with Mal-PEG5000. b) Showed *constructs labeled with Mal-PEG2000. Samples carried cysteine to serine exchanges in S*-HA background. Samples were detected using an anti-HA antibody.

4.3 Influence of disulfide bonds on antigenicity

To analyze the influence of disulfide bonds and free sulfides on the epitope of SVP we treated secreted particles with either NEM to block free cysteines or with DTT to reduce disulfide bonds. These samples from cell culture were sent to the diagnostic lab of the virology department at the Klinikum rechts der Isar. They were analyzed in an Abbot Architect HBsAg ELISA according to the standard procedures.

In Figure 4.19 a) the influence of NEM on the detectability is visible. With increasing amount of NEM the IU/ml detected was decreasing. However, it did not reach 0. And it was not a linear phenomenon, rather a logarithmic one. The same effect was there when DTT was added, the values decreased, but did not reach 0. The decrease in the NEM and DTT samples was comparable, as the values all cluster around the same value for the different concentrations.

To investigate if secretion of SVP was sufficient for the establishment of the epitope, different secretion competent constructs were analyzed. The supernatant was collected three dpt and directly transferred to the diagnostics department. The results from the sandwich ELISA can be seen in Figure 4.20. S-HA was detected with a mean of 1650 IU/ml. The different constructs were all below 1 IU/ml, which was very close to the cut-off of the machine. So all the constructs which were detected in SN (except S-SSS which served as a negative control) did not react with the diagnostic ELISA. We knew from the experiment before (Figure 4.19) that the test was sensitive to free SH groups as well as disulfide bonds. It seemed that secretion alone is no proof of the correct folding of S proteins.

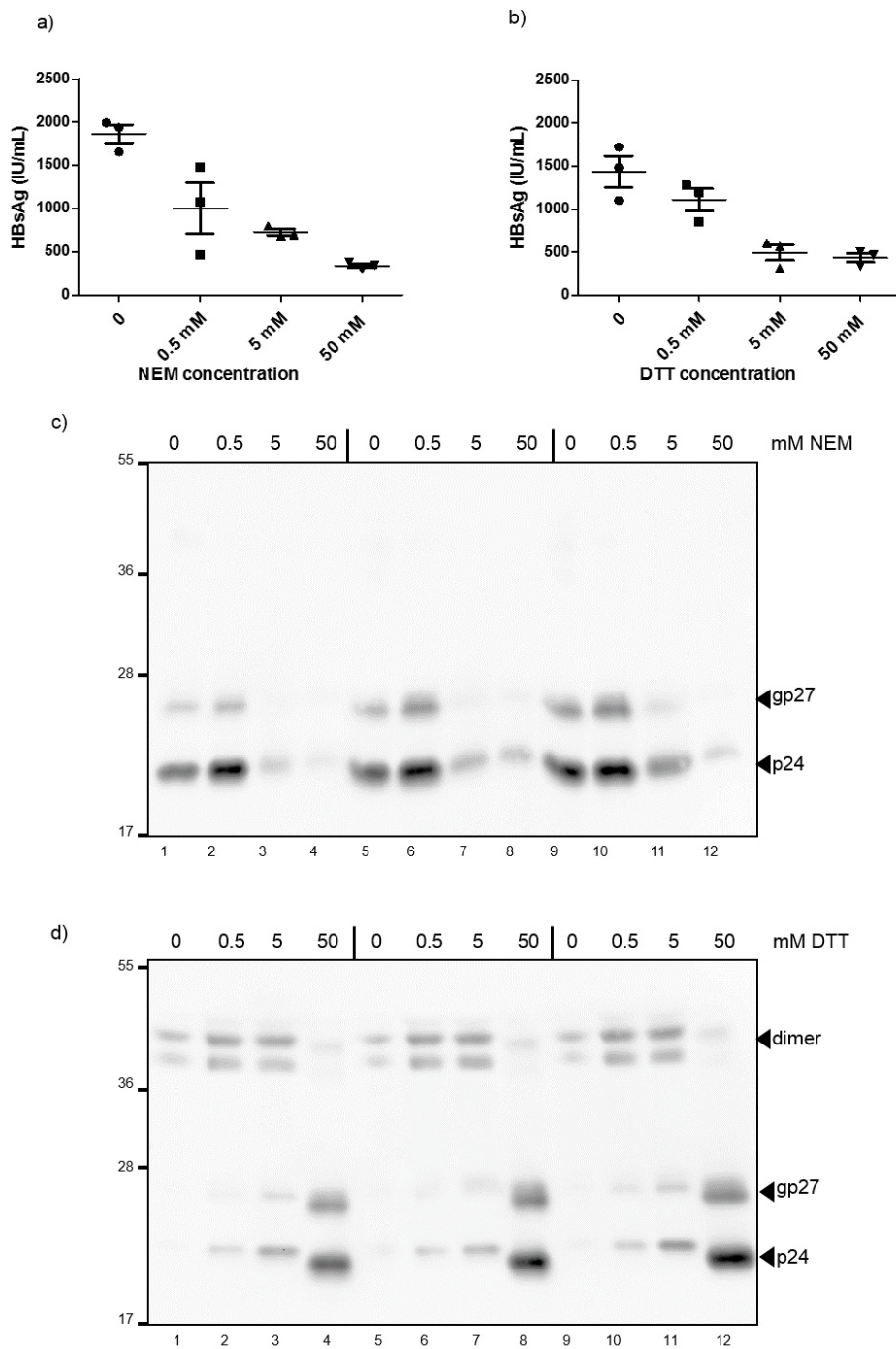


Figure 4.19: **Analysis of the antigenicity of wt S** Supernatant of wt S was collected three dpt and treated with different amounts of NEM or DTT. The samples were either analyzed via an Architect ELISA at the diagnostics department (a) and b)) or via WB (c) and d)). All three replicates are shown. In WB HB1 antibody was used to detect the samples.

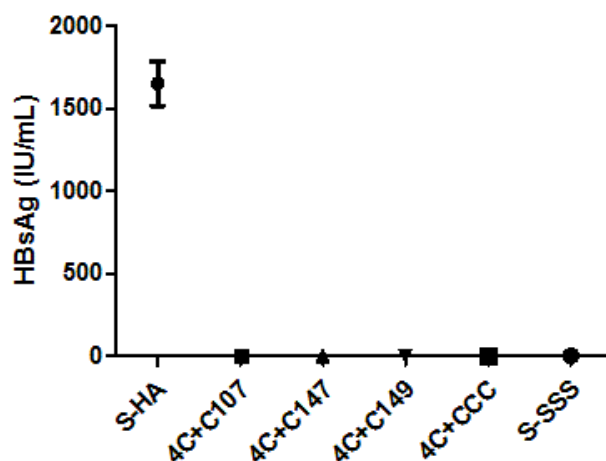


Figure 4.20: **Analysis of the antigenicity of secretion competent constructs** Supernatant of wt S was collected three dpt. The samples were analyzed via an Architect ELISA at the diagnostics department. All three replicates are shown.

4.4 Comparison of human SVP and SVP from yeast for vaccination

As described above, S proteins expressed in yeast cells are used for the production of the HBV vaccine. The samples used here were produced as so called "Cuban" strain (kind gift from Ulla Protzer). Due to the fact, that the samples were already highly purified, a Coomassie staining was performed. The samples were either treated with DTT (Figure 4.22 lane 2) or without DTT (lane 4) To analyze the disulfide pattern yHBsAg was labeled for free sulfides (lane 6) and for oxidized thiols (lane 7).

To begin with, yHBs is only present as p24, as yeast cells did not glycosylate S proteins. In contrast to patient samples or samples from eucaryotic cell culture, yeast samples were not mainly dimeric. When DTT was not added (lane 4), the particles were so extensively cross-linked through disulfide bonds, that the material was not running into the gel at all. So the size exceeded 250 kDa significantly.

Labeling of free thiols (lane 6) did not lead to a major shift. The main form was still monomer at 24 kDa and only a minor proportion ran at the boundary of stacking and separating gel. This would correspond to labeling of all 14 cysteines. On the contrary when disulfide bonds were labeled, no monomer was visible. All of the material shifted and was detectable at a height corresponding to 14 added Mal-PEG5000. This would indicate that all cysteines formed disulfide bonds, although it was not clear if inter- or intramolecular ones.

The results showed a different bonding pattern and as a next step we analyzed the influence

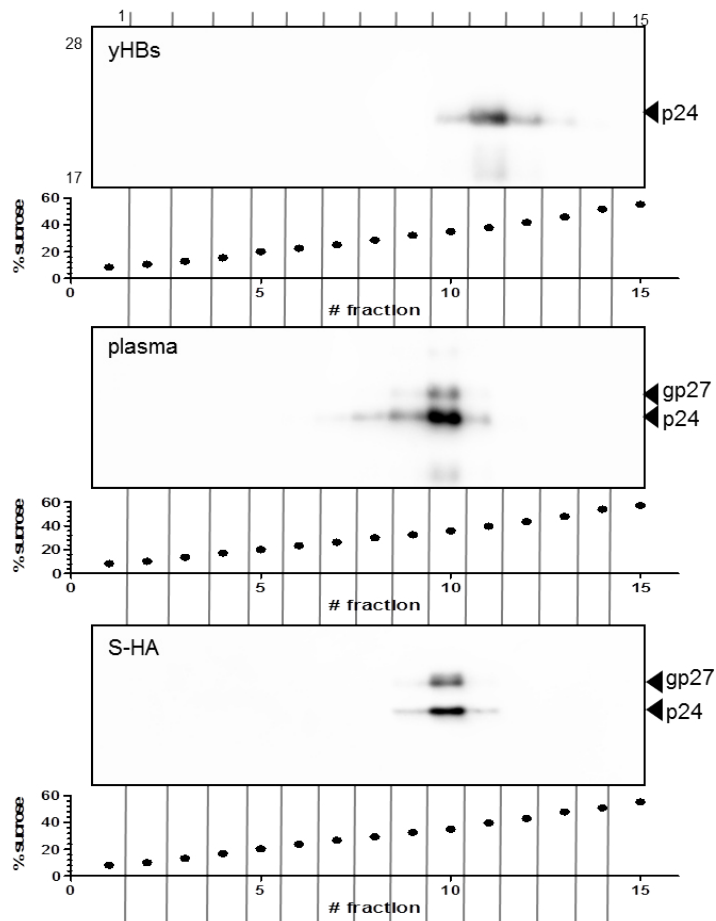


Figure 4.21: **Analysis of yeast HBs on sucrose gradient** Supernatant of S-HA was collected three dpt. The samples were loaded on top of a sucrose gradient. yHBs and plasma were analyzed using HB1-ab. S-HA was detected using HA-ab.

on the overall structure of the yeast particles. So sucrose gradient density centrifugation was performed with yeast samples, plasma samples and S-HA from cell culture. In Figure 4.21 the results can be seen. SVP from cell culture and from donors were both present in fraction 10, but yHBs had its main peak in fraction 11. This indicated also a different, denser structure of the SVP produced in yeast in comparison with human and eucaryotic cell culture samples.

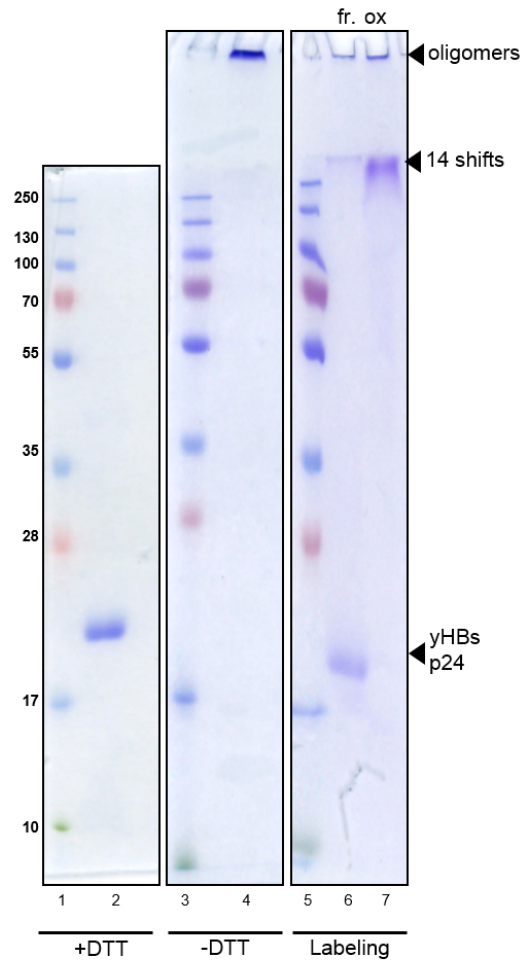


Figure 4.22: **Coomassie staining of yeast derived SVP +/- DTT and labeled for free and bound cysteines** Purified yeast samples were either treated with (2) or without DTT (4) or labeled for free (6) or oxidized cysteines (7). Samples were loaded on a SDS-gel and stained with Coomassie.

5 Discussion

5.1 Mal-PEG labeling as a method for analysis of cysteine status in secreted viral particles

Mal-PEG labeling or pegylation is used for mass-tagging of cysteines in proteins²⁶². The advantages are that for every SH group only one mass-tag is added, the reaction takes place under neutral pH conditions or below pH 7, the occurring adduct is stable in detergents and it is relatively specific^{261,266}.

Labeling of proteins with Mal-PEG was already used for human and yeast PDI, DsbD from *E.coli*, p53, acyl-coenzyme A:cholesterol acyltransferase and several plant proteins^{260,262,267-272}. One shortcoming of the method is that the sizes of the shifts do not correspond to the indicated mass of the PEG-tail. This means that Mal-PEG5000 does not cause an increase of 5 kDa in Western blot^{261,272}. This can be due to protein solvation and Mal-PEG's weak interaction with SDS^{268-270,272}. In this work we quantified the shift size in our experimental system and calculated it to be 12 ± 2.7 kDa, which was in accordance with the result from Lu and Deutsch which stated the shift to be ≥ 10 kDa²⁶¹. This group used a protein with around 25 kDa in size, comparable to S, and generated up to six shifts in their work²⁶¹. When our analysis of the shift (cf. Figure 4.13) was performed on their data a shift of 19 ± 4.7 kDa was the result. Another problem with our protein was the high number of cysteines. With 14 cysteine residues in S a maximum increase of ~ 205 kDa would be possible. This would result in a band at around 220 kDa in Western blot. So the first analysis was conducted with 4C+C107, which contains only five cysteines in total, and resulted in a shift of around 100 kDa. The data used for the analysis of the shift size did not include five shifts cf. Figure 4.12. The maximum number analyzed was four tags. So these measurement calculated a size of 84 kDa for four shifts. The increase from shift number 3 to 4 in this case was 19 kDa. So mathematically we can extrapolate this data, and calculate the size of S with five added tags to be around 103 kDa in 4C+C107. Furthermore, five shifts of a protein with circa 25 kDa in Lu and Deutsch's results would correspond to 119 kDa²⁶¹. As this corresponds to our observed 100 kDa result, the labeling of all five cysteines in 4C+C107 was achieved theoretically. Meaning all cysteine were accessible.

In a next step we tried to label all 14 cysteines in S-HA (Figure 4.12). The detectable band ran at around 230 kDa. However, at this sizes the migration pattern is not that accurate and not easy to determine. The band should theoretically run at around 220 KDa. Our result could therefore indicate that we labeled all 14 cysteines, but it could also only 13 or 12 could not be ruled out. Due to the fact that in this area the measurements and calculations are relatively uncertain.

It was also known that labeling of cysteines which are vicinal could cause problems^{267,270,273}. In S we have three cysteines directly next to each other, C137, C138 and C139. So it was impossible to determine if all of them could be labeled at the same time. So we cannot state for sure that all cysteines, especially the C13X, are all accessible at the same time.

This could be an explanation why not all cysteines could be labeled in Figure 4.17 c). A cysteine can either be free or oxidized and therefore be incorporated in a disulfide bond. So when a construct is labeled for free and oxidized cysteines, the sum should be the number of cysteines present in the protein. The results for S-HA revealed six free cysteines and seven oxidized ones. In total, S-HA carries 14 cysteines, so one of them was not labeled. This can be due to the fact that some of them are located too closely to each other in the primary sequence of S. Of course, the influence would only occur when the status of the two adjacent cysteines is the same. Nevertheless, the four cysteines in CL were accessible, so distances of only four cysteines (C65-C69) can be labeled with Mal-PEG5000 at the same time.

Besides, another obvious effect after labeling was the "ladder" which was generated. So most of the time more than one clear band was detectable. Sometimes protein monomers were still visible after labeling, for example S*-HA in (Figure 4.16). Or the labeling did not cause one clear shift but some or all of the shifts below were also visible as a "ladder" (Figure 4.17). This could be a hint to incomplete labeling, but when labeling yHBs almost all the material shifted and one clear band was visible in the Coomassie staining (Figure 4.22). Both experiments were performed with the same protocol. So maybe the high protein content in the lysate or the SN negatively influenced the labeling reaction. This ladder effect was visible in most of the papers published, sometimes stronger sometimes weaker^{260,262,267-272}. Lu and Deutsch found an influence of the labeling time on the ladder, but could not reduce side bands completely²⁶¹. As the effect was visible when labeled for free and for disulfide bonds in samples, the root cause seemed to be Mal-PEG itself. Even with a smaller Mal-PEG (2000) we still could see the ladder appearing after labeling. So this effect could not be reduced completely with cell culture samples. To sum it up, using a maleimide to mass-tag free and oxidized cysteines was a good way to examine the status of cysteines in S proteins. It was the first time to assign 13 out of 14 cysteines in secreted particles to be free or disulfide-linked. The protocol itself is easily adaptable to other proteins. Shortcomings of this methods are the number of cysteines detectable on Western blots, as good resolutions were only achieved with up to five shifts in S-

HA. Another problem was that we could not label all 14 cysteines, probably caused by cysteines neighboring each other directly.

5.2 The main form of S in SVP was dimeric

Most of the hypothesis concerning the form of S in SVP stated, that S assembles in oligomeric structures, though the influence was not only assigned to disulfide bonds^{150,151,274-276}. Gilbert et al. performed a microscopy analysis of secreted particles and concluded that S forms dimers²⁵⁹. Earlier dimers were described as the main structure recognized by antibodies produced after vaccination²⁷⁷.

Analyzing plasma without DTT revealed dimers which could only be connected via cysteines (Figure 4.5). This phenotype could be resembled with transient transfection of wt S and S-HA constructs into Huh7 cells. As SDS was added before loading the samples on an SDS-gel, the influence of lipids or other chemical bonds was diminished. In conclusion non-covalent bonds, which are denatured using SDS, could be the reason for the proposed oligomers in SVP postulated by other groups²⁷⁸. So for example electrostatic interactions or van der Waals forces could connect the dimers to higher oligomers.

Furthermore after 30 min dimers were again detectable in SN (Figure 4.5d)). The cells had been transcribing and translating S already for three days, which means that inside the cell a reservoir of translated proteins in different stages of maturation were present. So the time span could only cover the secretion process of proteins which were already inserted into vesicles and located close to the membrane. Huovila et al. described in their pulse-chase experiments, that they could detect S in SN after 2 h¹⁵². However, they analyzed the whole process of protein synthesis in their experiments, with the use of labeled methionine. Additionally, they described the formation of dimers as an early and quickly occurring process, taking place in the ER. In contrast to our findings Huovila et al. described oligomer formation in a pre-Golgi and post-ER compartment which did not contain PDI¹⁵². They could also show that S oligomers could be reduced to dimers when PDI was added to the corresponding environment¹⁵². We could show that disulfide-linked dimers were the main form in secreted subviral particles, and it was possible that these dimers were formed in the ER through PDI. However formation of disulfide-linked higher oligomers could not be shown in our experimental set-up. Nevertheless formation of oligomers through non-covalent bonds or the lipids of the SVP could not be ruled out, as we were focusing on disulfide bonds with our analysis.

C107 had the biggest impact on dimer formation of S. The construct 4C+C107 had the strongest dimer signal in secreted particles (Figure 4.8). The influence of C107 was known, as Mangold and Streek showed that exchange of this cysteine to alanine blocked secretion^{150,151}. In the 4C background, also either C147 or C149 alone were sufficient to form dimers and were secreted.

So it was supposed that the mutant C107A from Mangold et al. should be secreted, as it carries C147 and C149. Though the intensities in our experiments were very weak compared to S-HA (cf. Figure 4.8). Possibly, the signal from the other group in their experimental set-up with pulse-chase labeling was not strong enough to be recognized as such.

In lysate also dimers were visible. Yet it seemed that a certain threshold needed to be overcome to trigger the secretion. When the intensity of dimers and monomers was quantified, the proportion of dimers needed to exceed 10 %. Huovila et al. described that S oligomers were formed in the presence of PDI¹⁵². So it can be speculated that the quality control system of the ER requires S to be dimeric to be processed. What can be stated was that the constructs were inserted into the ER, as the glycosylation pattern was visible. As N-glycosylation only occurs within the ER, the insertion took place in all mutant constructs. As a consequence monomers, or incorrectly folded S proteins needed to be removed again from the ER to be degraded through the ubiquitin pathway in the cytosol^{279,280}.

This could be one possible explanation why some secretion-deficient constructs showed dimers in lysate. As our lysate blot always detects and displays different stages of protein maturation at the same time, the dimers detected are incorrectly folded and bound to be removed from the ER to be degraded. Indicating that these constructs were incorrectly folded, we could assume that in total up to 7 % of S proteins were misfolded and targeted for degradation.

Another hypothesis could be that only dimers were permitted to process to the Golgi compartment and therefore the secretory pathway. However, a problem could be that with dimer proportions below 10 % no particles could be formed. An explanation could be that a certain portion of dimers was needed to assemble to generate a particle and that for this simply not enough were present in close proximity at the same time point.

Not much is known about the way and steps S takes to be released from the cell as SVP. So if there was no direct process arranging the proteins to form SVP and we assumed a random process for budding of SVP, the trigger for that might be the correct number of S accumulating in close proximity. It is striking that spherical SVP have a more or less defined diameter of 20 nm and therefore also a defined curvature and a defined number of proteins^{137,172}. Based on this assumption, one could propose that some of our mutants did not form enough dimers in lysate so that at a later time point enough dimers were present to bud and form particles, which could be released as SVP.

5.3 A disulfide bond in the CL

The sequence of the CL was known to be highly conserved throughout *orthohepadnaviruses*. So in a first step the conservation of this region and of the cysteines throughout the *hepadnavirus* evolution was evaluated. Recently, a new group of hepadnaviruses was discovered which do not carry the envelope and are therefore called nakednaviruses²⁸¹. It is speculated by the authors that this early ancestor gained the envelope through insertion. So there was a split within the *hepadnavirus* between enveloped and non-enveloped viruses. Evolutionary the furthest away from *orthohepadnaviruses* containing S proteins are the parahepadnavirus. This group is the first diverging lineage in the clade of enveloped viruses, which was found in fish. They carry an envelope but lack the LL, which makes them a good comparison for sequence analysis of the S-ORF²⁸¹.

The analysis revealed that, as predicted, the LL showed no sequence similarity, due to the fact that this trait was gained later in the phylogenetic tree. The two TM domains, CL and the amphipathic helix, showed the highest identity ranging from 41 - 67 % (Figure 5.1). Within the CL three out of four cysteines are conserved, and also the distance between the residues is the same as in HBV circulating today. The cysteines corresponding to C76 in HBV had no equivalence in the fish sequence. Also nine other cysteines (the eight in LL and one in HCR) were not found in the out-branched sequence. There were only four cysteines in total in the fish sequence, the fourth one being present in the TM2 domain. It was located 5 aa residues before the corresponding C90 from the human sequence. So here we could show that the cysteines assigned to the CL loop today are highly conserved among enveloped *hepadnaviruses*.

One dogma in cell biology is that the redox state in the cytoplasm is too reducing to facilitate disulfide bond formation²⁸²⁻²⁸⁴. The only well described disulfide bonds formed in the cytoplasm of different cell types are influenced by reactive oxygen species (ROS)^{285,286}. In our experimental set-up this effect can mainly be neglected, as only transfection was performed with the cells. Besides the pH value in cell culture did not indicate major changes throughout the four days of culture in the plates. So it was a very remarkable feature of SVP that inside the CL evidence for a disulfide bond was found. After labeling for disulfide bonds 4C+C107 showed three shifts: one from the intermolecular bond establishing the dimer and two unassigned ones (cf. Figure 4.17). In CL four cysteines were present (C48, C65, C69 and C76) which were not dimeric in lysate (Figure 4.8), so they did not form an intermolecular bond, but an intramolecular bond. This was the first experimental proof for an intramolecular disulfide bond established in the cytoplasm of a cell, without special proteins encoded or oxidative stress.

As a fact, there are viruses which encode their own oxidative folding pathway, like vaccinia virus²⁸⁷⁻²⁸⁹. During the assembly process of this virus, proteins which are not located in the lumen of the ER become disulfide-linked²⁶⁵. Similarly to the findings presented here, in the

domain	identity (%)	sequence
N terminal	0	1 MGSAFQGLSF 10 W
		1 MENITSG 7 H
TM1	41	11 DLWVLFVLLVLLVFFLLIK 29 W
		8 FLGPELL VLQAGFFLLTR 24 H
CL	45	30 IHTILKAAD WWLISRSFLG TQTC PF RNTESPTSMHFKTD CP LTC GF RWTLV 82 W
		25 ILTIPQSLDSWW TSLNFLGGSPV CL GQNSQSPTSNHSPT SC PI CP GYRWM CL 77 H
TM2	54	83 RRSIIIF LC ILALVVIFWYLMawe 105 W
		78 RRFIIIFL CL IF LLVLLD 99 H
LL	0	106 PFT 108 W
		100 YQGM LPVCP LIPG STT ST GPCKTCT TPAQGNSMF FPSC CK TK PTDGN CTC IP IPSSW 156 H
amphipathic helix	67	109 AFVKRLWELGSV 120 W
		157 AFAKYLWEWASV 168 H
HCR	13	121 LGSYIFSHLSSQLGSVPTIQFIALLT WMIFYSHIPVWLH FL SEVTSWH FL QNGGF 176 W
		169 RFSWLSLLVPFVQWFVGLSPTVWLSAIWMMWYWG PS LYSIV SP FIPL PIFF CLWVYI 226 H

Figure 5.1: **Comparison of sequence similarities in HBsAg between fish and human**
 Analysis was sub-divided into the different sections of the S protein. Cysteines are marked in bold

vaccinia virus disulfide bonds were also detected on the cytoplasmic surface of integral proteins²⁶⁵. In contrast, they have specialized proteins catalyzing this process.

S is co-translationally inserted into the ER membrane and through several chemical interactions sets up a complex structure. It is known that already established and buried disulfide bonds cannot be reduced, not even inside the cytoplasm²⁸⁵. This could also be the case for the S protein. Suffner has already shown that the TM2 domain was interacting with the TM2 domain of a second S protein²⁵³. Here we demonstrated that dimers are set up by several intermolecular disulfide bonds. So it is possible, that the CL forms a complex structure which shields the cysteines in the loop form surrounding reducing cytoplasm. In conclusion, disulfide bonds which are established in this structure cannot be chemically reduced and cannot be isomerized. Besides, enzymes which can catalyze an isomerization of disulfide bonds are only present in the ER lumen²⁹⁰.

The formation of disulfide bonds itself is a process that does not need certain enzymes. An experimental procedure exists that is called "Dynamic Disulfide Scanning" which is used in transmembrane domains^{291,292}. There cysteines are inserted through mutations at different positions in TM domains of two proteins. These two proteins are stated to interact when close proximity exists between the residues and a disulfide bridge forms between the two proteins²⁹¹. This indicates that it is sufficient for cysteines to form disulfide bonds if they are close enough

and are not influenced by the surrounding milieu. Close enough means, that an established bond can be maintained over a distance of 2.3 Å²⁹³. This could also explain why it was not possible to determine the exact position of the disulfide bond in the CL. If the cysteines were all within the range of 2.3 Å to each other, bridges could occur between all of them. So it is possible that this disulfide bond is not a directed and catalyzed process, but a result of proximity.

This process seems essential, as the exchange of one of these cysteines in wt-background was sufficient to block secretion and also had a very strong dominant negative effect on secretion of S-HA (Figure 4.15). S-HA could not be secreted until a ratio of 16:1 wt:mutant was transfected. One model would be that the incorporation of a single mutant S in a SVP is sufficient to block secretion. Detected SVP in SN would then be particles which do not, by chance, contain a single mutated S protein. However, this would take place with a probability of $(\frac{16}{17})^{100} = 0.0023 = 0.23\%$. This does not correspond to the intensities measured in Figure 4.15. The 1:16 band was not 0.23 % as strong as S-HA alone.

Another explanation would be that in a single SVP with approximately 100 S proteins, a certain number of mutant proteins would be sufficient to inhibit the secretion of the whole particle. From the intensities of secreted particles in comparison to S-HA, we can draw statistical conclusions. Using the cumulative binomial distribution function, we can calculate the probability of a certain number of mutants being incorporated in a particle just by chance. In math the cumulative binomial distribution is described as

$$f(k, n, p) = Pr(k; n, p) = P(X = k) = \binom{n}{k} p^k (1 - p)^{n-k} \quad (5.1)$$

n = number of trials

k = number of successes

p = success probability for each trial

In our case $X=k$ is wrong, as we do not describe a fixed number of mutated S being inserted into a particle, but a maximum number of mutants. This means $X \leq k$. This however changes the formula to

$$f(k, n, p) = P(X \leq k) = \sum_{i=0}^k \binom{n}{i} p^i (1 - p)^{n-i} \quad (5.2)$$

The formula now sums up the single possibilities until the value k is reached. This means the probability of k-x, ., k-2, k-1 and k are calculated and the probabilities are summed up to answer the question: How likely is it, that maximum k mutated S proteins are inserted in one particle. A calculation of different probabilities with k values between 1 and 10 could be performed and the results could be compared with the secretion efficacy in Figure 4.15. If we took a ratio of 1:16 into account for our calculations, the parameters could be assumed as follows:

$$\begin{aligned}
n &= \text{number of } S \text{ proteins in one SVP} && = 100 \\
k &= \text{number of mutated proteins} \\
p &= \text{probability for insertion of mutated } S && = 1/17
\end{aligned}$$

With this we can calculate the probabilities for the different maximum values of k .

Table 5.1: Calculated probabilities according to formula 5.2. The different maximum values for k range from 1-10.

$X (X \leq k)$	P [%]
1	1.69
2	6.20
3	15.41
4	29.35
5	46.08
6	62.62
7	76.50
8	86.58
9	93.02
10	96.67

Comparison of these probabilities with the intensities of the secreted proteins at 1:16 in Figure 4.15 could hint at the maximum number of mutated S proteins inserted in SVP which still enabled secretion. The intensities in WB were 8.7 % (C48), 15.1 % (C65S), 11.1 % (C69) and 48.4 % (C76S) in comparison to S-HA. This would correspond to a maximum number of 3-5 mutated S in 100 S proteins in total. Interestingly this corresponded to the number of mutants we would expect if they were equally distributed:

$$k_{\text{equal.distr.}} = p * n = \frac{1}{17} * 100 = 5.88 \quad (5.3)$$

The impact of the exchange mutations differ in their influence with C48S having the strongest effect. In this case statistically only two mutated S were tolerable within 100 S-HA proteins.

A disulfide bond in the CL was also proposed earlier by Guerrero et al.²⁹⁴. However, they suggested an intermolecular bridge involving C48. Moreover, the influence of cysteines on the secretion had been investigated earlier by Mangold and Streek¹⁵⁰. For the cysteines in

CL they found out that C48, C65 and C69 are essential, but that C76 is dispensable. In contrast, we showed that also C76 was essential. The difference in the systems was the use of COS-7 cells, a monkey kidney cell line, the exchange of cysteine to alanine, the immune precipitation with a HBsAg antibody and the pulse-labeling. An effect of the cell line arising from monkeys can mainly be ruled out. HBV strains infecting monkeys like woolly monkey hepatitis B virus (WMHBV) or capuchin monkey hepatitis B virus (CMHBV) all carry a cysteine at position C76, so an influence through evolutionary selection can be ruled out. The only effect on secretion could arise from the exchange to alanine, instead of our cysteine. We exchanged the polar cysteine to a polar serine. Mangold and Streek used alanine instead, which is nonpolar. This could be an explanation, but is only speculative at this point.

To sum it up, the CL loop contains a disulfide bond which cannot directly be assigned to two cysteines. From the fact that the 4C construct is not dimeric in lysate, it can be concluded, that it needs to be an intramolecular disulfide bond. Through complex secondary and tertiary structures the disulfide bond may be shielded from the reducing environment of the cytoplasm. This bond is also complex enough to be conserved through the secretion process, as it was also detectable in secreted particles. Besides, the four cysteines in the CL are essential for secretion and have a dominant negative effect on the secretion of S-HA. Furthermore, this effect seemed to be "dose-dependent" on the number of mutant S proteins incorporated in the SVP.

5.4 Mapping of disulfide bonds and free sulfides in the S protein of HBV

The structure of S is not completely determined. Not only the disulfide bonds which are needed for the epitope are clearly assigned to certain residues. Also only two of the four transmembrane domains are experimentally proven¹⁴⁴. In contrast to the capsid, which was expressed in *E. coli* and was crystallized in 1999²⁹⁵, no structural analysis to this resolution was achieved with the envelope of S till today. One of the main problems is that the envelope proteins cannot be expressed in *E. coli*⁶¹⁻⁶⁴. Other expression systems also had major shortcomings, like the already discussed expression of S in yeast systems. To begin with, it was analyzed how conserved cysteine residues in S are among circulating sequences today, based on a data set generated by Schittl and Bruß²⁹⁶. The dataset was retrieved from NCBI and contained 3579 full length HBV sequences. The data for the 14 cysteine positions was retrieved and analyzed for conservation. So the cysteines at the indicated positions were counted and all other amino acids were summed up to calculate fractions. C221 was the least conserved one, with only 93.6 % of cysteine at the position. The results of the total numbers can be seen in Figure 5.2. Cysteines at position C76 and C221 are the most variable ones among all cysteines. However

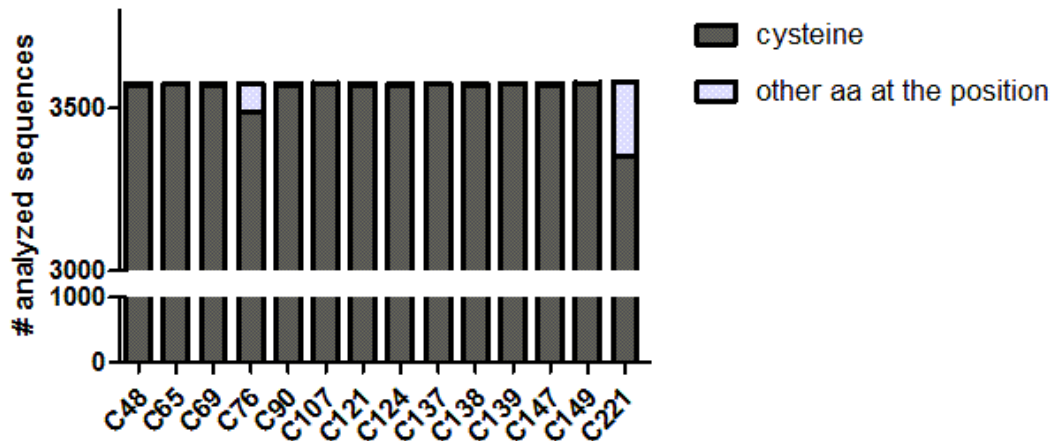


Figure 5.2: **Variability at the cysteine position among sequences from NCBI** The dataset from Schittl and Bruss²⁹⁶ was used for the analysis in which they retrieved 3579 full length HBV genome sequences from NCBI. Here the cysteine positions in S were analyzed. The total number of cysteines was counted and all other aa which were present at the indicated position.

they appear in more than 90 % of the sequences retrieved from NCBI. Overall cysteines are highly conserved among circulating strains today, indicating an important function within the protein.

Several models from previous studies came to different and mainly contradicting results concerning the disulfide bonding patten in S^{275,276,297}. Proposed was a double loop structure with disulfide bonds between C124-C137 and C139-C147²⁹⁷. But also a single loop with one bond between C121-C124 was proposed²⁷⁵. Mangold and Streek presumed two intermolecular bonds forming dimers and oligomers involving C121 and C147²⁷⁶. Furthermore, they proposed that at least one of the cysteines 76, 90 and 221 carries a free sulfide.

Labeling of all oxidized and all free cysteines in S-HA SN revealed seven oxidized and six free ones. It is known that S contains 14 cysteines, so one was not labeled in the experiment shown in Figure 4.17. This could mean that in reality it was either 8:6 or 7:7 oxidized:free cysteines. Due to the fact that S was dimeric, intermolecular disulfide bonds were needed to stabilize that protein interaction.

In fact, the number of intermolecular bonds can be even or uneven. Intramolecular bonds are always set up between two cysteines in the same protein and therefore need to cause an even numbered shift. We found that the dimer was stabilized through three intermolecular disulfide bonds. Knowing that intramolecular bonds always are even numbered, labels for oxidized cysteine in total needed to be uneven. $3 + 2*x = \text{inter} + \text{intra} = \text{total}$.

In conclusion, only seven oxidized and seven free cysteines were reasonable. Assigning three

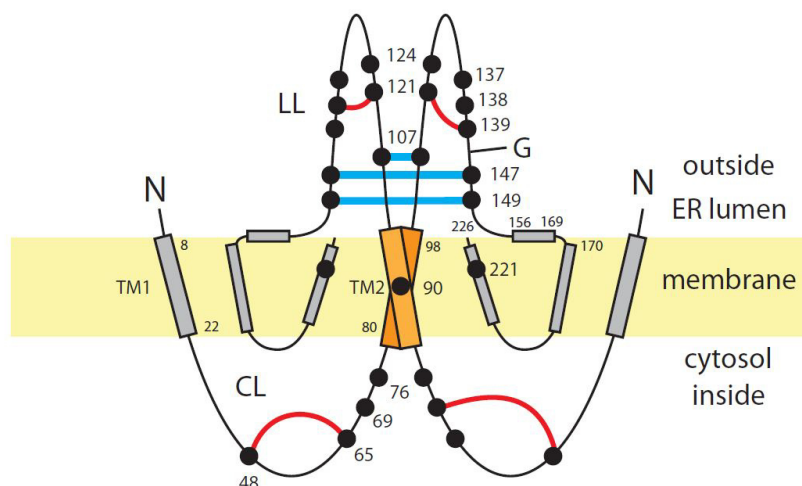


Figure 5.3: **Proposed model of the S protein dimer** Structural model of the S protein dimer with the symmetrical intermolecular disulfide bonds (blue). The proposed intramolecular bonds could not be pinpointed to specific positions and could only be assigned to a protein domain (red). Free SH groups were arranged accordingly, however C90 and C211 were shown to be free.

intermolecular bonds to the dimer stabilization leaves four residues incorporated in intramolecular cysteines. Two of these are located in the CL but could not be pinpointed down to certain positions (Figure 4.16).// We assume that disulfide bonds can only be established within the same "compartment" of the protein meaning that one intramolecular bond is either present between the two cysteines in the TM or in the LL. Franziska Zörndlein analyzed in her Master thesis (Figure 6.1) the shifts in 6C. She could show, that when labeled for disulfides, there was no difference between 4C and 6C. This in turn indicated that the two TM cysteines were free. So the missing shifts, corresponding to an intramolecular disulfidebond, needed to be located within the LL.

It could also be shown that one of the free cysteines was exposed on the surface of secreted particles. The position could be narrowed down to C137, C138 or C139 Figure 4.18. So with regard to the results presented in this work, the model with a double loop structure established through two bonds in LL including C149 could be refuted. However, the model from Ohnuma with a disulfide bond between C121 and C124 could be included in our existing working hypothesis²⁷⁵. This was the only model proposed so far, which did match with the results we presented in this work.

Last but not least, we could prove the prediction of Mangold and Streek that at least one of the three cysteines (C76, C90, C221) was free²⁷⁶. C90 and C221 were shown to be free and C76

could be free, although we could not assign the bond or the free -SH groups in the CL. Besides, the same group stated that C121 and C147 both form an intermolecular bridge to form dimers and oligomers. With the 4C+C147 construct forming dimers in SVP one of the two could be verified. However, the influence of C121 could not be shown with this experimental set-up. A possible explanation could be that the bridge of C121 would form later in the process and would need an initial contact, formed via C107, C147 and C149. A shortcoming of this model would be that another cysteine needs to form an intermolecular bond in a later step. Otherwise it would not match with our total number of oxidized cysteines.

With regard to the antigenicity we found out that disulfide bonds are essential for the epitope and the reactivity in Architect ELISA. Nevertheless, the restoration of the dimerization properties did not restore the ELISA signal. This suggested that another structural feature was necessary. The samples which were used for ELISA were used in WB as well. In Figure 4.19 when 5 mM of DTT were added to the samples, monomers were visible. In comparison the monomers with 5 mM DTT ran higher in the gel than the 50 mM DTT monomers. An explanation for this effect could be that the disulfide bonds were not completely reduced, this can also be seen in the strong dimer signal. So the monomers were still linked through cysteines, causing a different structure and letting the monomers run higher in the gel. This proposed intramolecular disulfide bond could have an influence on the ELISA signal. It is supposed that a domain between aa 137 and aa 147 is particularly interesting with respect to the epitope, as changes in this area disabled surface antigen recognition by neutralizing antibodies^{298,299}.

The epitope or epitopes detected in this ELISA are not published by the manufacturer. They described in their manual for the ARCHITECT HBsAg that they can detect the common escape mutant G145A with wt sensitivity. It was not clear, if the assay uses different antibodies or only one. It is described that monoclonal antibodies are used and in the description of the conjugate it is stated: "Conjugate: Anti-HBs (Goat, IgG) Acridinium Labeled Conjugate in MES buffer with protein stabilizers" (http://www.illexmedical.com/files/PDF/HBsAg_ARC.pdf).

We found out, that secretion alone was not sufficient for detection in this ELISA. So the structure established through intermolecular disulfide bonds was not enough to trigger binding of the antibodies in the system. Due to the fact, that the signal in Figure 4.19 did not reach 0, we assumed that more than one antibody was used. Nevertheless, an influence of the predicted intramolecular disulfide bond on the epitope was assumed. So the area between aa 121 and aa 139 might drastically influence the assay and therefore the epitope.

5.5 SVP from yeast differ from human SVP

Yeast cells are used for the production of HBsAg due to safety and cost reasons³⁰⁰. Nevertheless, HBsAg is neither secreted from yeast cells nor glycosylated^{52,63-71}. This leads to extensive purification and maturation steps during harvesting⁷³. KSCN treatment used in preparation has a strong denaturing effect on yHBs. It is therefore supposed that the disulfides generated under this conditions differ from native disulfides⁷². Nevertheless, an isomerization after removal of KSCN and incubation at 37 °C is proposed leading to a more native conformation of yHBsAg⁷². The yeast samples analyzed here did not show the same results we found in human and cell culture material. Yeast material was neither dimeric, nor did it carry free sulfides. All cysteines were linked in intra- and intermolecular disulfide bonds and no cysteine was free. When the material was not treated with DTT prior to loading, it was so extensively cross-linked that it did not run into the SDS-gel (Figure 4.22). The difference in the overall structure could also be shown in sucrose-density centrifugation. Human samples ran mainly in fraction 10 while yeast samples ran mainly in fraction 11. This indicated that the yeast particles sediment quicker than human plasma samples. Nevertheless, this can be a hint at the mass or the overall size which differs from plasma samples.

In summary, S from yeast cells differ from human or cell culture samples in their morphology and in their disulfide bond pattern. An explanation can be that the different connections in yHBs lead to an altered structure of the particle, which then differs in size. The disulfide bonds are set up artificially during the purification process and through the chemical treatment. All of them are linked in the end, although we showed that also free SH groups are part of SVP.

5.6 S protein oligomerization reveals influence of C65 and the TM2 domain

Suffner already showed that FACS-FRET analysis was a valid method to investigate the influence of certain domains or single mutations on the oligomerization properties of S²⁵³. In the beginning, the topology of the fusion constructs were analyzed, as it was not clear if the addition of the YFP or BFP influenced the insertion of the S proteins in the ER membrane³⁰¹. It was clear that the orientation of the LL was correct, as the typical glycosylation pattern was visible in Figure 4.2. Nevertheless, any influence of the large fusion protein added to the N terminus of S needed to be ruled out. After preparation of microsomes the proteins were digested with trypsin, but without prior opening of the lipids with NP40 no digestion was visible. This indicated correct insertion of the proteins into the ER. However, when the fused type I secretion signal was deleted from the sequence (YFP*-S and BFP*-S), BFP*-S behaved differently than BFP-S. The migration pattern in the gel and the stability towards trypsin treatment changed.

BFP-S ran higher in the gel than BFP*-S due to covalent modifications in the ER²⁵⁸. The influence of TM2 on the oligomerization has already been proven before^{253,302}. In combination with exchange of all cysteines in CL and the point mutation C65S (S-CS-C65S-TM2) the FRET signal could be almost completely reduced. This was interpreted as no interaction. However the exchange of TM2 with a poly-alanine sequence and the mutation C65S did not reduce FRET signals inside cells (S-C65S-TM2). This could be explained with the results discussed above. As in the construct (S-C65S-TM2) the C107, C147 and C149 were all present, a dimer was stabilized in the lysate, which was detectable as a very strong interaction, with a high FRET-signal. The influence of the exchanged TM2 seemed not to hinder this interaction. It was possible that the two interactions were independent from each other and in lysate the disulfide bonds were compensating the TM2-TM2 interaction. Besides the influence of TM2 and the cysteines in the LL, a striking impact of C65 was demonstrated. This was also shown with the co-transfection experiments performed earlier. The proposed disulfide bond in LL could be an explanation for the influence of the exchange of this cysteine. Why only this cysteine had such a huge impact on FACS-FRET, cannot be elucidated.

5.7 Outlook

To determine the missing positions of the predicted disulfide bond, further constructs could be cloned. The exchange of pairwise cysteines from C121 to C139 (10 constructs) and the subsequent labeling should reveal the disulfide bond. A more structural approach could be the determination of disulfide bonds through mass-spectrometry. Problems with S proteins are in this case that native S proteins are not cleaved by trypsin. But it could be a possibility to generate cleaving sites at determined positions which do not influence the predicted disulfide bond.

Also an analysis of the secretion pathway through microscopy or separation of the organelles would be beneficial. If the compartments through which SVP are secreted were known, the influence of pH, enzymes or other specific properties could be elucidated. As a consequence, the different steps in maturation of SVP could be analyzed and assigned to distinguished cellular compartments.

Another method would be NMR in combination with nanodiscs. In nanodiscs the dimer can be inserted into a compartment with phospholipids. This approach is mainly used for membrane proteins and was used with proteins containing only one transmembrane domain or several TM domains. The advantage of this method would be the possibility to visualize the dimer in a membrane. With this, the native conformation can be kept and the loops would be analyzed with the TM domains being inserted in a membrane-like structure. Problems which needed to be addressed would be how to insert S into the disc. As a first step the proteins (in our case SVP)

needed to be purified and then the proteins can be transiently solubilized with a detergent in the presence of phospholipids and an encircling amphipathic helical protein belt^{303,304}. Dimers which were established through disulfide bonds were rather stable in our set-up, so that the incorporation of dimers into nanodiscs should be possible.

If the proteins were inserted into the discs, those could be analyzed using NMR and generating high-resolution results of the dimer and the bonds establishing the structure. If this approach works, interesting comparisons would be with the fish hepadnaviruses or the duck hepatitis B virus (DHBV). Both of them only carry the envelope but do not contain the LL. This could show the influence of the LL on structure and stability of SVP.

Bibliography

- [1] A. Lurman, Eine icterus epidemic *Berl Klin Wochenschr*, vol. 22, no. 20, p. 23, 1885.
- [2] B. S. Blumberg and H. J. Alter, A new antigen in leukemia sera *Jama*, vol. 191, no. 7, pp. 541–546, 1965.
- [3] A. Prince, Relation of Australia and SH antigens *Lancet*, vol. 2, no. 7565, pp. 462 – 463, 1968.
- [4] D. Dane, C. Cameron, and M. Briggs, Virus-like particles in serum of patients with Australia-antigen-associated hepatitis *The Lancet*, vol. 295, no. 7649, pp. 695–698, 1970.
- [5] WHO, “Hepatitis b fact sheet.”
- [6] C. W. Shepard, E. P. Simard, L. Finelli, A. E. Fiore, and B. P. Bell, Hepatitis B virus infection: epidemiology and vaccination *Epidemiol Rev*, vol. 28, pp. 112–25, 2006. Shepard, Colin W Simard, Edgar P Finelli, Lyn Fiore, Anthony E Bell, Beth P Journal Article Review United States Epidemiol Rev. 2006;28:112-25. Epub 2006 Jun 5.
- [7] D. Ganem and A. M. Prince, Hepatitis B virus infection—natural history and clinical consequences *New England Journal of Medicine*, vol. 350, no. 11, pp. 1118–1129, 2004.
- [8] D. Lavanchy, Hepatitis B virus epidemiology, disease burden, treatment, and current and emerging prevention and control measures *Journal of viral hepatitis*, vol. 11, no. 2, pp. 97–107, 2004.
- [9] A. Schweitzer, J. Horn, R. T. Mikolajczyk, G. Krause, and J. J. Ott, Estimations of worldwide prevalence of chronic hepatitis B virus infection: a systematic review of data published between 1965 and 2013 *The Lancet*, vol. 386, no. 10003, pp. 1546–1555, 2015.
- [10] D. Ganem, Persistent infection of humans with hepatitis B virus: mechanisms and consequences *Review of Infectious Diseases*, vol. 4, no. 5, pp. 1026–1047, 1982.
- [11] L. G. Davis, D. Weber, and S. Lemon, Horizontal transmission of hepatitis B virus *The Lancet*, vol. 333, no. 8643, pp. 889–893, 1989.

- [12] G. B. Yao, Importance of perinatal versus horizontal transmission of hepatitis B virus infection in China *Gut*, vol. 38 Suppl 2, pp. S39–42, 1996. Yao, G B Journal Article Review England *Gut*. 1996;38 Suppl 2:S39-42.
- [13] E. Franco, B. Bagnato, M. G. Marino, C. Meleleo, L. Serino, and L. Zaratti, Hepatitis B: Epidemiology and prevention in developing countries *World journal of hepatology*, vol. 4, no. 3, p. 74, 2012.
- [14] M. J. Alter, Epidemiology and prevention of hepatitis B in *Seminars in liver disease*, vol. 23-01, pp. 039–046, Copyright© 2002 by Thieme Medical Publishers, Inc., 333 Seventh Avenue, New York, NY 10001, USA. Tel.:+ 1 (212) 584-4662, 2003.
- [15] V. W. Wong, H. Reesink, H. H. Ip, P. N. Lelie, E. Reerink-Brongers, C. Yeung, and H. Ma, Prevention of the HBsAg carrier state in newborn infants of mothers who are chronic carriers of HBsAg and HBeAg by administration of hepatitis-B vaccine and hepatitis-B immunoglobulin: double-blind randomised placebo-controlled study *The Lancet*, vol. 323, no. 8383, pp. 921–926, 1984.
- [16] Z.-Y. Xu, C.-B. Liu, D. P. Francis, R. H. Purcell, Z.-L. Gun, S.-C. Duan, R.-J. Chen, H. S. Margolis, C.-H. Huang, and J. E. Maynard, Prevention of perinatal acquisition of hepatitis B virus carriage using vaccine: preliminary report of a randomized, double-blind placebo-controlled and comparative trial *Pediatrics*, vol. 76, no. 5, pp. 713–718, 1985.
- [17] I. C. o. T. o. Viruses, A. King, M. Adams, E. Lefkowitz, and E. Carstens, *Virus Taxonomy: Classification and Nomenclature of Viruses : Ninth Report of the International Committee on Taxonomy of Viruses*. Academic Press, 2011.
- [18] S. Schaefer, Hepatitis B virus taxonomy and hepatitis B virus genotypes *World Journal of Gastroenterology*, vol. 13, no. 1, p. 14, 2007.
- [19] C. Chu and A. S. Lok, Clinical significance of hepatitis B virus genotypes *Hepatology*, vol. 35, no. 5, pp. 1274–1276, 2002.
- [20] H. Norder, A. Courouce, P. Coursaget, J. Echevarria, S. Lee, I. Mushahwar, B. Robertson, S. Locarnini, and L. Magnius, Genetic diversity of hepatitis B virus strains derived worldwide: genotypes, subgenotypes, and HBsAg subtypes *Intervirology*, vol. 47, pp. 289 – 309, 2004.
- [21] A. Kramvis, K. Arakawa, M. C. Yu, R. Nogueira, D. O. Stram, and M. C. Kew, Relationship of serological subtype, basic core promoter and precore mutations to genotypes/subgenotypes of hepatitis B virus *Journal of medical virology*, vol. 80, no. 1, pp. 27–46, 2008.

- [22] B. K. Kim, P. A. Revill, and S. H. Ahn, HBV genotypes: relevance to natural history, pathogenesis and treatment of chronic hepatitis B *Antiviral therapy*, vol. 16, no. 8, p. 1169, 2011.
- [23] S. Tong, J. Li, J. R. Wands, and Y.-m. Wen, Hepatitis B virus genetic variants: biological properties and clinical implications *Emerging microbes & infections*, vol. 2, no. 3, p. e10, 2013.
- [24] A. Kramvis, Genotypes and genetic variability of hepatitis B virus *Intervirology*, vol. 57, no. 3-4, pp. 141–150, 2014.
- [25] S. Tong and P. Revill, Overview of hepatitis B viral replication and genetic variability *Journal of hepatology*, vol. 64, no. 1, pp. S4–S16, 2016.
- [26] E. Orito, M. Mizokami, Y. Ina, E. N. Moriyama, N. Kameshima, M. Yamamoto, and T. Gojobori, Host-independent evolution and a genetic classification of the hepadnavirus family based on nucleotide sequences *Proceedings of the National Academy of Sciences*, vol. 86, no. 18, pp. 7059–7062, 1989.
- [27] D. Paraskevis, G. Magiorkinis, E. Magiorkinis, S. Ho, R. Belshaw, J. Allain, and A. Hatzakis, Dating the origin and dispersal of hepatitis B virus infection in humans and primates *Hepatology*, vol. 57, pp. 908 – 916, 2013.
- [28] R. S. Tedder, S. L. Bissett, R. Myers, and S. Ijaz, The ‘Red Queen’ dilemma—running to stay in the same place: reflections on the evolutionary vector of HBV in humans *Antivir Ther*, vol. 18, no. 3, 2013.
- [29] I. E. Andernach, O. E. Hunewald, and C. P. Muller, Bayesian inference of the evolution of HBV/E *PLoS One*, vol. 8, no. 11, p. e81690, 2013.
- [30] M. A. Fares and E. C. Holmes, A revised evolutionary history of hepatitis B virus (HBV) *Journal of molecular evolution*, vol. 54, no. 6, pp. 807–814, 2002.
- [31] S. Günther, G. Sommer, F. Von Breunig, A. Iwanska, T. Kalinina, M. Sterneck, and H. Will, Amplification of full-length hepatitis B virus genomes from samples from patients with low levels of viremia: frequency and functional consequences of PCR-introduced mutations *Journal of clinical microbiology*, vol. 36, no. 2, pp. 531–538, 1998.
- [32] R. Bouckaert, M. V. Alvarado-Mora, J. R. Pinho, *et al.*, Evolutionary rates and HBV: issues of rate estimation with Bayesian molecular methods *Antivir Ther*, vol. 18, no. 3 Pt B, pp. 497–503, 2013.

- [33] A. Kramvis, M. Kew, and G. Francois, Hepatitis B virus genotypes *Vaccine*, vol. 23, no. 19, pp. 2409–2423, 2005.
- [34] A. Kramvis and M. Kew, Relationship of genotypes of hepatitis B virus to mutations, disease progression and response to antiviral therapy *Journal of viral hepatitis*, vol. 12, no. 5, pp. 456–464, 2005.
- [35] H. Yu, Q. Yuan, S.-X. Ge, H.-Y. Wang, Y.-L. Zhang, Q.-R. Chen, J. Zhang, P.-J. Chen, and N.-S. Xia, Molecular and phylogenetic analyses suggest an additional hepatitis B virus genotype “I” *PloS one*, vol. 5, no. 2, p. e9297, 2010.
- [36] K. Tatematsu, Y. Tanaka, F. Kurbanov, F. Sugauchi, S. Mano, T. Maeshiro, T. Nakayoshi, M. Wakuta, Y. Miyakawa, and M. Mizokami, A genetic variant of hepatitis B virus divergent from known human and ape genotypes isolated from a Japanese patient and provisionally assigned to new genotype J *Journal of virology*, vol. 83, no. 20, pp. 10538–10547, 2009.
- [37] W. Shi, Z. Zhang, C. Ling, W. Zheng, C. Zhu, M. J. Carr, and D. G. Higgins, Hepatitis B virus subgenotyping: history, effects of recombination, misclassifications, and corrections *Infection, genetics and Evolution*, vol. 16, pp. 355–361, 2013.
- [38] P. Coursaget, B. Yvonnet, J. Chotard, P. Vincelot, M. Sarr, C. Diouf, J. Chiron, and I. Diop-Mar, Age-and sex-related study of hepatitis B virus chronic carrier state in infants from an endemic area (Senegal) *Journal of medical virology*, vol. 22, no. 1, pp. 1–5, 1987.
- [39] N. C. Tassopoulos, G. J. Papaevangelou, M. H. Sjogren, A. Roumeliotou-Karayannis, J. L. Gerin, and R. H. Purcell, Natural history of acute hepatitis B surface antigen-positive hepatitis in Greek adults *Gastroenterology*, vol. 92, no. 6, pp. 1844–1850, 1987.
- [40] R. P. Beasley, Hepatitis B virus. The major etiology of hepatocellular carcinoma *Cancer*, vol. 61, no. 10, pp. 1942–1956, 1988.
- [41] C. Seeger and W. S. Mason, Hepatitis B Virus Biology *Microbiology and Molecular Biology Reviews*, vol. 64, no. 1, pp. 51–68, 2000. 0003[PII] 10704474[pmid] *Microbiol Mol Biol Rev*.
- [42] B. Rehermann and M. Nascimbeni, Immunology of hepatitis B virus and hepatitis C virus infection *Nature Reviews Immunology*, vol. 5, no. 3, pp. 215–229, 2005.
- [43] M. Dandri and S. Locarnini, New insight in the pathobiology of hepatitis B virus infection *Gut*, vol. 61, no. Suppl 1, pp. i6–i17, 2012.

- [44] T. Bauer, M. Sprinzl, and U. Protzer, Immune control of hepatitis B virus *Digestive Diseases*, vol. 29, no. 4, pp. 423–433, 2011.
- [45] J. Ott, G. Stevens, J. Groeger, and S. Wiersma, Global epidemiology of hepatitis B virus infection: new estimates of age-specific HBsAg seroprevalence and endemicity *Vaccine*, vol. 30, no. 12, pp. 2212–2219, 2012.
- [46] J. H. MacLachlan and B. C. Cowie, Hepatitis B virus epidemiology *Cold Spring Harbor perspectives in medicine*, vol. 5, no. 5, p. a021410, 2015.
- [47] R. Beasley, L. Hwang, C. Lin, C. Stevens, K. Wang, T. Sun, F. Hsieh, and W. Szmuness, Hepatitis B immune globulin (HBIG) efficacy in the interruption of perinatal transmission of hepatitis B virus carrier state *Initial report of a randomised double-blind placebo-controlled trial. Lancet*, vol. 2, no. 8243, pp. 388 – 393, 1981.
- [48] R. P. Beasley, L. Y. Hwang, G. C. Lee, C. C. Lan, C. H. Roan, F. Y. Huang, and C. L. Chen, Prevention of perinatally transmitted hepatitis B virus infections with hepatitis B immune globulin and hepatitis B vaccine *Lancet*, vol. 2, no. 8359, pp. 1099–102, 1983. Beasley, R P Hwang, L Y Lee, G C Lan, C C Roan, C H Huang, F Y Chen, C L Clinical Trial Journal Article Randomized Controlled Trial Research Support, Non-U.S. Gov't England *Lancet*. 1983 Nov 12;2(8359):1099-102.
- [49] B. J. McMahon, W. L. Alward, D. B. Hall, W. L. Heyward, T. R. Bender, D. P. Francis, and J. E. Maynard, Acute hepatitis B virus infection: relation of age to the clinical expression of disease and subsequent development of the carrier state *J Infect Dis*, vol. 151, no. 4, pp. 599–603, 1985. McMahon, B J Alward, W L Hall, D B Heyward, W L Bender, T R Francis, D P Maynard, J E Journal Article United states *J Infect Dis*. 1985 Apr;151(4):599-603.
- [50] E. E. Mast, H. S. Margolis, A. E. Fiore, E. W. Brink, S. T. Goldstein, S. A. Wang, L. A. Moyer, B. P. Bell, and M. J. Alter, A comprehensive immunization strategy to eliminate transmission of hepatitis B virus infection in the United States *MMWR*, vol. 54, no. 16, pp. 1–32, 2005.
- [51] T. Moriyama, S. Guilhot, K. Klopchin, B. Moss, C. A. Pinkert, R. D. Palmiter, R. L. Brinster, O. Kanagawa, and F. V. Chisari, Immunobiology and pathogenesis of hepatocellular injury in hepatitis B virus transgenic mice *Science*, vol. 248, no. 4953, pp. 361–364, 1990.
- [52] J. Stephenne, Recombinant versus plasma-derived hepatitis B vaccines: issues of safety, immunogenicity and cost-effectiveness *Vaccine*, vol. 6, no. 4, pp. 299–303, 1988.

- [53] G. A. Cabral, F. Marciano-Cabral, G. A. Funk, Y. Sanchez, F. B. Hollinger, J. L. Melnick, and G. R. Dreesman, Cellular and humoral immunity in guinea pigs to two major polypeptides derived from hepatitis B surface antigen *Journal of General Virology*, vol. 38, no. 2, pp. 339–350, 1978.
- [54] W. H. Organization *et al.*, Hepatitis B vaccines. *Weekly epidemiological record*, vol. 84, no. 40, pp. 405–419, 2009.
- [55] W. J. McAleer, E. B. Buynak, R. Z. Maigetter, D. E. Wampler, W. J. Miller, and M. R. Hilleman, Human hepatitis B vaccine from recombinant yeast *Nature*, vol. 307, no. 5947, p. 178, 1984.
- [56] M. Hilleman, Yeast recombinant hepatitis B vaccine *Infection*, vol. 15, no. 1, pp. 3–7, 1987.
- [57] E. Mast, F. Mahoney, M. Kane, and H. Margolis, Hepatitis B vaccine *Vaccines*, vol. 5, pp. 205–42, 2004.
- [58] S. R. Bialek, W. A. Bower, R. Novak, L. Helgenberger, S. B. Auerbach, I. T. Williams, and B. P. Bell, Persistence of protection against hepatitis B virus infection among adolescents vaccinated with recombinant hepatitis B vaccine beginning at birth: a 15-year follow-up study *The Pediatric infectious disease journal*, vol. 27, no. 10, pp. 881–885, 2008.
- [59] S. Viviani, A. Jack, A. Hall, N. Maine, M. Mendy, R. Montesano, and H. Whittle, Hepatitis B vaccination in infancy in The Gambia: protection: against carriage at 9 years of age *Vaccine*, vol. 17, no. 23-24, pp. 2946–2950, 1999.
- [60] A. Floreani, V. Baldo, M. Cristofolletti, G. Renzulli, A. Valeri, C. Zanetti, and R. Trivello, Long-term persistence of anti-HBs after vaccination against HBV: an 18 year experience in health care workers *Vaccine*, vol. 22, no. 5-6, pp. 607–610, 2004.
- [61] J. C. Edman, R. A. Hallewell, P. Valenzuela, H. M. Goodman, and W. J. Rutter, Synthesis of hepatitis B surface and core antigens in *E. coli* *Nature*, vol. 291, no. 5815, p. 503, 1981.
- [62] Y. Fujisawa, Y. Ito, R. Sasada, Y. Ono, K. Igarashi, R. Marumoto, M. Kikuchi, and Y. Sugino, Direct expression of hepatitis B surface antigen gene in *E coli* *Nucleic acids research*, vol. 11, no. 11, pp. 3581–3591, 1983.
- [63] E.-J. Kim, Y.-K. Park, H.-K. Lim, Y.-C. Park, and J.-H. Seo, Expression of hepatitis B surface antigen S domain in recombinant *Saccharomyces cerevisiae* using GAL1 promoter *Journal of biotechnology*, vol. 141, no. 3-4, pp. 155–159, 2009.

- [64] P. Valenzuela, A. Medina, W. Rutter, G. Ammerer, and B. Hall, Synthesis and assembly of hepatitis B virus surface antigen particles in yeast *Nature*, vol. 298, pp. 347 – 350, 1982.
- [65] Z. A. Janowicz, K. Melber, A. Merckelbach, E. Jacobs, N. Harford, M. Comberbach, and C. P. Hollenberg, Simultaneous expression of the S and L surface antigens of hepatitis B, and formation of mixed particles in the methylotrophic yeast, *Hansenula polymorpha* *Yeast*, vol. 7, no. 5, pp. 431–443, 1991.
- [66] J. Cregg, J. Tschopp, C. Stillman, R. Siegel, M. Akong, W. Craig, R. Buckholz, K. Madden, P. Kellaris, G. Davis, *et al.*, High-Level Expression and Efficient Assembly of Hepatitis B Surface Antigen in the Methylotrophic Yeast, *Pichia Pastoris* *Nature Biotechnology*, vol. 5, no. 5, p. 479, 1987.
- [67] E. Patzer, G. Nakamura, C. Simonsen, A. Levinson, and R. Brands, Intracellular assembly and packaging of hepatitis B surface antigen particles occur in the endoplasmic reticulum *Journal of virology*, vol. 58, no. 3, pp. 884–892, 1986.
- [68] S. Kuroda, T. Miyazaki, S. Otaka, and Y. Fujisawa, *Saccharomyces cerevisiae* can release hepatitis B virus surface antigen (HBsAg) particles into the medium by its secretory apparatus *Applied microbiology and biotechnology*, vol. 40, no. 2-3, pp. 333–340, 1993.
- [69] A. Vassileva, D. A. Chugh, S. Swaminathan, and N. Khanna, Expression of hepatitis B surface antigen in the methylotrophic yeast *Pichia pastoris* using the GAP promoter *Journal of biotechnology*, vol. 88, no. 1, pp. 21–35, 2001.
- [70] H. Lünsdorf, C. Gurramkonda, A. Adnan, N. Khanna, and U. Rinas, Virus-like particle production with yeast: ultrastructural and immunocytochemical insights into *Pichia pastoris* producing high levels of the Hepatitis B surface antigen *Microbial cell factories*, vol. 10, no. 1, p. 48, 2011.
- [71] C. Gurramkonda, A. Adnan, T. Gäbel, H. Lünsdorf, A. Ross, S. K. Nemani, S. Swaminathan, N. Khanna, and U. Rinas, Simple high-cell density fed-batch technique for high-level recombinant protein production with *Pichia pastoris*: Application to intracellular production of Hepatitis B surface antigen *Microbial cell factories*, vol. 8, no. 1, p. 13, 2009.
- [72] Q. Zhao, Y. Wanga, D. Freedb, T.-M. Fub, J. A. Gimenez, R. D. Sitrina, and M. W. Washabaugh, Maturation of recombinant hepatitis B virus surface antigen particles *Human vaccines*, vol. 2, no. 4, pp. 174–180, 2006.

- [73] C. Gurramkonda, M. Zahid, S. K. Nemani, A. Adnan, S. K. Gudi, N. Khanna, T. Ebensen, H. Lünsdorf, C. A. Guzmán, and U. Rinas, Purification of hepatitis B surface antigen virus-like particles from recombinant *Pichia pastoris* and in vivo analysis of their immunogenic properties *Journal of Chromatography B*, vol. 940, pp. 104–111, 2013.
- [74] M.-F. Yuen and C.-L. Lai, Treatment of chronic hepatitis B: Evolution over two decades *Journal of gastroenterology and hepatology*, vol. 26, pp. 138–143, 2011.
- [75] N. A. Terrault, N. H. Bzowej, K.-M. Chang, J. P. Hwang, M. M. Jonas, and M. H. Murad, AASLD guidelines for treatment of chronic hepatitis B *Hepatology*, vol. 63, no. 1, pp. 261–283, 2016.
- [76] F. Dianzani, Biological basis for the clinical use of interferon. *Gut*, vol. 34, no. 2 Suppl, pp. S74–S76, 1993.
- [77] L. P. Jordheim, D. Durantel, F. Zoulim, and C. Dumontet, Advances in the development of nucleoside and nucleotide analogues for cancer and viral diseases *Nature reviews Drug discovery*, vol. 12, no. 6, p. 447, 2013.
- [78] M. G. Ghany and E. C. Doo, Antiviral resistance and hepatitis B therapy *Hepatology*, vol. 49, no. S5, pp. S174–S184, 2009.
- [79] Y.-S. Lim, Management of antiviral resistance in chronic hepatitis B *Gut and liver*, vol. 11, no. 2, p. 189, 2017.
- [80] H. Yan, G. Zhong, G. Xu, W. He, Z. Jing, Z. Gao, Y. Huang, Y. Qi, B. Peng, H. Wang, L. Fu, M. Song, P. Chen, W. Gao, B. Ren, Y. Sun, T. Cai, X. Feng, J. Sui, and W. Li, Sodium taurocholate cotransporting polypeptide is a functional receptor for human hepatitis B and D virus *eLife*, vol. 1, p. e00049, 2012. 00049[PII] 23150796[pmid] eLife.
- [81] P. Bogomolov, A. Alexandrov, N. Voronkova, M. Macievich, K. Kokina, M. Petrachenkova, T. Lehr, F. A. Lempp, H. Wedemeyer, M. Haag, *et al.*, Treatment of chronic hepatitis D with the entry inhibitor myrcludex B: First results of a phase Ib/IIa study *Journal of hepatology*, vol. 65, no. 3, pp. 490–498, 2016.
- [82] P. Gripon, I. Cannie, and S. Urban, Efficient inhibition of hepatitis B virus infection by acylated peptides derived from the large viral surface protein *Journal of virology*, vol. 79, no. 3, pp. 1613–1622, 2005.
- [83] J. Lucifora and U. Protzer, Attacking hepatitis B virus cccDNA—The holy grail to hepatitis B cure *Journal of hepatology*, vol. 64, no. 1, pp. S41–S48, 2016.

- [84] J. Lucifora, Y. Xia, F. Reisinger, K. Zhang, D. Stadler, X. Cheng, M. F. Sprinzl, H. Koppensteiner, Z. Makowska, T. Volz, C. Remouchamps, W.-M. Chou, W. E. Thasler, N. Hüser, D. Durantel, T. J. Liang, C. Münk, M. H. Heim, J. L. Browning, E. Dejardin, M. Dandri, M. Schindler, M. Heikenwalder, and U. Protzer, Specific and Nonhepatotoxic Degradation of Nuclear Hepatitis B Virus cccDNA *Science*, vol. 343, no. 6176, pp. 1221–1228, 2014.
- [85] C. Seeger and J. A. Sohn, Targeting hepatitis B virus with CRISPR/Cas9 *Molecular Therapy-Nucleic Acids*, vol. 3, 2014.
- [86] J. Summers, A. O’Connell, and I. Millman, Genome of hepatitis B virus: restriction enzyme cleavage and structure of DNA extracted from Dane particles *Proceedings of the National Academy of Sciences*, vol. 72, no. 11, pp. 4597–4601, 1975.
- [87] J. W. Habig and D. D. Loeb, Template switches during plus-strand DNA synthesis of duck hepatitis B virus are influenced by the base composition of the minus-strand terminal redundancy *Journal of virology*, vol. 77, no. 23, pp. 12412–12420, 2003.
- [88] D. D. Loeb, K. J. Gulya, and R. Tian, Sequence identity of the terminal redundancies on the minus-strand DNA template is necessary but not sufficient for the template switch during hepadnavirus plus-strand DNA synthesis. *Journal of virology*, vol. 71, no. 1, pp. 152–160, 1997.
- [89] J. E. Tavis, S. Perri, and D. Ganem, Hepadnavirus reverse transcription initiates within the stem-loop of the RNA packaging signal and employs a novel strand transfer. *Journal of virology*, vol. 68, no. 6, pp. 3536–3543, 1994.
- [90] C. Seeger, D. Ganem, and H. E. Varmus, Biochemical and genetic evidence for the hepatitis B virus replication strategy *Science*, vol. 232, no. 4749, pp. 477–484, 1986.
- [91] A. Dejean, L. Bougueleret, K. Grzeschik, and P. Tiollais, Hepatitis B virus DNA integration in a sequence homologous to v-erb-A and steroid receptor genes in a hepatocellular carcinoma *Nature*, vol. 322, pp. 70 – 72, 1986.
- [92] F. Sattler and W. S. Robinson, Hepatitis B viral DNA molecules have cohesive ends *Journal of virology*, vol. 32, no. 1, pp. 226–233, 1979.
- [93] W. Gerlich and W. Robinson, Hepatitis B virus contains protein attached to the 5’ terminus of its complete DNA strand *Cell*, vol. 21, pp. 801 – 809, 1980.
- [94] R. Bartenschlager and H. Schaller, Hepadnaviral assembly is initiated by polymerase binding to the encapsidation signal in the viral RNA genome *The EMBO journal*, vol. 11, no. 9, p. 3413, 1992.

- [95] J. Lien, C. E. Aldrich, and W. S. Mason, Evidence that a capped oligoribonucleotide is the primer for duck hepatitis B virus plus-strand DNA synthesis. *Journal of virology*, vol. 57, no. 1, pp. 229–236, 1986.
- [96] B. L. Slagle, O. M. Andrisani, M. J. Bouchard, C. G. Lee, J.-H. J. Ou, and A. Siddiqui, Technical standards for hepatitis B virus X protein (HBx) research *Hepatology*, vol. 61, no. 4, pp. 1416–1424, 2015.
- [97] A. Gallina, F. Bonelli, L. Zentilin, G. Rindi, M. Muttini, and G. Milanesi, A recombinant hepatitis B core antigen polypeptide with the protamine-like domain deleted self-assembles into capsid particles but fails to bind nucleic acids *Journal of virology*, vol. 63, no. 11, pp. 4645–4652, 1989.
- [98] F. Birnbaum and M. Nassal, Hepatitis B virus nucleocapsid assembly: primary structure requirements in the core protein. *Journal of virology*, vol. 64, no. 7, pp. 3319–3330, 1990.
- [99] T. Hatton, S. Zhou, and D. Standring, RNA-and DNA-binding activities in hepatitis B virus capsid protein: a model for their roles in viral replication. *Journal of virology*, vol. 66, no. 9, pp. 5232–5241, 1992.
- [100] M. Nassal, The arginine-rich domain of the hepatitis B virus core protein is required for pregenome encapsidation and productive viral positive-strand DNA synthesis but not for virus assembly *Journal of virology*, vol. 66, no. 7, pp. 4107–4116, 1992.
- [101] Z. Tan, K. Pionek, N. Unchwaniwala, M. L. Maguire, D. D. Loeb, and A. Zlotnick, The interface between HBV capsid proteins affects self-assembly, pgRNA packaging, and reverse transcription *Journal of virology*, pp. JVI-03545, 2015.
- [102] S. Zhou and D. N. Standring, Hepatitis B virus capsid particles are assembled from core-protein dimer precursors *Proceedings of the National Academy of Sciences*, vol. 89, no. 21, pp. 10046–10050, 1992.
- [103] A. M. Roseman, J. A. Berriman, S. A. Wynne, P. J. G. Butler, and R. A. Crowther, A structural model for maturation of the hepatitis B virus core *Proceedings of the National Academy of Sciences of the United States of America*, vol. 102, no. 44, pp. 15821–15826, 2005.
- [104] R. Crowther, N. Kiselev, B. Böttcher, J. Berriman, G. Borisova, V. Ose, and P. Pumpens, Three-dimensional structure of hepatitis B virus core particles determined by electron cryomicroscopy *Cell*, vol. 77, no. 6, pp. 943–950, 1994.

- [105] J.-H. Ou, O. Laub, and W. J. Rutter, Hepatitis B virus gene function: the precore region targets the core antigen to cellular membranes and causes the secretion of the e antigen *Proceedings of the National Academy of Sciences*, vol. 83, no. 6, pp. 1578–1582, 1986.
- [106] D. Milich and T. J. Liang, Exploring the biological basis of hepatitis B e antigen in hepatitis B virus infection *Hepatology*, vol. 38, no. 5, pp. 1075–1086, 2003.
- [107] V. Bruss and W. Gerlich, Formation of transmembraneous hepatitis B e-antigen by co-translational in vitro processing of the viral precore protein *Virology*, vol. 163, pp. 268 – 275, 1988.
- [108] M. A. DiMattia, N. R. Watts, S. J. Stahl, J. M. Grimes, A. C. Steven, D. I. Stuart, and P. T. Wingfield, Antigenic switching of hepatitis B virus by alternative dimerization of the capsid protein *Structure*, vol. 21, no. 1, pp. 133–142, 2013.
- [109] M. T. Chen, J.-N. Billaud, M. Sällberg, L. G. Guidotti, F. V. Chisari, J. Jones, J. Hughes, and D. R. Milich, A function of the hepatitis B virus precore protein is to regulate the immune response to the core antigen *Proceedings of the National Academy of Sciences*, vol. 101, no. 41, pp. 14913–14918, 2004.
- [110] C. Chang, G. Enders, R. Sprengel, N. Peters, H. E. Varmus, and D. Ganem, Expression of the precore region of an avian hepatitis B virus is not required for viral replication. *Journal of virology*, vol. 61, no. 10, pp. 3322–3325, 1987.
- [111] Y.-F. Liaw, HBeAg seroconversion as an important end point in the treatment of chronic hepatitis B *Hepatology international*, vol. 3, no. 3, pp. 425–433, 2009.
- [112] L. Magnusius and A. Espmark, A new antigen complex co-occurring with Australia antigen *Acta Pathol Microbiol Scand B Microbiol Immunol*, vol. 80, pp. 335 – 337, 1972.
- [113] G. Radziwill, W. Tucker, and H. Schaller, Mutational analysis of the hepatitis B virus P gene product: domain structure and RNase H activity *Journal of virology*, vol. 64, no. 2, pp. 613–620, 1990.
- [114] G. H. Wang and C. Seeger, The reverse transcriptase of hepatitis B virus acts as a protein primer for viral DNA synthesis *Cell*, vol. 71, no. 4, pp. 663–70, 1992. Wang, G H Seeger, C AI-24972/AI/NIAID NIH HHS/United States AI-30544/AI/NIAID NIH HHS/United States CA-06927/CA/NCI NIH HHS/United States Journal Article Research Support, Non-U.S. Gov't Research Support, U.S. Gov't, P.H.S. United states Cell. 1992 Nov 13;71(4):663-70.

- [115] S. A. Jones and J. Hu, Hepatitis B virus reverse transcriptase: diverse functions as classical and emerging targets for antiviral intervention *Emerging microbes & infections*, vol. 2, no. 9, p. e56, 2013.
- [116] R. Bartenschlager and H. Schaller, The amino-terminal domain of the hepadnaviral P-gene encodes the terminal protein (genome-linked protein) believed to prime reverse transcription. *The EMBO journal*, vol. 7, no. 13, pp. 4185–4192, 1988.
- [117] M. Bavand, M. Feitelson, and O. Laub, The hepatitis B virus-associated reverse transcriptase is encoded by the viral pol gene. *Journal of virology*, vol. 63, no. 2, pp. 1019–1021, 1989.
- [118] L. Chang, R. Hirsch, D. Ganem, and H. Varmus, Effects of insertional and point mutations on the functions of the duck hepatitis B virus polymerase. *Journal of virology*, vol. 64, no. 11, pp. 5553–5558, 1990.
- [119] J. Hu and C. Seeger, [11] Expression and characterization of hepadnavirus reverse transcriptases in *Methods in enzymology*, vol. 275, pp. 195–208, Elsevier, 1996.
- [120] F. Zoulim and C. Seeger, Reverse transcription in hepatitis B viruses is primed by a tyrosine residue of the polymerase. *Journal of virology*, vol. 68, no. 1, pp. 6–13, 1994.
- [121] M. Weber, V. Bronsema, H. Bartos, A. Bosserhoff, R. Bartenschlager, and H. Schaller, Hepadnavirus P protein utilizes a tyrosine residue in the TP domain to prime reverse transcription. *Journal of virology*, vol. 68, no. 5, pp. 2994–2999, 1994.
- [122] S. A. Jones, R. Boregowda, T. E. Spratt, and J. Hu, In vitro epsilon RNA-dependent protein priming activity of human hepatitis B virus polymerase *Journal of virology*, pp. JVI-07137, 2012.
- [123] M. M. Minor and B. L. Slagle, Hepatitis B virus HBx protein interactions with the ubiquitin proteasome system *Viruses*, vol. 6, no. 11, pp. 4683–4702, 2014.
- [124] M. van Regenmortel and B. Mahy, *Desk Encyclopedia of General Virology*. Elsevier Science, 2010.
- [125] J. Summers and W. S. Mason, Replication of the genome of a hepatitis B-like virus by reverse transcription of an RNA intermediate *Cell*, vol. 29, no. 2, pp. 403–15, 1982. Summers, J Mason, W S Journal Article Research Support, Non-U.S. Gov't Research Support, U.S. Gov't, P.H.S. United states Cell. 1982 Jun;29(2):403-15.

- [126] J. Lucifora, S. Arzberger, D. Durantel, L. Belloni, M. Strubin, M. Levrero, F. Zoulim, O. Hantz, and U. Protzer, Hepatitis B virus X protein is essential to initiate and maintain virus replication after infection *J Hepatol*, vol. 55, pp. 996 – 1003, 2011.
- [127] F. Zoulim, J. Saputelli, and C. Seeger, Woodchuck hepatitis virus X protein is required for viral infection in vivo *Journal of virology*, vol. 68, no. 3, pp. 2026–2030, 1994.
- [128] S. A. Becker, T.-H. Lee, J. S. Butel, and B. L. Slagle, Hepatitis B virus X protein interferes with cellular DNA repair *Journal of virology*, vol. 72, no. 1, pp. 266–272, 1998.
- [129] M. J. Bouchard, L.-H. Wang, and R. J. Schneider, Calcium signaling by HBx protein in hepatitis B virus DNA replication *Science*, vol. 294, no. 5550, pp. 2376–2378, 2001.
- [130] T. L. Gearhart and M. J. Bouchard, The hepatitis B virus X protein modulates hepatocyte proliferation pathways to stimulate viral replication *Journal of virology*, vol. 84, no. 6, pp. 2675–2686, 2010.
- [131] S. Rawat and M. J. Bouchard, The hepatitis B virus (HBV) HBx protein activates AKT to simultaneously regulate HBV replication and hepatocyte survival *Journal of virology*, vol. 89, no. 2, pp. 999–1012, 2015.
- [132] D. Sir, Y. Tian, W.-l. Chen, D. K. Ann, T.-S. B. Yen, and J.-h. J. Ou, The early autophagic pathway is activated by hepatitis B virus and required for viral DNA replication *Proceedings of the National Academy of Sciences*, vol. 107, no. 9, pp. 4383–4388, 2010.
- [133] S.-J. Kim, M. Khan, J. Quan, A. Till, S. Subramani, and A. Siddiqui, Hepatitis B virus disrupts mitochondrial dynamics: induces fission and mitophagy to attenuate apoptosis *PLoS pathogens*, vol. 9, no. 12, p. e1003722, 2013.
- [134] X.-D. Zhang, Y. Wang, and L.-H. Ye, Hepatitis B virus X protein accelerates the development of hepatoma *Cancer biology & medicine*, vol. 11, no. 3, p. 182, 2014.
- [135] B. L. Slagle and M. J. Bouchard, Role of HBx in hepatitis B virus persistence and its therapeutic implications *Current opinion in virology*, vol. 30, pp. 32–38, 2018.
- [136] M. Geng, X. Xin, L.-Q. Bi, L.-T. Zhou, and X.-H. Liu, Molecular mechanism of hepatitis B virus X protein function in hepatocarcinogenesis *World journal of gastroenterology: WJG*, vol. 21, no. 38, p. 10732, 2015.
- [137] K. Heermann, U. Goldmann, W. Schwartz, T. Seyffarth, H. Baumgarten, and W. Gerlich, Large surface proteins of hepatitis B virus containing the pre-s sequence *J Virol*, vol. 52, pp. 396 – 402, 1984.

- [138] R. Cattaneo, H. Will, N. Hernandez, and H. Schaller, Signals regulating hepatitis B surface antigen transcription *Nature*, vol. 305, no. 5932, p. 336, 1983.
- [139] S. Y. Sheu and S. J. Lo, Preferential ribosomal scanning is involved in the differential synthesis of the hepatitis B viral surface antigens from subgenomic transcripts *Virology*, vol. 188, no. 1, pp. 353–357, 1992.
- [140] W. Stibbe and W. H. Gerlich, Structural relationships between minor and major proteins of hepatitis B surface antigen *Journal of virology*, vol. 46, no. 2, pp. 626–628, 1983.
- [141] T. K. Tolle, D. Glebe, M. Linder, D. Linder, S. Schmitt, R. Geyer, and W. H. Gerlich, Structure and Glycosylation Patterns of Surface Proteins from Woodchuck Hepatitis Virus *Journal of Virology*, vol. 72, no. 12, pp. 9978–9985, 1998. 0914[PII] 9811735[pmid] J Virol.
- [142] V. Bruss, Hepatitis B virus morphogenesis *World J Gastroenterol*, vol. 13, no. 1, pp. 65–73, 2007. Bruss, Volker Journal Article Review China World J Gastroenterol. 2007 Jan 7;13(1):65-73.
- [143] B. Eble, V. Lingappa, and D. Ganem, Hepatitis B surface antigen: an unusual secreted protein initially synthesized as a transmembrane polypeptide. *Molecular and cellular biology*, vol. 6, no. 5, pp. 1454–1463, 1986.
- [144] B. E. Eble, D. R. MacRae, V. R. Lingappa, and D. Ganem, Multiple topogenic sequences determine the transmembrane orientation of the hepatitis B surface antigen *Mol Cell Biol*, vol. 7, no. 10, pp. 3591–601, 1987. Eble, B E MacRae, D R Lingappa, V R Ganem, D Journal Article United states Mol Cell Biol. 1987 Oct;7(10):3591-601.
- [145] R. Patient, C. Hourieux, and P. Roingeard, Morphogenesis of hepatitis B virus and its subviral envelope particles *Cellular microbiology*, vol. 11, no. 11, pp. 1561–1570, 2009.
- [146] H. Stirk, J. Thornton, and C. Howard, Atopological Model for Hepatitis B Surface Antigen *Intervirology*, vol. 33, no. 3, pp. 148–158, 1992.
- [147] N. Sonveaux, K. Conrath, C. Capiou, R. Brasseur, E. Goormaghtigh, and J.-M. Ruyschaert, The topology of the S protein in the yeast-derived hepatitis B surface antigen particles. *Journal of Biological Chemistry*, vol. 269, no. 41, pp. 25637–25645, 1994.
- [148] B. Persson and P. Argos, Prediction of transmembrane segments in proteins utilising multiple sequence alignments 1994.
- [149] D. L. Peterson, N. Nath, and F. Gavilanes, Structure of hepatitis B surface antigen. Correlation of subtype with amino acid sequence and location of the carbohydrate moiety. *Journal of biological chemistry*, vol. 257, no. 17, pp. 10414–10420, 1982.

- [150] C. Mangold and R. E. Streeck, Mutational analysis of the cysteine residues in the hepatitis B virus small envelope protein. *Journal of virology*, vol. 67, no. 8, pp. 4588–4597, 1993.
- [151] C. M. Mangold, F. Unckell, M. Werr, and R. E. Streeck, Secretion and antigenicity of hepatitis B virus small envelope proteins lacking cysteines in the major antigenic region *Virology*, vol. 211, no. 2, pp. 535–543, 1995.
- [152] A. Huovila, A. M. Eder, and S. D. Fuller, Hepatitis B surface antigen assembles in a post-ER, pre-Golgi compartment *The Journal of cell biology*, vol. 118, no. 6, pp. 1305–1320, 1992.
- [153] G. Wunderlich and V. Bruss, Characterization of early hepatitis B virus surface protein oligomers *Archives of virology*, vol. 141, no. 7, pp. 1191–1205, 1996.
- [154] D. H. Persing, H. Varmus, and D. Ganem, The preS1 protein of hepatitis B virus is acylated at its amino terminus with myristic acid. *Journal of virology*, vol. 61, no. 5, pp. 1672–1677, 1987.
- [155] B. E. Eble, V. R. Lingappa, and D. Ganem, The N-terminal (pre-S2) domain of a hepatitis B virus surface glycoprotein is translocated across membranes by downstream signal sequences *J Virol*, vol. 64, no. 3, pp. 1414–9, 1990. Eble, B E Lingappa, V R Ganem, D Journal Article Research Support, U.S. Gov't, P.H.S. United states *J Virol*. 1990 Mar;64(3):1414-9.
- [156] Y. Liu, E. Simsek, P. Norton, G. Sinnathamby, R. Philip, T. Block, T. Zhou, and A. Mehta, The role of the downstream signal sequences in the maturation of the HBV middle surface glycoprotein: development of a novel therapeutic vaccine candidate *Virology*, vol. 365, no. 1, pp. 10–19, 2007.
- [157] D. Fernholz, M. Stemler, M. Brunetto, F. Bonino, and H. Will, Replicating and virion secreting hepatitis B mutant virus unable to produce preS2 protein *Journal of hepatology*, vol. 13, pp. S102–S104, 1991.
- [158] V. Bruss and D. Ganem, The role of envelope proteins in hepatitis B virus assembly *Proceedings of the National Academy of Sciences*, vol. 88, no. 3, pp. 1059–1063, 1991.
- [159] V. Bruss, X. Lu, R. Thomssen, and W. Gerlich, Post-translational alterations in transmembrane topology of the hepatitis B virus large envelope protein. *The EMBO journal*, vol. 13, no. 10, pp. 2273–2279, 1994.
- [160] P. Ostapchuk, P. Hearing, and D. Ganem, A dramatic shift in the transmembrane topology of a viral envelope glycoprotein accompanies hepatitis B viral morphogenesis. *The EMBO journal*, vol. 13, no. 5, pp. 1048–1057, 1994.

- [161] R. Prange and R. E. Streeck, Novel transmembrane topology of the hepatitis B virus envelope proteins. *The EMBO journal*, vol. 14, no. 2, pp. 247–256, 1995.
- [162] E. Grgacic, C. Kuhn, and H. Schaller, Hepadnavirus envelope topology: insertion of a loop region in the membrane and role of S in L protein translocation *Journal of virology*, vol. 74, no. 5, pp. 2455–2458, 2000.
- [163] C. Lambert and R. Prange, Dual topology of the hepatitis B virus large envelope protein determinants influencing post-translational pre-S translocation *Journal of Biological Chemistry*, vol. 276, no. 25, pp. 22265–22272, 2001.
- [164] C. Lambert, S. Mann, and R. Prange, Assessment of determinants affecting the dual topology of hepadnaviral large envelope proteins *Journal of general virology*, vol. 85, no. 5, pp. 1221–1225, 2004.
- [165] H. Löffler-Mary, M. Werr, and R. Prange, Sequence-specific repression of cotranslational translocation of the hepatitis B virus envelope proteins coincides with binding of heat shock protein Hsc70 *Virology*, vol. 235, no. 1, pp. 144–152, 1997.
- [166] C. Lambert and R. Prange, Chaperone action in the posttranslational topological reorientation of the hepatitis B virus large envelope protein: Implications for translocational regulation *Proceedings of the National Academy of Sciences*, vol. 100, no. 9, pp. 5199–5204, 2003.
- [167] D.-Y. Cho, G.-H. Yang, C. J. Ryu, and H. J. Hong, Molecular chaperone GRP78/BiP interacts with the large surface protein of hepatitis B virus in vitro and in vivo *Journal of virology*, vol. 77, no. 4, pp. 2784–2788, 2003.
- [168] K. Awe, C. Lambert, and R. Prange, Mammalian BiP controls posttranslational ER translocation of the hepatitis B virus large envelope protein *FEBS letters*, vol. 582, no. 21–22, pp. 3179–3184, 2008.
- [169] D. Glebe and S. Urban, Viral and cellular determinants involved in hepadnaviral entry *World Journal of gastroenterology*, vol. 13, no. 1, p. 22, 2007.
- [170] F. Gavilanes, J. M. Gonzalez-Ros, and D. L. Peterson, Structure of hepatitis B surface antigen. Characterization of the lipid components and their association with the viral proteins. *Journal of biological chemistry*, vol. 257, no. 13, pp. 7770–7777, 1982.
- [171] L. P. Aggerbeck and D. L. Peterson, Electron microscopic and solution X-ray scattering observations on the structure of hepatitis B surface antigen *Virology*, vol. 141, no. 1, pp. 155–161, 1985.

- [172] D. Ganem and H. Varmus, The molecular biology of the hepatitis B viruses *Annual review of biochemistry*, vol. 56, no. 1, pp. 651–693, 1987.
- [173] D. L. Peterson, The structure of hepatitis B surface antigen and its antigenic sites *BioEssays*, vol. 6, no. 6, pp. 258–262, 1987.
- [174] P. Vanlandschoot, F. Van Houtte, A. Roobrouck, A. Farhoudi, and G. Leroux-Roels, Hepatitis B virus surface antigen suppresses the activation of monocytes through interaction with a serum protein and a monocyte-specific receptor *Journal of general virology*, vol. 83, no. 6, pp. 1281–1289, 2002.
- [175] Y. Chen, H. Wei, R. Sun, and Z. Tian, Impaired function of hepatic natural killer cells from murine chronic HBsAg carriers *International immunopharmacology*, vol. 5, no. 13-14, pp. 1839–1852, 2005.
- [176] M. L. Op den Brouw, R. S. Binda, M. H. Van Roosmalen, U. Protzer, H. L. Janssen, R. G. Van Der Molen, and A. M. Woltman, Hepatitis B virus surface antigen impairs myeloid dendritic cell function: a possible immune escape mechanism of hepatitis B virus *Immunology*, vol. 126, no. 2, pp. 280–289, 2009.
- [177] L. Novellino, R. L. Rossi, F. Bonino, D. Cavallone, S. Abrignani, M. Pagani, and M. R. Brunetto, Circulating hepatitis B surface antigen particles carry hepatocellular microRNAs *PloS one*, vol. 7, no. 3, p. e31952, 2012.
- [178] Y. Kondo, M. Ninomiya, E. Kakazu, O. Kimura, and T. Shimosegawa, Hepatitis B surface antigen could contribute to the immunopathogenesis of hepatitis B virus infection *ISRN gastroenterology*, vol. 2013, 2013.
- [179] D. H. Persing, H. E. Varmus, and D. Ganem, Inhibition of secretion of hepatitis B surface antigen by a related presurface polypeptide *Science*, vol. 234, no. 4782, pp. 1388–1391, 1986.
- [180] J.-H. Ou and W. J. Rutter, Regulation of secretion of the hepatitis B virus major surface antigen by the preS-1 protein. *Journal of virology*, vol. 61, no. 3, pp. 782–786, 1987.
- [181] P. K. Chua, M.-H. Lin, and C. Shih, Potent inhibition of human Hepatitis B virus replication by a host factor Vps4 *Virology*, vol. 354, no. 1, pp. 1–6, 2006.
- [182] C. Lambert, T. Döring, and R. Prange, Hepatitis B virus maturation is sensitive to functional inhibition of ESCRT-III, Vps4, and γ 2-adaptin *Journal of virology*, vol. 81, no. 17, pp. 9050–9060, 2007.

- [183] T. Watanabe, E. M. Sorensen, A. Naito, M. Schott, S. Kim, and P. Ahlquist, Involvement of host cellular multivesicular body functions in hepatitis B virus budding *Proceedings of the National Academy of Sciences*, vol. 104, no. 24, pp. 10205–10210, 2007.
- [184] R. Prange, Host factors involved in hepatitis B virus maturation, assembly, and egress *Medical microbiology and immunology*, vol. 201, no. 4, pp. 449–461, 2012.
- [185] P. Roingeard and C. Sureau, Ultrastructural analysis of hepatitis B virus in HepG2-transfected cells with special emphasis on subviral filament morphogenesis *Hepatology*, vol. 28, no. 4, pp. 1128–1133, 1998.
- [186] R. Patient, C. Hourieux, P.-Y. Sizaret, S. Trassard, C. Sureau, and P. Roingeard, Hepatitis B virus subviral envelope particle morphogenesis and intracellular trafficking *Journal of virology*, vol. 81, no. 8, pp. 3842–3851, 2007.
- [187] C. Sureau and J. Salisse, A conformational heparan sulfate binding site essential to infectivity overlaps with the conserved hepatitis B virus a-determinant *Hepatology*, vol. 57, pp. 985 – 994, 2013.
- [188] A. Schulze, P. Gripon, and S. Urban, Hepatitis B virus infection initiates with a large surface protein–dependent binding to heparan sulfate proteoglycans *Hepatology*, vol. 46, no. 6, pp. 1759–1768, 2007.
- [189] C. M. Leistner, S. Gruen-Bernhard, and D. Glebe, Role of glycosaminoglycans for binding and infection of hepatitis B virus *Cellular microbiology*, vol. 10, no. 1, pp. 122–133, 2008.
- [190] Y. Ni, F. A. Lempp, S. Mehrle, S. Nkongolo, C. Kaufman, M. Fälth, J. Stindt, C. Königer, M. Nassal, and R. Kubitz, Hepatitis B and D viruses exploit sodium taurocholate co-transporting polypeptide for species-specific entry into hepatocytes *Gastroenterology*, vol. 146, no. 4, pp. 1070–1083. e6, 2014.
- [191] V. Bruss, J. Hagelstein, E. Gerhardt, and P. R. Galle, Myristylation of the large surface protein is required for hepatitis B virus in vitro infectivity *Virology*, vol. 218, no. 2, pp. 396–9, 1996. Bruss, V Hagelstein, J Gerhardt, E Galle, P R Journal Article Research Support, Non-U.S. Gov't United states Virology. 1996 Apr 15;218(2):396-9.
- [192] P. Gripon, J. Le Seyec, S. Rumin, and C. Guguen-Guillouzo, Myristylation of the hepatitis B virus large surface protein is essential for viral infectivity *Virology*, vol. 213, no. 2, pp. 292–299, 1995.
- [193] M. Blanchet and C. Sureau, Analysis of the cytosolic domains of the hepatitis B virus envelope proteins for their function in viral particle assembly and infectivity *Journal of virology*, vol. 80, no. 24, pp. 11935–11945, 2006.

- [194] M. Blanchet and C. Sureau, Infectivity determinants of the hepatitis B virus pre-S domain are confined to the N-terminal 75 amino acid residues *Journal of virology*, vol. 81, no. 11, pp. 5841–5849, 2007.
- [195] D. R. Macrae, V. Bruss, and D. Ganem, Myristylation of a duck hepatitis B virus envelope protein is essential for infectivity but not for virus assembly *Virology*, vol. 181, no. 1, pp. 359–363, 1991.
- [196] D. Glebe, S. Urban, E. Knoop, N. Cag, P. Krass, S. Grun, A. Bulavaite, K. Sasnauskas, and W. Gerlich, Mapping of the hepatitis B virus attachment site by infection-inhibiting preS1 lipopeptides using Tupaia hepatocytes *Gastroenterology*, vol. 129, pp. 234 – 245, 2005.
- [197] C. Lepère-Douard, M. Trotard, J. Le Seyec, and P. Gripon, The first transmembrane domain of the hepatitis B virus large envelope protein is crucial for infectivity *Journal of virology*, vol. 83, no. 22, pp. 11819–11829, 2009.
- [198] T. Tu and S. Urban, Virus entry and its inhibition to prevent and treat hepatitis B and hepatitis D virus infections *Current opinion in virology*, vol. 30, pp. 68–79, 2018.
- [199] M. Kann, A. Schmitz, and B. Rabe, Intracellular transport of hepatitis B virus *World J Gastroenterol*, vol. 13, no. 1, pp. 39–47, 2007. Kann, Michael Schmitz, Andre Rabe, Birgit Journal Article Research Support, Non-U.S. Gov’t Review China World J Gastroenterol. 2007 Jan 7;13(1):39-47.
- [200] B. Rabe, A. Vlachou, N. Pante, A. Helenius, and M. Kann, Nuclear import of hepatitis B virus capsids and release of the viral genome *Proc Natl Acad Sci USA*, vol. 100, pp. 9849 – 9854, 2003.
- [201] W. H. Gerlich and W. S. Robinson, Hepatitis B virus contains protein attached to the 5’ terminus of its complete DNA strand *Cell*, vol. 21, no. 3, pp. 801–9, 1980. Gerlich, W H Robinson, W S Journal Article Research Support, Non-U.S. Gov’t Research Support, U.S. Gov’t, P.H.S. United states Cell. 1980 Oct;21(3):801-9.
- [202] K. L. Molnar-Kimber, J. Summers, J. M. Taylor, and W. S. Mason, Protein covalently bound to minus-strand DNA intermediates of duck hepatitis B virus *J Virol*, vol. 45, no. 1, pp. 165–72, 1983. Molnar-Kimber, K L Summers, J Taylor, J M Mason, W S AI-15166-04/AI/NIAID NIH HHS/United States CA-09035-07/CA/NCI NIH HHS/United States CA-22651-05/CA/NCI NIH HHS/United States etc. Journal Article Research Support, Non-U.S. Gov’t Research Support, U.S. Gov’t, P.H.S. United states J Virol. 1983 Jan;45(1):165-72.

- [203] C.-T. Bock, P. Schranz, C. H. Schröder, and H. Zentgraf, Hepatitis B virus genome is organized into nucleosomes in the nucleus of the infected cell *Virus genes*, vol. 8, no. 2, pp. 215–229, 1994.
- [204] M. Nassal, HBV cccDNA: viral persistence reservoir and key obstacle for a cure of chronic hepatitis B *Gut*, pp. gutjnl–2015, 2015.
- [205] S. Schreiner and M. Nassal, A role for the host DNA damage response in hepatitis B virus cccDNA formation—and beyond? *Viruses*, vol. 9, no. 5, p. 125, 2017.
- [206] J. S. Tuttleman, C. Pourcel, and J. Summers, Formation of the pool of covalently closed circular viral DNA in hepadnavirus-infected cells *Cell*, vol. 47, no. 3, pp. 451–60, 1986. Tuttleman, J S Pourcel, C Summers, J CA-06927/CA/NCI NIH HHS/United States R0-AI15166/AI/NIAID NIH HHS/United States Journal Article Research Support, U.S. Gov't, P.H.S. United states *Cell*. 1986 Nov 7;47(3):451-60.
- [207] J. E. Newbold, H. Xin, M. Tencza, G. Sherman, J. Dean, S. Bowden, and S. Locarnini, The covalently closed duplex form of the hepadnavirus genome exists in situ as a heterogeneous population of viral minichromosomes *J Virol*, vol. 69, no. 6, pp. 3350–7, 1995. Newbold, J E Xin, H Tencza, M Sherman, G Dean, J Bowden, S Locarnini, S 5K11DE00312/DE/NIDCR NIH HHS/United States Journal Article Research Support, U.S. Gov't, P.H.S. United states *J Virol*. 1995 Jun;69(6):3350-7.
- [208] C. Brechot, C. Pourcel, A. Louise, B. Rain, and P. Tiollais, Presence of integrated hepatitis B virus DNA sequences in cellular DNA of human hepatocellular carcinoma *Nature*, vol. 286, no. 5772, p. 533, 1980.
- [209] C. Saitta, G. Tripodi, A. Barbera, A. Bertuccio, A. Smedile, A. Ciancio, G. Raffa, A. Sangiovanni, G. Navarra, G. Raimondo, *et al.*, Hepatitis B virus (HBV) DNA integration in patients with occult HBV infection and hepatocellular carcinoma *Liver International*, vol. 35, no. 10, pp. 2311–2317, 2015.
- [210] H. Hai, A. Tamori, and N. Kawada, Role of hepatitis B virus DNA integration in human hepatocarcinogenesis *World Journal of Gastroenterology: WJG*, vol. 20, no. 20, p. 6236, 2014.
- [211] E. B. Stephens and R. W. Compans, Assembly of animal viruses at cellular membranes *Annual Reviews in Microbiology*, vol. 42, no. 1, pp. 489–516, 1988.
- [212] A. G. Cole, Modulators of HBV capsid assembly as an approach to treating hepatitis B virus infection *Current opinion in pharmacology*, vol. 30, pp. 131–137, 2016.

- [213] J. Beck and M. Nassal, Hepatitis B virus replication *World Journal of Gastroenterology : WJG*, vol. 13, no. 1, pp. 48–64, 2007. 17206754[pmid] *World J Gastroenterol*.
- [214] R. Bartenschlager, M. Junker-Niepmann, and H. Schaller, The P gene product of hepatitis B virus is required as a structural component for genomic RNA encapsidation. *Journal of virology*, vol. 64, no. 11, pp. 5324–5332, 1990.
- [215] R. C. Hirsch, J. E. Lavine, L.-j. Chang, H. E. Varmus, and D. Ganem, Polymerase gene products of hepatitis B viruses are required for genomic RNA packaging as well as for reverse transcription 1990.
- [216] M. Nassal and A. Rieger, A bulged region of the hepatitis B virus RNA encapsidation signal contains the replication origin for discontinuous first-strand DNA synthesis. *Journal of virology*, vol. 70, no. 5, pp. 2764–2773, 1996.
- [217] H. Will, W. Reiser, T. Weimer, E. Pfaff, M. Büscher, R. Sprengel, R. Cattaneo, and H. Schaller, Replication strategy of human hepatitis B virus. *Journal of Virology*, vol. 61, no. 3, pp. 904–911, 1987.
- [218] S. Staprans, D. Loeb, and D. Ganem, Mutations affecting hepadnavirus plus-strand DNA synthesis dissociate primer cleavage from translocation and reveal the origin of linear viral DNA. *Journal of virology*, vol. 65, no. 3, pp. 1255–1262, 1991.
- [219] T. Gerelsaikhon, J. Tavis, and V. Bruss, Hepatitis B virus nucleocapsid envelopment does not occur without genomic DNA synthesis *J Virol*, vol. 70, pp. 4269 – 4274, 1996.
- [220] F. Zoulim, New insight on hepatitis B virus persistence from the study of intrahepatic viral cccDNA *Journal of hepatology*, vol. 42, no. 3, pp. 302–308, 2005.
- [221] P. K. Chua, M.-H. Lin, and C. Shih, Potent inhibition of human Hepatitis B virus replication by a host factor Vps4 *Virology*, vol. 354, no. 1, pp. 1–6, 2006.
- [222] C. Lambert, T. Döring, and R. Prange, Hepatitis B virus maturation is sensitive to functional inhibition of ESCRT-III, Vps4, and gamma2-adaptin *Journal of virology*, vol. 81, no. 17, pp. 9050–9060, 2007.
- [223] T. Watanabe, E. M. Sorensen, A. Naito, M. Schott, S. Kim, and P. Ahlquist, Involvement of host cellular multivesicular body functions in hepatitis B virus budding *Proceedings of the National Academy of Sciences*, vol. 104, no. 24, pp. 10205–10210, 2007.
- [224] S. Urban, A. Schulze, M. Dandri, and J. Petersen, The replication cycle of hepatitis B virus *Journal of hepatology*, vol. 52, no. 2, pp. 282–284, 2010.

- [225] B. Jiang, K. Himmelsbach, H. Ren, K. Boller, and E. Hildt, Subviral hepatitis B virus filaments, like infectious viral particles, are released via multivesicular bodies *Journal of virology*, vol. 90, no. 7, pp. 3330–3341, 2016.
- [226] W. Gerlich, Medical Virology of Hepatitis B: how it began and where we are now *Virology Journal*, vol. 10, no. 1, p. 239, 2013.
- [227] B. S. Mamathambika and J. C. Bardwell, Disulfide-linked protein folding pathways *Annual review of cell and developmental biology*, vol. 24, pp. 211–235, 2008.
- [228] C. S. Sevier and C. A. Kaiser, Conservation and diversity of the cellular disulfide bond formation pathways *Antioxidants & redox signaling*, vol. 8, no. 5-6, pp. 797–811, 2006.
- [229] B. P. Tu and J. S. Weissman, Oxidative protein folding in eukaryotes: mechanisms and consequences *The Journal of cell biology*, vol. 164, no. 3, pp. 341–346, 2004.
- [230] J. Berg, J. Tymoczko, G. Gatto, L. Stryer, A. Held, G. Maxam, L. Seidler, B. Häcker, and B. Jarosch, *Stryer Biochemie*. Springer Berlin Heidelberg, 2017.
- [231] D. W. Reid and C. V. Nicchitta, Diversity and selectivity in mRNA translation on the endoplasmic reticulum *Nature reviews Molecular cell biology*, vol. 16, no. 4, p. 221, 2015.
- [232] T. A. Rapoport, Protein translocation across the eukaryotic endoplasmic reticulum and bacterial plasma membranes *Nature*, vol. 450, no. 7170, p. 663, 2007.
- [233] I. Braakman and D. N. Hebert, Protein folding in the endoplasmic reticulum *Cold Spring Harbor perspectives in biology*, vol. 5, no. 5, p. a013201, 2013.
- [234] P. Fagone and S. Jackowski, Membrane phospholipid synthesis and endoplasmic reticulum function *Journal of lipid research*, vol. 50, no. Supplement, pp. S311–S316, 2009.
- [235] D. N. Hebert, S. C. Garman, and M. Molinari, The glycan code of the endoplasmic reticulum: asparagine-linked carbohydrates as protein maturation and quality-control tags *Trends in cell biology*, vol. 15, no. 7, pp. 364–370, 2005.
- [236] D. E. Clapham, Calcium signaling *Cell*, vol. 131, no. 6, pp. 1047–1058, 2007.
- [237] L. Westrate, J. Lee, W. Prinz, and G. Voeltz, Form follows function: the importance of endoplasmic reticulum shape *Annual review of biochemistry*, vol. 84, pp. 791–811, 2015.
- [238] C. H. Jan, C. C. Williams, and J. S. Weissman, Principles of ER cotranslational translocation revealed by proximity-specific ribosome profiling *Science*, vol. 346, no. 6210, p. 1257521, 2014.

- [239] D. S. Schwarz and M. D. Blower, The endoplasmic reticulum: structure, function and response to cellular signaling *Cellular and Molecular Life Sciences*, vol. 73, no. 1, pp. 79–94, 2016.
- [240] R. J. Deshaies, S. L. Sanders, D. A. Feldheim, and R. Schekman, Assembly of yeast Sec proteins involved in translocation into the endoplasmic reticulum into a membrane-bound multisubunit complex *Nature*, vol. 349, no. 6312, p. 806, 1991.
- [241] P. Walter and G. Blobel, Translocation of proteins across the endoplasmic reticulum. II. Signal recognition protein (SRP) mediates the selective binding to microsomal membranes of in-vitro-assembled polysomes synthesizing secretory protein. *The Journal of cell biology*, vol. 91, no. 2, pp. 551–556, 1981.
- [242] P. Walter, I. Ibrahimi, and G. Blobel, Translocation of proteins across the endoplasmic reticulum. I. Signal recognition protein (SRP) binds to in-vitro-assembled polysomes synthesizing secretory protein. *The Journal of cell biology*, vol. 91, no. 2, pp. 545–550, 1981.
- [243] N. J. Bulleid, Disulfide bond formation in the mammalian endoplasmic reticulum *Cold Spring Harbor perspectives in biology*, vol. 4, no. 11, p. a013219, 2012.
- [244] L. Ellgaard and L. W. Ruddock, The human protein disulphide isomerase family: substrate interactions and functional properties *EMBO reports*, vol. 6, no. 1, pp. 28–32, 2005.
- [245] I. Braakman and N. J. Bulleid, Protein folding and modification in the mammalian endoplasmic reticulum *Annual review of biochemistry*, vol. 80, pp. 71–99, 2011.
- [246] M. G. Pollard, K. J. Travers, and J. S. Weissman, Ero1p: a novel and ubiquitous protein with an essential role in oxidative protein folding in the endoplasmic reticulum *Molecular cell*, vol. 1, no. 2, pp. 171–182, 1998.
- [247] A. R. Frand and C. A. Kaiser, The ERO1 gene of yeast is required for oxidation of protein dithiols in the endoplasmic reticulum *Molecular cell*, vol. 1, no. 2, pp. 161–170, 1998.
- [248] A. Cabibbo, M. Pagani, M. Fabbri, M. Rocchi, M. R. Farmery, N. J. Bulleid, and R. Sitia, ERO1-L, a human protein that favors disulfide bond formation in the endoplasmic reticulum *Journal of Biological Chemistry*, vol. 275, no. 7, pp. 4827–4833, 2000.
- [249] M. Pagani, M. Fabbri, C. Benedetti, A. Fassio, S. Pilati, N. J. Bulleid, A. Cabibbo, and R. Sitia, Endoplasmic reticulum oxidoreductin 1- β (ERO1-L β), a human gene induced

- in the course of the unfolded protein response *Journal of Biological Chemistry*, vol. 275, no. 31, pp. 23685–23692, 2000.
- [250] E. Gross, D. B. Kastner, C. A. Kaiser, and D. Fass, Structure of Ero1p, source of disulfide bonds for oxidative protein folding in the cell *Cell*, vol. 117, no. 5, pp. 601–610, 2004.
- [251] H. Nakabayashi, K. Taketa, K. Miyano, T. Yamane, and J. Sato, Growth of human hepatoma cell lines with differentiated functions in chemically defined medium *Cancer research*, vol. 42, no. 9, pp. 3858–3863, 1982.
- [252] E. Gerhardt and V. Bruss, Phenotypic mixing of rodent but not avian hepadnavirus surface proteins into human hepatitis B virus particles *Journal of virology*, vol. 69, no. 2, pp. 1201–1208, 1995.
- [253] S. Suffner, N. Gerstenberg, M. Patra, P. Ruibal, A. Orabi, M. Schindler, and V. Bruss, Domains of the hepatitis B virus small surface protein S mediating oligomerization *Journal of virology*, pp. JVI-02232, 2018.
- [254] C. Banning, J. Votteler, D. Hoffmann, H. Koppensteiner, M. Warmer, R. Reimer, F. Kirchhoff, U. Schubert, J. Hauber, and M. Schindler, A flow cytometry-based FRET assay to identify and analyse protein-protein interactions in living cells *PloS one*, vol. 5, no. 2, p. e9344, 2010.
- [255] L. Zheng, U. Baumann, and J.-L. Reymond, An efficient one-step site-directed and site-saturation mutagenesis protocol *Nucleic acids research*, vol. 32, no. 14, pp. e115–e115, 2004.
- [256] H. Liu and J. H. Naismith, An efficient one-step site-directed deletion, insertion, single and multiple-site plasmid mutagenesis protocol *BMC biotechnology*, vol. 8, no. 1, p. 91, 2008.
- [257] O. Laub, L. Rall, M. Truett, Y. Shaul, D. Standring, P. Valenzuela, and W. Rutter, Synthesis of hepatitis B surface antigen in mammalian cells: expression of the entire gene and the coding region. *Journal of virology*, vol. 48, no. 1, pp. 271–280, 1983.
- [258] L. M. Costantini, O. M. Subach, M. Jauregui-Berry-Bravo, V. V. Verkhusha, and E. L. Snapp, Cysteineless non-glycosylated monomeric blue fluorescent protein, secBFP2, for studies in the eukaryotic secretory pathway *Biochemical and biophysical research communications*, vol. 430, no. 3, pp. 1114–1119, 2013.
- [259] R. J. Gilbert, L. Beales, D. Blond, M. N. Simon, B. Y. Lin, F. V. Chisari, D. I. Stuart, and D. J. Rowlands, Hepatitis B small surface antigen particles are octahedral *Proceedings of the National Academy of Sciences*, vol. 102, no. 41, pp. 14783–14788, 2005.

- [260] L. Nikkanen, J. Toivola, and E. Rintamäki, Crosstalk between chloroplast thioredoxin systems in regulation of photosynthesis *Plant, cell & environment*, vol. 39, no. 8, pp. 1691–1705, 2016.
- [261] J. Lu and C. Deutsch, Pegylation: a method for assessing topological accessibilities in Kv1. 3 *Biochemistry*, vol. 40, no. 44, pp. 13288–13301, 2001.
- [262] L. Makmura, M. Hamann, A. Areopagita, S. Furuta, A. Muñoz, and J. Momand, Development of a sensitive assay to detect reversibly oxidized protein cysteine sulfhydryl groups *Antioxidants and Redox Signaling*, vol. 3, no. 6, pp. 1105–1118, 2001.
- [263] R. Julithe, G. Abou-Jaoudé, and C. Sureau, Modification of the hepatitis B virus envelope protein glycosylation pattern interferes with secretion of viral particles, infectivity, and susceptibility to neutralizing antibodies *Journal of virology*, vol. 88, no. 16, pp. 9049–9059, 2014.
- [264] S. Suffner, *Mutationsanalyse der Oligomerisierung des kleinen Hepatitis B Virus Hüllproteins S und ihr Einfluss auf die Partikelbildung des Hepatitis B und D Virus*. PhD thesis, Technische Universität München, 2016.
- [265] J. K. Locker and G. Griffiths, An unconventional role for cytoplasmic disulfide bonds in vaccinia virus proteins *The Journal of cell biology*, vol. 144, no. 2, pp. 267–279, 1999.
- [266] J. R. Winther and C. Thorpe, Quantification of thiols and disulfides *Biochimica et Biophysica Acta (BBA)-General Subjects*, vol. 1840, no. 2, pp. 838–846, 2014.
- [267] H. Peled-Zehavi, S. Avital, and A. Danon, Methods of redox signaling by plant thioredoxins *Methods in Redox Signaling, D. Das, ed (New Rochelle, NY: Mary Ann Liebert)*, pp. 251–256, 2010.
- [268] R. Xiao, B. Wilkinson, A. Solovyov, J. R. Winther, A. Holmgren, J. Lundström-Ljung, and H. F. Gilbert, The contributions of protein disulfide isomerase and its homologues to oxidative protein folding in the yeast endoplasmic reticulum *Journal of Biological Chemistry*, vol. 279, no. 48, pp. 49780–49786, 2004.
- [269] C. Appenzeller-Herzog and L. Ellgaard, In vivo reduction-oxidation state of protein disulfide isomerase: the two active sites independently occur in the reduced and oxidized forms *Antioxidants & redox signaling*, vol. 10, no. 1, pp. 55–64, 2008.
- [270] F. Katzen and J. Beckwith, Role and location of the unusual redox-active cysteines in the hydrophobic domain of the transmembrane electron transporter DsbD *Proceedings of the National Academy of Sciences*, vol. 100, no. 18, pp. 10471–10476, 2003.

- [271] W. Hsiao-Huei, J. A. THOMAS, and J. MOMAND, p53 protein oxidation in cultured cells in response to pyrrolidine dithiocarbamate: a novel method for relating the amount of p53 oxidation in vivo to the regulation of p53-responsive genes *Biochemical Journal*, vol. 351, no. 1, pp. 87–93, 2000.
- [272] Z.-Y. Guo, C. C. Chang, X. Lu, J. Chen, B.-L. Li, and T.-Y. Chang, The disulfide linkage and the free sulfhydryl accessibility of acyl-coenzyme A: cholesterol acyltransferase 1 as studied by using mPEG5000-maleimide *Biochemistry*, vol. 44, no. 17, pp. 6537–6546, 2005.
- [273] M. Schwaller, B. Wilkinson, and H. F. Gilbert, Reduction-reoxidation cycles contribute to catalysis of disulfide isomerization by protein-disulfide isomerase *Journal of Biological Chemistry*, vol. 278, no. 9, pp. 7154–7159, 2003.
- [274] G. Abou-Jaoudé and C. Sureau, Entry of hepatitis delta virus requires the conserved cysteine residues of the hepatitis B virus envelope protein antigenic loop and is blocked by inhibitors of thiol-disulfide exchange *Journal of virology*, vol. 81, no. 23, pp. 13057–13066, 2007.
- [275] H. Ohnuma, E. Takai, A. Machida, F. Tsuda, H. Okamoto, T. Tanaka, M. Naito, E. Munekata, K. Miki, and Y. Miyakawa, Synthetic oligopeptides bearing a common or subtypic determinant of hepatitis B surface antigen. *The Journal of Immunology*, vol. 145, no. 7, pp. 2265–2271, 1990.
- [276] C. Mangold, F. Unckell, M. Werr, and R. Streeck, Analysis of intermolecular disulfide bonds and free sulfhydryl groups in hepatitis B surface antigen particles *Archives of virology*, vol. 142, no. 11, pp. 2257–2267, 1997.
- [277] N. thi Man, B. Mat, P. N. Tran, G. Morris, *et al.*, Structural relationships between hepatitis B surface antigen in human plasma and dimers from recombinant vaccine: a monoclonal antibody study *Virus research*, vol. 21, no. 2, pp. 141–154, 1991.
- [278] R. Corley, *A Guide to Methods in the Biomedical Sciences*. A Guide to Methods in the Biomedical Sciences, Springer US, 2006.
- [279] M. H. Smith, H. L. Ploegh, and J. S. Weissman, Road to ruin: targeting proteins for degradation in the endoplasmic reticulum *Science*, vol. 334, no. 6059, pp. 1086–1090, 2011.
- [280] J. A. Olzmann, R. R. Kopito, and J. C. Christianson, The mammalian endoplasmic reticulum-associated degradation system *Cold Spring Harbor perspectives in biology*, vol. 5, no. 9, p. a013185, 2013.

- [281] C. Lauber, S. Seitz, S. Mattei, A. Suh, J. Beck, J. Herstein, J. Börold, W. Salzburger, L. Kaderali, J. A. Briggs, *et al.*, Deciphering the origin and evolution of hepatitis B viruses by means of a family of non-enveloped fish viruses *Cell Host & Microbe*, vol. 22, no. 3, pp. 387–399, 2017.
- [282] J. R. Gaut and L. M. Hendershot, The modification and assembly of proteins in the endoplasmic reticulum *Current opinion in cell biology*, vol. 5, no. 4, pp. 589–595, 1993.
- [283] A. Helenius, T. Marquardt, and I. Braakman, The endoplasmic reticulum as a protein-folding compartment *Trends in cell biology*, vol. 2, no. 8, pp. 227–231, 1992.
- [284] C. Hwang, A. J. Sinskey, and H. F. Lodish, Oxidized redox state of glutathione in the endoplasmic reticulum *Science*, vol. 257, no. 5076, pp. 1496–1502, 1992.
- [285] M. J. Saaranen and L. W. Ruddock, Disulfide bond formation in the cytoplasm *Antioxidants & redox signaling*, vol. 19, no. 1, pp. 46–53, 2013.
- [286] R. C. Cumming, N. L. Andon, P. A. Haynes, M. Park, W. H. Fischer, and D. Schubert, Protein disulfide bond formation in the cytoplasm during oxidative stress *Journal of biological chemistry*, vol. 279, no. 21, pp. 21749–21758, 2004.
- [287] T. G. Senkevich, C. L. White, E. V. Koonin, and B. Moss, Complete pathway for protein disulfide bond formation encoded by poxviruses *Proceedings of the National Academy of Sciences*, vol. 99, no. 10, pp. 6667–6672, 2002.
- [288] T. G. Senkevich, A. S. Weisberg, and B. Moss, Vaccinia virus E10R protein is associated with the membranes of intracellular mature virions and has a role in morphogenesis *Virology*, vol. 278, no. 1, pp. 244–252, 2000.
- [289] T. G. Senkevich, B. M. Ward, and B. Moss, Vaccinia virus A28L gene encodes an essential protein component of the virion membrane with intramolecular disulfide bonds formed by the viral cytoplasmic redox pathway *Journal of virology*, vol. 78, no. 5, pp. 2348–2356, 2004.
- [290] S. Akagi, A. Yamamoto, T. Yoshimori, R. Masaki, R. Ogawa, and Y. Tashiro, Distribution of protein disulfide isomerase in rat hepatocytes. *Journal of Histochemistry & Cytochemistry*, vol. 36, no. 12, pp. 1533–1542, 1988.
- [291] C. Klenner and A. Kuhn, Dynamic disulfide scanning of the membrane-inserting Pf3 coat protein reveals multiple YidC substrate contacts *Journal of Biological Chemistry*, vol. 287, no. 6, pp. 3769–3776, 2012.

- [292] M. A. Danielson, R. B. Bass, and J. J. Falke, Cysteine and disulfide scanning reveals a regulatory α -helix in the cytoplasmic domain of the aspartate receptor *Journal of Biological Chemistry*, vol. 272, no. 52, pp. 32878–32888, 1997.
- [293] R. Bhattacharyya, D. Pal, and P. Chakrabarti, Disulfide bonds, their stereospecific environment and conservation in protein structures *Protein Engineering Design and Selection*, vol. 17, no. 11, pp. 795–808, 2004.
- [294] E. Guerrero, D. Peterson, and F. Franco, *Model for the Protein Arrangement in HBsAg Particles Based on Physical and Chemical Studies*. 1988.
- [295] S. Wynne, R. Crowther, and A. Leslie, The crystal structure of the human hepatitis B virus capsid *Molecular cell*, vol. 3, no. 6, pp. 771–780, 1999.
- [296] B. Schittl and V. Bruss, Mutational profiling of the variability of individual amino acid positions in the hepatitis B virus matrix domain *Virology*, vol. 458–459, no. 0, pp. 183–189, 2014.
- [297] W. F. Carman, Vaccine-associated mutants of hepatitis B virus in *Viral Hepatitis and Liver Disease*, pp. 243–247, Springer, 1994.
- [298] J. M. Lee and S. H. Ahn, Quantification of HBsAg: basic virology for clinical practice *World journal of gastroenterology: WJG*, vol. 17, no. 3, p. 283, 2011.
- [299] B. A. Antoni, I. RODRÍGUEZ-CRESPO, J. GÓMEZ-GUTIÉRREZ, M. Nieto, D. Peterson, and F. Gavilanes, Site-directed mutagenesis of cysteine residues of hepatitis B surface antigen Analysis of two single mutants and the double mutant *European journal of biochemistry*, vol. 222, no. 1, pp. 121–127, 1994.
- [300] L. J. Frost, M. R. Reich, *et al.*, *Access: how do good health technologies get to poor people in poor countries?* Harvard Center for Population and Development Studies, 2008.
- [301] E. L. Snapp, Fluorescent proteins: a cell biologist’s user guide *Trends in cell biology*, vol. 19, no. 11, pp. 649–655, 2009.
- [302] V. D. Siegler and V. Bruss, Role of transmembrane domains of hepatitis B virus small surface proteins in subviral-particle biogenesis *Journal of virology*, vol. 87, no. 3, pp. 1491–1496, 2013.
- [303] T. H. Bayburt and S. G. Sligar, Membrane protein assembly into Nanodiscs *FEBS letters*, vol. 584, no. 9, pp. 1721–1727, 2010.

- [304] T. H. Bayburt, Y. V. Grinkova, and S. G. Sligar, Self-assembly of discoidal phospholipid bilayer nanoparticles with membrane scaffold proteins *Nano Letters*, vol. 2, no. 8, pp. 853–856, 2002.

6 Appendix

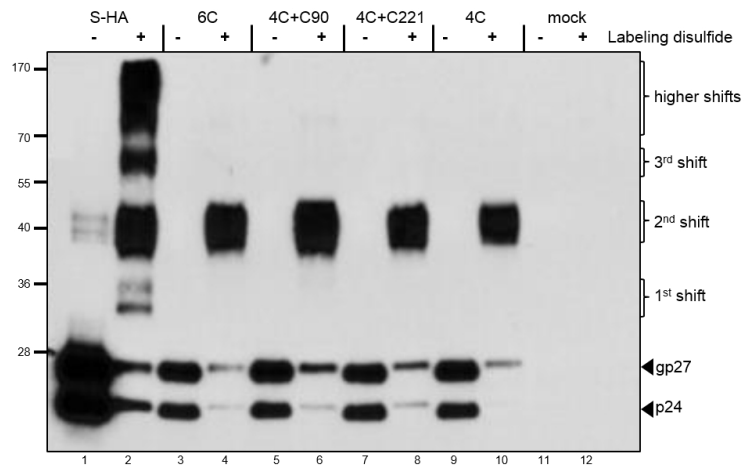


Figure 6.1: Picture adapted from Master Thesis of Franziska Zörndlein. Labeling of disulfide bonds in lysate of different constructs regarding cysteines in TM domains. Samples were taken 3 dpt and labeled with Mal-PEG5000 with respect to disulfide bonds. anti-HA antibody.

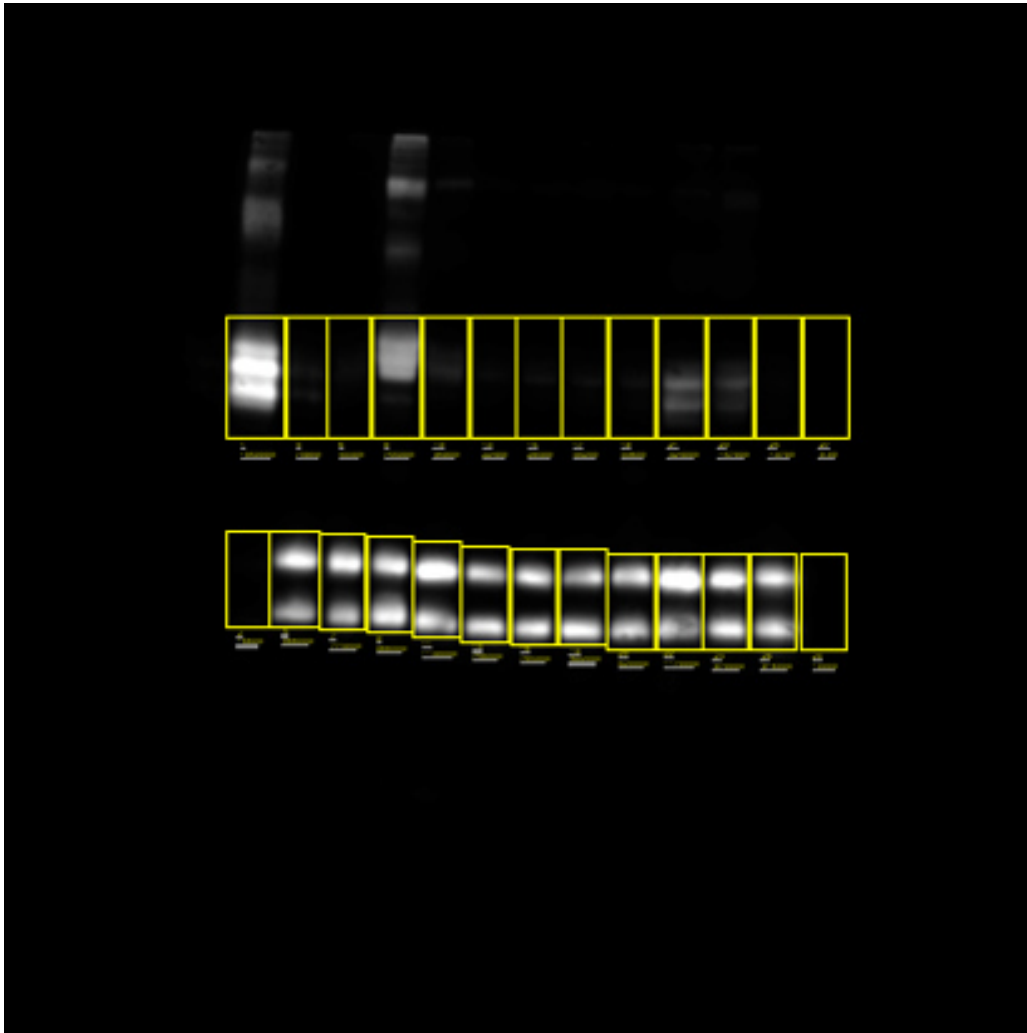


Figure 6.2: Graphic corresponding to the intensity analysis in Figure 4.9. The rectangles drawn for the intensity analysis can be seen in the inverted picture of lysate -DTT.

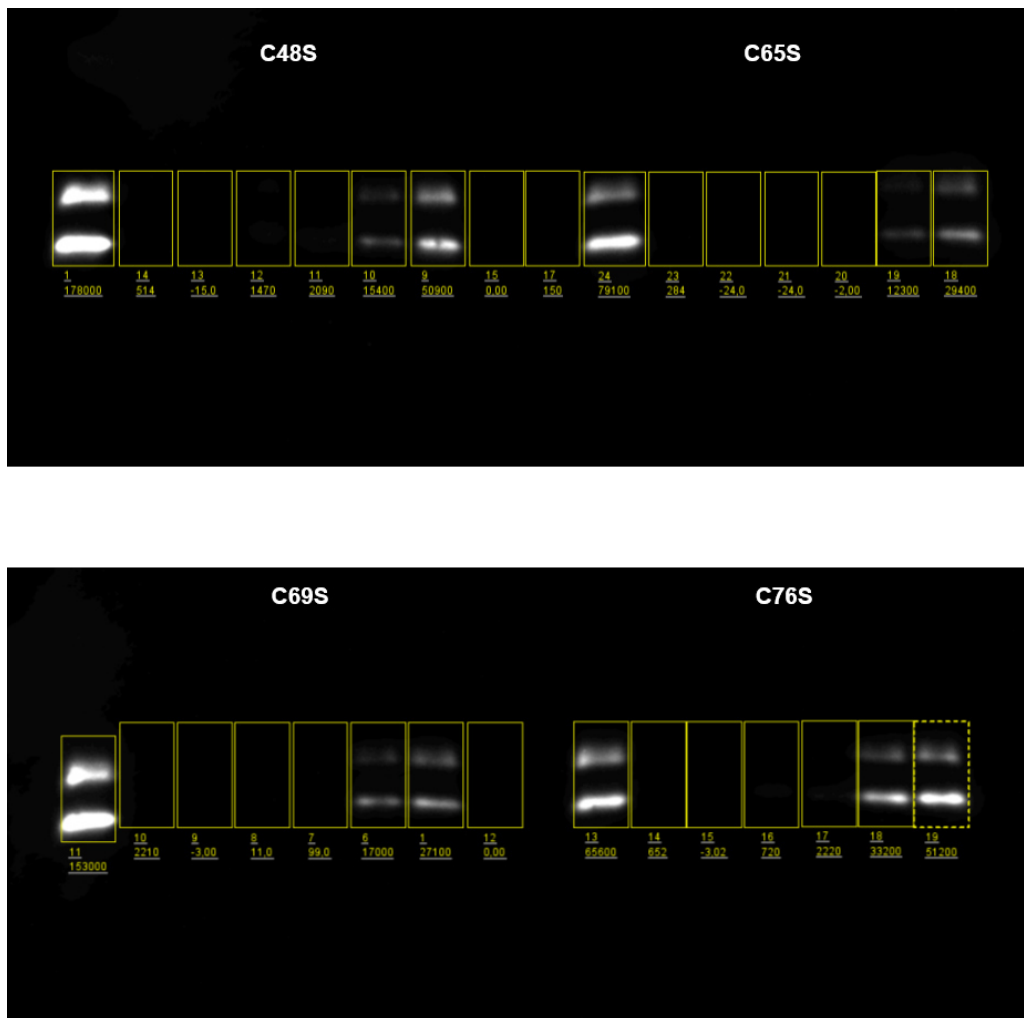


Figure 6.3: Graphic corresponding to the intensity analysis in Figure 4.15. The rectangles drawn for the intensity analysis can be seen in the inverted picture of the four SN blots.

7 Acknowledgments

First of all I want to thank Volker Bruss for the opportunity to do my PhD thesis in his lab and for the very interesting topic of my work. The great working atmosphere was derived by the fact that I did not have the feeling that I worked *for* him, but *with* him. I appreciated his professional and personal guidance and always had the feeling that our discussions were at eye-level.

Next, I want to thank Dieter Langosch for being the official supervisor of my thesis. And Ruth Brack-Werner and Thomas Floss for their time and the fruitful discussions at my Thesis Committee Meetings.

The working atmosphere at the institute was really special and supportive which, of course, was only possible with the people shaping this. I have enjoyed the easy way of collaboration, the mutual support, the helping hands and the open-minded people. I won a lot of friends during my time here and I enjoyed going to work every day. Special thanks to the students, interns and assistants who were a great help to me.

Also a big "thank you" to Nina and Claudia who helped me with all questions regarding English grammar and punctuation, or statistical and combinatorial problems.

I want to express my gratitude to my family, especially my father who always supported me. He was always interested in my studies and my work and we had a lot of critical and open-minded discussions. Thank you!

Last but not least a big thank you to my husband Michael for his encouragement and his support. And in some stages of my thesis for his unending patience!

Lebenslauf

PERSÖNLICHE ANGABEN

Name Nadine King, geb. Gerstenberg
Geburtsdatum/-ort 19.12.1990 in Buchloe
Familienstand verheiratet

WERDEGANG

11/2015 – heute **Promotion | Technische Universität München und Helmholtz Zentrum München**

Wissenschaftlerin in der Arbeitsgruppe von Prof. Volker Bräu – Forschung im Bereich Sekundärstruktur der Hüllproteine von Hepatitis B mit besonderem Fokus auf Disulfidbrücken

10/2013 – 09/2015 **MSc: Biologie Technische Universität München | München**

Titel der Abschlussarbeit: In-vitro-Infektion von HepG2-NTCP-Zellen mit ausgewählten Hepatitis-B-Virus-Mutanten | Institut für Virologie

09/2013 **Praktikum | GeneArt (jetzt Thermo Fisher Scientific), Regensburg**

Praktikum in wechselnden Gruppen mit Schwerpunkt auf der Herstellung kundenspezifischer Gene und Oligonukleotide

10/2010 – 09/2013 **BSc: Biologie Technische Universität München | München**

Titel der Abschlussarbeit: Kodierung des echo-akustischen Flussfeldes im auditorischen Kortex von Fledermäusen: Einfluss des seitlichen Objektabstandes | Institut für Zoologie

09/2000 – 08/2010 **Abitur Joseph-Bernhart Gymnasium | Türkheim**

Liste der Veröffentlichungen

PUBLIKATIONEN

Suffner, S., **Gerstenberg, N.**, Patra, M., Ruibal, P., Orabi, A., Schindler, M., & Bruss, V. (2018). Domains of the hepatitis B virus small surface protein S mediating oligomerization. Journal of virology, JVI-02232.

Bartenstein, S. K., **Gerstenberg, N.**, Vanderelst, D., Peremans, H., & Firzlaff, U. (2014). Echo-acoustic flow dynamically modifies the cortical map of target range in bats. Nature communications, 5, 4668.

KONFERENZTEILNAHMEN

Suffner, S., **Gerstenberg, N.**, Schindler M., & Bruss V. Mutational analysis of HBV S protein oligomerization
26TH ANNUAL MEETING OF THE SOCIETY FOR VIROLOGY | Münster | April 2016

Gerstenberg N., Zörndlein F., Suffner S., & Bruss V. Mapping of disulfide bonds in the hepatitis B virus small envelope protein S
27TH ANNUAL MEETING OF THE SOCIETY FOR VIROLOGY | Marburg | März 2017

Gerstenberg N., Zörndlein F., Schöllkopf A., & Bruss V. Mapping of disulfide bonds in the hepatitis B virus small envelope protein S
28TH ANNUAL MEETING OF THE SOCIETY FOR VIROLOGY | Würzburg | März 2018

King N., Zörndlein F., & Bruss V. Mapping disulfide bonds in the hepatitis B virus small envelope protein S
INTERNATIONAL HBV MEETING | Taormina, Italy | October 2018

AUSZEICHNUNGEN

- Travel Grant zum internationalen HBV meeting (\$750 Travel Grant) | Hepatitis B Foundation (2018)
- Goldmedaille und Top 16 beim iGEM-Wettbewerb | iGEM Foundation (2013)